서남극 퇴적물 미세조직의 현미경 관찰을 통한 퇴적과정과 기후변화

Study on sedimentary processes and climate change based on microscopic observations of sediment microstructures in West Antarctic

부산대학교

제 출 문

극지연구소장 귀하

본 보고서를 “ 과거온난기의 서남극 빙상 후퇴 및 해양 순환 변화 연구”과제의 위탁연구“서남극 퇴적물 미세조직의 현미경 관찰을 통한 퇴적과정과 기후변화”과제의 최종보고서로 제출합니다.

2026 . 1 . 30

(본과제)	총괄연구책임자	: 유 규 철
	위탁연구기관명	: 부 산 대 학 교
	위탁연구책임자	: 김 부 근
	위탁참여연구원	: 하 상 범
	“	: 최 혁
	“	: 양 주 연

보고서 초록

위탁연구과제명	서남극 퇴적물 미세조직의 현미경 관찰을 통한 퇴적과정과 기후변화 연구				
위탁연구책임자	김 부 근	해당단계 참여연구원수	4	해당단계 연구비	100,000,000원
연구기관명 및 소속부서명	부산대학교	참여기업명			
국제공동연구	상대국명 :	상대국연구기관명 :			
요약(연구결과를 중심으로 개조식 500자이내)				보고서 면수	85

- 로스해 북서부 중앙 분지에서 회수된 코어 LC42에는 지난 약 100만 년 동안 퇴적된 세 가지 뚜렷한 퇴적상, 즉 빙산기원퇴적물(IRD)이 거의 없는 생물교란된 사질이질, IRD가 풍부한 괴상 사질이질, 그리고 엽리 머드가 서로 교호하며 분포함
- 빙하기 동안에는 전진하는 빙하 아래에서 방출된 유백색 융빙수 플룸에 의해, 과거에 퇴적되어 반고결 상태에 있던 규조류 풍부 퇴적물이 침식·재작용되며 이러한 엽리 머드층이 하향 퇴적된 것으로 판단됨
- 남극 대륙 주변부에서 기후–생산성 모델을 구축하고 고기후를 해석함에 있어, 생물기원 입자의 재순환 효과를 충분히 고려하지 않을 경우 고기후 해석의 오류에 이를 수 있음을 강조함
- 서부 로스해 드라이갈스키 분지 북부의 코어 퇴적물은 쇄설물이 풍부한 이질성 머디 디아믹톤, 쇄설물이 풍부한 사질 디아믹톤, 괴상 이질, 엽리 머드, 생물교란 이질, 괴상 사질이질, 생물교란 사질이질의 총 7개 퇴적상으로 구분되며, 퇴적상의 조합은 퇴적 진화 과정에 따라 네 개의 암상 단위를 정의함
- 마지막 최대빙기 이후, 드라이갈스키 분지 북부에서의 고환경 변화와 빙하성 해양 퇴적 진화는 홀로세 동안의 기후 변화뿐만 아니라, 빙상의 동역학과 빙붕 활동과도 밀접하게 연관되어 있었음을 보여줌

색 인 어 (각 5개 이상)	한 글	로스해, 고환경, 고기후, 시추코아
	영 어	Ross Sea, Paleoenvironment, Paleoclimate, Sediment core

요 약 문

Ⅰ. 제 목

- 서남극 퇴적물 미세조직의 현미경 관찰을 통한 퇴적과정과 기후변화 연구

Ⅱ. 연구개발의 목적 및 필요성

- 서남극 코아 퇴적물에 보존된 엽리층 미세조직을 박편의 현미경 관찰과 연마편의 전자현미경 관찰 등 다양한 분석을 통하여 빙상의 발달 및 후퇴와 관련된 해양순환 및 기후변화 정보를 획득함
- 로스해 드라이갈스키 분지 코아퇴적물의 다양한 분석을 통하여 마지막 빙하기 이후 빙상의 발달 및 후퇴와 관련된 해양순환 및 기후변화를 복원함

Ⅲ. 연구개발의 내용 및 범위

- 서남극 코아 퇴적물의 엽리층 미세조직 특성 파악
- 드라이갈스키 분지 해역의 고환경 복원

Ⅳ. 연구개발결과

- 로스해 북서부 중앙 분지에서 회수된 코어 LC42에는 지난 약 100만 년 동안 퇴적된 세 가지 뚜렷한 퇴적상, 즉 빙산기원퇴적물(IRD)이 거의 없는 생물교란된 사질이질, IRD가 풍부한 괴상 사질이질, 그리고 엽리 머드가 서로 교호하며 분포함
- 빙하기 동안에는 전진하는 빙하 아래에서 방출된 유백색 융빙수 플룸에 의해, 과거에 퇴적되어 반고결 상태에 있던 규조류 풍부 퇴적물이 침식·재작용되며

이러한 엽리 머드층이 하향 퇴적된 것으로 판단됨

- 남극 대륙 주변부에서 기후–생산성 모델을 구축하고 고기후를 해석함에 있어, 생물기원 입자의 재순환 효과를 충분히 고려하지 않을 경우 고기후 해석의 오류에 이를 수 있음을 강조함
- 서부 로스해 드라이갈스키 분지 북부의 코어 퇴적물은 쇄설물이 풍부한 이질성 머디 디아믹톤, 쇄설물이 풍부한 사질 디아믹톤, 괴상 이질, 엽리 머드, 생물교란 이질, 괴상 사질이질, 생물교란 사질이질의 총 7개 퇴적상으로 구분되며, 퇴적상의 조합은 퇴적 진화 과정에 따라 네 개의 암상 단위를 정의함
- 마지막 최대빙기 이후, 드라이갈스키 분지 북부에서의 고환경 변화와 빙하성 해양 퇴적 진화는 홀로세 동안의 기후 변화뿐만 아니라, 빙상의 동역학과 빙붕 활동과도 밀접하게 연관되어 있었음을 보여줌

Ⅴ. 연구개발결과의 활용계획

- 본 연구에서 축적된 자료와 해석 결과는 국내외 연구진의 교육·인력 양성 측면에서도 활용되며, 차세대 극지 연구 인력의 전문성 강화로 이어지는 인적 자원 양성 효과는 장기적으로 국내 극지 과학의 지속 가능성을 높이는 데 기여함
- 본 연구의 논문실적은 국제 학술지 게재에 그치지 않고, 국제 공동 시추 자료 해석 고도화, 빙상–기후 모델 검증, 대형 극지 연구 기획, 인력 양성 및 학문적 표준 정립 등 다양한 분야에서 실질적으로 활용됨

S U M M A R Y
(영 문 요 약 문)

Ⅰ. Title

– Study on sedimentary processes and climate change based on microscopic observations of sediment microstructures in West Antarctic sediments.

Ⅱ. Purpose and Necessity of R&D

– Through integrated analyses of laminated sediment microstructures preserved in West Antarctic core sediments—including petrographic microscope observations of thin sections and electron microscope analyses of polished sections—this study obtained information on ocean circulation and climate change associated with ice-sheet advance and retreat.

– Based on comprehensive analyses of core sediments from the Drygalski Basin in the Ross Sea, this study reconstructed ocean circulation and climate changes related to ice-sheet development and retreat since the Last Glacial Maximum.

Ⅲ. Contents and Extent of R&D

– Characterization of laminated sediment microstructures in West Antarctic core sediments

– Paleoenvironmental reconstruction of the Drygalski Basin region

Ⅳ. R&D Results

- Core LC42 retrieved from the Central Basin of the northwestern Ross Sea contains three distinct sediment facies (IRD (ice-rafted debris)-poor bioturbated sandy mud, IRD-rich massive sandy mud, and laminated mud) that are interleaved with each other and deposited over the last 1 Ma.
- During the glacial periods, these laminated muds were deposited downward by milky plumes of meltwater discharged underneath the advancing glaciers that scoured the earlier-deposited and semi-consolidated diatom-rich sediments.
- Our study highlights that the recycling of biogenic particles should be precautious to avoid the fallacy of paleoclimatic interpretation in formulating climate-productivity models in the Antarctic continental margin.
- Using the four gravity (and box) cores obtained from the northern Drygalski Basin in the western Ross Sea, the core sediments were classified into the seven sediment facies: clast-rich muddy diamicton, clast-rich sandy diamicton, massive mud, laminated mud, bioturbated mud, massive sandy mud, and bioturbated sandy mud and the association of these sediment facies define the four lithologic units in terms of the depositional evolution.
- Since the LGM, the paleoenvironmental change and glaciomarine depositional evolution on the northern Drygalski Basin were closely linked with the ice sheet dynamics and ice shelf activity, in addition to the climate change during the Holocene.

Ⅴ. Application Plans of R&D Results

– The data and interpretive results accumulated through this study are also utilized for education and human resource development among domestic and international research communities, contributing to the training of next-generation polar scientists. In the long term, this human capacity–building effect enhances the sustainability of polar science research in Korea.

– The publication outcomes of this study extend beyond international journal articles and are practically applied to advancing the interpretation of international collaborative drilling datasets, validating ice-sheet–climate models, planning large-scale polar research initiatives, fostering scientific manpower, and establishing academic standards in polar science.

목 차

제 1 장 서론

1 절. 전 지구적 기후변화의 가속화와 새로운 위기 국면

산업혁명 이후 인위적인 온실가스 배출 증가로 인해 지구 평균기온은 전례 없는 속도로 상승하고 있다. 이러한 온난화는 단순한 기온 변화에 그치지 않고 해수면 상승, 기후대 및 생태계의 재편, 사막화 확산, 담수 자원의 고갈, 태풍의 강도와 빈도 변화, 극한 강수의 증가 등 복합적이고 상호 연계된 문제를 야기하고 있다. 특히 최근 수십 년간 관측된 극한기상 현상은 기존 기후 변동성의 범위를 넘어서는 양상을 보이며, 이는 사회·경제·안보 전반에 걸쳐 중대한 위협으로 인식되고 있다.

기후변화의 이러한 가속화는 단기적인 완화 정책만으로는 대응이 어렵고, 중·장기적 관점에서 지구 시스템의 근본적인 변화를 이해하는 과학적 기반이 필수적임을 시사한다. 특히 해수면 상승은 연안 저지대와 대도시에 직접적인 피해를 초래할 뿐만 아니라, 국가 간 분쟁과 대규모 이주를 유발할 수 있는 잠재적 요인으로 작용한다. 따라서 미래 해수면 변동의 규모와 속도를 보다 정확히 예측하는 것은 기후변화 대응 전략 수립의 핵심 과제라 할 수 있다.

2 절. 남극 빙상의 중요성과 해수면 상승의 결정적 요인

전 세계 담수의 약 60%가 남극 빙상에 저장되어 있다는 점에서, 남극은 지구 기후 시스템의 핵심 구성 요소라 할 수 있다. 남극 빙상은 대기 및 해양 온도 변화에 민감하게 반응하며, 그 질량 변화는 전 지구 평균 해수면 변동에 직접적인 영향을 미친다. 위성 관측과 중력 자료를 기반으로 한 최근 분석에 따르면, 1992년 이후 남극 빙하의 유실 속도는 과거에 비해 약 3배 이상 가속화되었으며, 특히 서남극 빙상에서 전체 유실량의 약 70%가 집중되고 있는 것으로 보고되었다(The IMBIE team, 2018).

서남극 빙상은 해저 기반이 해수면보다 낮은 해양빙상(marine-based ice sheet) 구조를 갖고 있어, 해수 온도 상승과 빙저 침식에 매우 취약하다. 이러한 특성으로 인해 빙상 붕괴가 일단 시작되면 되돌리기 어려운 비가역적 변화가 발생할 가능성이 크다. 실제로 다수의 빙하가 붕괴 임계점(tipping point)에 근접해 있다는 연구 결과는, 남극 빙상 변화가 단순한 미래 가능성이 아니라 현재 진행 중인 위기임을 명확히 보여준다.

3절. 미래 빙상-기후 모델과 장기적 해수면 상승

빙상과 기후를 결합한 수치모델 연구는 남극 빙하 변화가 장기적으로 지구 환경에 미칠 영향을 정량적으로 제시하고 있다. DeConto와 Pollard(2016)의 연구에 따르면, 온실가스 배출이 지속될 경우 남극 빙하 유실로 인한 전 지구 평균 해수면 상승은 2100년까지 1 m 이상, 2500년에는 15 m 이상에 이를 가능성이 있다. 이러한 수치는 기존 연안 방재 및 도시 계획의 전제를 근본적으로 재검토해야 할 필요성을 제기한다.

특히 수백 년에서 수천 년 규모의 장기 전망은 단순한 학술적 관심을 넘어, 문명 지속 가능성의 문제와 직결된다. 해수면이 수 미터 이상 상승할 경우 현재의 연안 도시 상당수가 존속 불가능해지며, 항만·산업단지·에너지 인프라 전반에 막대한 영향을 미칠 것이다. 따라서 빙상 변화의 장기적 거동을 이해하는 연구는 미래 세대의 생존과 직결된 필수 연구 영역이라 할 수 있다.

4절. 고기후 연구를 통한 미래 예측 불확실성 저감

미래 기후 예측의 가장 큰 한계 중 하나는 장기적인 빙상 반응에 대한 불확실성이다. 이를 극복하기 위한 핵심 접근법이 바로 과거 온난기의 지구 환경을 복원하는 고기후(paleoclimate) 연구이다. IPCC 제5차 평가보고서와 기후모델-고기후 비교 연구에 따르면, 현재와 같은 온난화 추세가 지속될 경우 2030년경에는 약 300만 년 전 플라이오세 중기의 기후 상태, 즉 현재보다 평균기온이 2-4℃ 높은 시기와 유사해질 것으로 전망된다. 더 나아가 2150년경에는 빙하가 거의 존재하지 않았던 약 5천만 년 전 에오세 온난기와 유사한 기후에 도달할 가능성도 제시되었다(Burke et al., 2018).

플라이오세와 에오세는 현재와 대륙 배치가 유사하거나, 혹은 온난화의 극단적 사례를 제공하는 시기로서, 미래 지구의 잠재적 상태를 이해하는 데 중요한 자연 실험실이라 할 수 있다. 이 시기 동안 남극 빙상이 어떻게 형성·후퇴·붕괴되었는지를 규명하는 것은, 빙상 모델의 물리 과정과 민감도를 검증하고 개선하는 데 결정적인 기여를 한다.

5절. 동아시아와 한반도에 대한 효과와 국가적 대응 필요성

남극 빙상 변화로 인한 해수면 상승과 기후 시스템 재편은 한반도를 포함한 동아시아 지역에도 중대한 영향을 미칠 것으로 예상된다. 한반도는 삼면이 바다로 둘러싸인 지리적 특성상 해수면 상승과 연안 침식에 취약하며, 극한 강수와 폭염, 태풍 경로 변화 등 복합적인 기후 리스크에 직면해 있다. 이러한 변화는 농업 생산성, 수자원 관리, 연안 생태계, 국민 안전에 직결되는 문제로 이어질 가능성이 크다.

그러나 현재 동아시아 지역의 미래 기후 전망은 여전히 높은 불확실성을 내포하고 있으며, 이는 남극을 포함한 극지 변화에 대한 이해 부족에서 비롯된 측면이 크다. 따라서 남극 빙상 연구는 단순한 극지 과학을 넘어, 동아시아 및 한반도의 기후 적응 전략 수립을 위한 과학적 근거를 제공하는 핵심 연구 분야라 할 수 있다.

6절. 국제 공동 연구의 필요성과 전략적 참여

남극 빙상과 과거 온난기 환경을 복원하기 위해서는 해저 및 빙하 퇴적물에 대한 직접적인 시료 확보가 필수적이다. 이를 위해 현재 국제 사회는 대규모 국제 공동 시추 프로그램을 추진하고 있으며, 고해상도 지질·지구화학·생물학적 기록을 확보함으로써 빙상-기후 상호작용을 정밀하게 규명하고자 하고 있다.

이러한 국제 공동 연구는 단일 국가의 역량만으로는 수행이 어려운 고난도·고비용 연구이지만, 참여를 통해 세계 최고 수준의 자료 접근과 연구 네트워크 구축이 가능하다. 또한 연구 결과는 기후 모델 개선, 해수면 상승 예측 고도화, 국제 기후 정책 논의에서의 과학적 발언권 강화로 이어질 수 있다. 따라서 해당 프로그램에 대한 적극적이고 전략적인 참여는 학술적 가치뿐만 아니라 국가적 위상 제고 측면에서도 매우 중요하다.

제 2 장 국내외 기술개발 현황

1 절. 국내 연구개발 동향

국내 남극 고환경 및 빙상 연구는 초기에는 마지막 빙하기 이후의 비교적 단기간에 해당하는 지역적 고해양 변화와 퇴적상 해석에 주로 집중되어 왔다. 이러한 연구들은 남극 주변 해역의 환경 변동을 이해하는 데 기초 자료를 제공하였으나, 수십만 년 이상에 걸친 장기 기후 변동과 빙상 진화 과정을 해석하는 데에는 한계가 존재하였다. 그러나 지난 십여 년간 연구 인프라와 연구 역량의 비약적인 발전을 통해 국내 남극 연구는 질적·양적 도약을 이루었다.

2009년 쇄빙연구선 아라온(ARAON)의 건조는 국내 남극 연구의 전환점이라 할 수 있다. 아라온의 취항으로 결빙 해역에서의 안정적인 관측과 시료 채취가 가능해졌으며, 그동안 접근이 제한적이었던 남극해 및 극지 해역에서의 본격적인 연구 수행이 가능해졌다. 특히 국제 공동 탐사 참여가 확대되면서 국내 연구진은 글로벌 극지 연구 네트워크에 본격적으로 편입되었고, 연구 주제 역시 지역적 해양 변화에서 빙상-해양-기후 상호작용을 포괄하는 방향으로 확장되었다.

2011년부터 2017년까지 추진된 장기 롱 코어링 시스템 구축 사업은 국내 고기후 연구의 시간적 한계를 크게 확장시켰다. 이 기간 동안 구축된 피스톤 코어링 및 장주기 퇴적물 시추 기술을 통해 수백만 년 규모의 장기 기후 기록 확보가 가능해졌으며, 국내의 해저 퇴적물 시추 능력은 세계 최고 수준에 근접하게 되었다. 이는 남극 빙상의 장기 진화와 고기후 변화 복원을 위한 핵심 기반 기술로 평가된다.

또한 2014년 장보고 과학기지의 설립은 국내 남극 연구의 공간적 확장을 가능하게 하였다. 기존의 남극반도 및 남극해 중심 연구에서 벗어나 로스해 지역까지 연구 영역이 확대되었으며, 이를 통해 동남극과 서남극을 아우르는 다지역 비교 연구가 가능해졌다. 여러 지역에서 획득된 자료를 종합적으로 분석함으로써 국지적 환경 변화 해석을 넘어 남극 빙상의 거시적 거동과 전 지구적 기후 시스템과의 연계를 해석할 수 있는 기반이 마련되었다. 특히 서남극 빙상 변화와 해수면 상승 문제에 대한 대응 연구 측면에서 장보고 기지는 전략적 거점 역할을 수행하고 있다.

이와 함께 학계와 정부출연연구기관 간의 공동연구, 국제 공동연구 참여 확대, 고정밀 연대측정 기법 및 다양한 퇴적물 프록시 분석 장비 도입을 통해 연구의 정밀도와 신뢰성이 크게 향상되었다. 방사성 동위원소 연대측정, 미량원소·동위원소 분석, 미세입자 및 생물기원 프록시 분석 등 다각적인 접근이 가능해지면서 남극

고환경 복원 연구의 깊이와 폭이 동시에 확장되고 있다.

이러한 인프라와 연구 역량의 축적을 통해, 국내 연구진은 SCAR(Scientific Committee on Antarctic Research) Horizon Scan에서 제시한 남극 빙상 안정성, 해수면 상승, 극지-저위도 기후 연계와 같은 세계적 핵심 과제에 실질적으로 기여할 수 있는 수준에 도달하였다. 이는 향후 국제 대형 공동 연구에서 주도적 역할을 수행할 수 있는 잠재력을 확보하였음을 의미한다.

2 절. 국외 연구개발 동향

최근 국외 남극 연구의 주요 흐름은 과거 온난기 동안의 남극 환경 복원과 그에 따른 빙상 안정성, 그리고 해수면 상승 기여도를 정량화하는 데 집중되고 있다. 미래 지구 평균기온 상승이 불가피한 상황에서 남극빙상이 어떤 임계 반응을 보일 것인지 예측하기 위한 과학적 근거를 확보하려는 국제적 노력의 일환이다.

특히 현재와 대기 중 이산화탄소 농도가 유사했던 플라이오세 온난기를 대상으로 한 연구들이 활발히 수행되고 있다. 다수의 지질·지구물리학적 증거에 따르면, 플라이오세 동안 동남극 빙상은 Wilkes Subglacial Basin 내부까지 후퇴한 것으로 해석되고 있다(Cook et al., 2013; Patterson et al., 2014; Reinardy et al., 2015). 이러한 고기후 복원 결과를 빙상 모델에 반영한 연구에서는 당시 전 지구 평균 해수면이 현재보다 약 17 m 높았을 가능성이 제시되었다(Pollard et al., 2015). 이는 동남극 빙상 역시 장기 온난화 조건하에서 결코 안정적이지 않을 수 있음을 시사하는 중요한 결과이다.

지난 마지막 해빙기 동안 관측된 급격한 해수면 상승 사건과 남극 빙상의 역할에 대한 연구도 중요한 국제적 이슈로 부각되고 있다. 약 17 ka에 발생한 비교적 이른 시기의 해수면 상승은 남극반도 빙상과 남동 웨델해 인근의 동남극 빙상 해빙과 관련되었을 가능성이 제기되었다. 더 나아가 스코시아해의 빙산기원퇴적물(IRD) 기록 분석 결과는 서남극 빙상의 후퇴가 Meltwater Pulse 1A와 같은 급격한 해수면 상승 사건의 주요 원인 중 하나였음을 지시하고 있다(Weber et al., 2014).

이와 같은 연구 성과를 바탕으로, 미래 지구 평균기온이 2℃ 이상 상승할 경우 남극 환경과 빙상이 어떻게 변화할 것인지에 대한 국제적 관심이 집중되고 있다. 이를 규명하기 위해 과거 온난기를 직접 추적할 수 있는 고해상도 퇴적 기록 확보가 필수적이며, 이에 따라 대규모 국제 공동 퇴적물 시추 프로그램이 활발히 추진되고 있다.

제 3 장 연구개발수행 내용 및 결과

1 절. Fallacy of paleoproductivity signals by the recycled biogenic components: case study in the Central Basin of the northwestern Ross Sea)

1. Introduction

Antarctic cryosphere and hydrosphere are vulnerable to the impact of orbital-scale climate change in terms of ice sheet activity (Prothro et al. 2020). As a consequence, contrasting sediments as exemplified by an interglacial open marine deposit and a glacial diamicton have been deposited on the Antarctic continental shelves during the warm and cold conditions, respectively, in association with the advance or retreat of ice sheet (Anderson et al. 1984; Domack et al. 1999; Domack and Powell 2018). On the other hand, in the Antarctic continental margin where the ice sheet was not grounded, the amount of ice-rafted debris (IRD) has been proposed as a key to distinguish interglacial and deglacial (IRD-rich) sediments from glacial (IRD-poor or absent) sediments (Anderson et al. 1979; Anderson 1999;Khim et al. 2017; Smith et al. 2019; Hillenbrand et al. 2021; Bollen et al. 2022).

The Ross Sea continental shelf is known for being a biological 'hot spot' in the Southern Ocean, connecting the biogenic silica production in the water column to the current pattern of biosiliceous sediment accumulation (Ledford-Hoffman et al. 1986;Dunbar et al. 1989; Langone et al. 1998). In the Ross Sea, during the glacial periods, the biological productivity was limited in most continental shelves due to the advancing ice sheet (Frignani et al. 1998; McKay et al. 2008), and it was also reduced in the distal continental margin, mainly due to the wider expansion of seasonal or permanent sea ice coverageand limited nutrient availability (Ceccaroniet al. 1998; Cunninghamet al. 1999). This confirms the coupling between climate and productivity (i.e., high productivity during warm interglacial), as verified from the numerous sedimentary records in the Ross Sea continental margin (Tolottiet al. 2013; Kim et al. 2020; Hartman et al. 2021; Li et al. 2022) as well as in the other Antarctic continental margin (Frank et al. 1995; Wu et al. 2017; Hillenbrand et al. 2021;

Lu et al. 2022).

Recently, a core RS15-LC42 (hereafter LC42) was collectednear the eastern flank of the Hallett Ridge in the Central Basin of the northwestern Ross Sea (Fig. 1). Khim et al. (2024) conducted the microscopic examination of the laminated mud layers in LC42, explaining that these laminated muds contain the components recycled by the transportation and redeposition of reworked sediments from the older deposits. In this study, we performed multi-analyses of the biogenic components (biogenic opal, total organic carbon [TOC], and total nitrogen [TN]) in this core and found out their extraordinary results, which contradicts climate-productivity model based on glaciomarine sediment deposition. Our novel finding suggests that the recycled biogenic particles of the laminated mud layers in LC42 are an important example against the climate-productivity model, warning that overly simplistic glaciomarine sedimentation should be precautious for the reliable paleoenvironmental interpretations in the Antarctic continental margin.

2. Materials and methods

The Central Basin is a deep semi-closed tectonic depression forming the slope basin located at the mouth of the JOIDES Basin in the northwestern Ross Sea (Fig. 1). During the austral summer of 2015, an 11.75 m-long core LC42 was collectedfrom the northwestern moat (71°49.40′S, 178°34.76′E, 2084 m water depth)in the Central Basin using jumbo gravity coring systemaboard I/B *Araon*. Optical images of LC42 were captured using ITRAX core scanner, and X-ray radiographic images were taken on 1-cm thick sediment slabs using X-ray inspection equipment (SOFTEX W-100W) at Korea Polar Research Institute (KOPRI). X-ray images were digitized to obtain the gray scale (0~255) of sediment brightness.

Total carbon (TC), total nitrogen (TN), and biogenic opal contents were measured at 5 cm intervals at KOPRI. Because of such low-resolution sampling, the dark and light lamina cannot be separated during the analysis. TC and TN content was determined using an organic elemental analyzer (FLASH, 2000 NC Analyzer) with an analytical precision of less than ±0.1%. Total inorganic carbon (TIC) content was measured using UIC CO_2 coulometer (Model CM5240) with an analytical precision of less than ±0.1%. Total organic carbon (TOC) content was calculated as the difference between TC and TIC content. Biogenic silica (Si_{BIO}) concentration was measured using a continuous flow analyzer (SKALAR SANplus Analyzer) and the wet-alkaline extraction method modified from DeMaster (1981). Biogenic opal content was calculated by multiplying Si_{BIO} concentration by 2.4 (Mortlock and Froelich 1989). The relative analytical error of Si_{BIO} concentration is less than 1%.

Grain size analysis was performed on the selected three horizons that represent the major sediment lithology. Organic matter was removed from the bulk sediments using 10% H_2O_2. Coarser fractions (>63 mm) were weighed at 1 phi interval using sieves, while finer fractions (<63 mm) were analyzed using a Micrometrics Sedigraph III 5120 at KOPRI.

To examine the componentry of laminated sediments, polished sections were prepared using a fluid displacive resin embedding technique modified from Pike and Kemp (1996). These sections were examined using scanning electron micro-scope (SEM) (×100–10000) with backscattered electron imagery (BSEI) of JEOL (JZA-8530F PLUS) Field-Emission Electron Probe Micro-Analyzer at Gyeongsang National University (Korea).

3. Results and discussion

(1) Sediment lithology, age, and glaciomarine deposition of LC42

Based on visual observations and examinations, the sediments of LC42 were divided into three facies: 1) IRD-poor bioturbated sandy mud, 2) IRD-rich massive sandy mud, and 3) laminated mud (Fig. 2, Supplement Fig. S1). This classification was confirmed by the grain size distribution (Fig. 2). In particular, the coarse-grained particles are absent in the laminated mud. Despite the repetition of these three sediment facies throughout the core, their vertical succession does not show cyclic pattern. It is worth noting that the uppermost part of the core is occupied by IRD-poor bioturbated sandy mud and IRD-rich massive sandy mud, which overlie the laminated mud (Fig. 2, Supplement Fig. S1). LC42 preserves eight intervals of laminated sediments with varying thicknesses (10 cm to about 2 m) throughout the core. The laminated sediments are devoid of IRD and bioturbation. The laminations consist of alternatingrelatively thicker light laminae and relatively thinner dark laminae

(Fig. 2 and Supplement Fig. S1). Khim et al. (2024) carried out the microscopic observation and backscattered electron imagery examination of these laminated muds, and reported that the light laminae consists of mostlyterrigenous angular to subangular silt-sized particles withdiatom fragments and eroded fossil-bearing sand-sized lumps and the dark laminae are composed of biogenic clays with very tiny pieces of fossils.

Ohneiser et al. (2019) reported the preliminary magneto-biostratigraphy of LC42 that contains the first appearance datum (0.57–0.65 Ma) of *Thalasssiosira antarctica* and the Matuyama–Brunhes boundary (0.781 Ma). Later, Bollen et al. (2022) confirmed that LC42 spans the last 1.34 Ma, based on a new magneto-biostratigraphic age model (Fig. 3). This implies that, if the glaciomarine sedimentation was continuous, there must be at least 10 orbital-scale (i.e., eccentricity) interglacial and glacial cycles during the deposition of LC42. Nonetheless, determining the precise age of each sediment facies and correlating with the interglacial-glacial cycles have proven challenging, despite the speculative correlation (Fig. 3) by Bollen et al. (2022). Thus, we cannot differentiate the interglacial and glacial cycles as well as the sedimentation rate change.

Based on the glaciomarine depositional processes in the Antarctic continental margins (Anderson, 1999; Domack and Powell 2018), IRD deposition increased during the warm period by more active calving and floating ice, whereas the lack of IRD seems to be due to the wide development of sea ice during the glacial period. Based on the temporal succession of sediment facies at the uppermost of core and application to the glaciomarine sedimentation, IRD-poor bioturbated sandy mud and IRD-rich massive mud might have been deposited during the interglacial and deglacial periods, whereas the laminated mud may represent glacial sediments without IRD(Anderson et al. 1979; Anderson 1999; Khim et al. 2017; Domack and Powell 2018). Recently, Bollen et al. (2022) reported the hypothesized schematic depositional conditions for three sediment facies in LC42. IRD-rich deposit was influenced by a combination of enhanced glacial calving during the glacial retreat and export of shelf water during interglacial and weak glacial periods. In contrast, IRD-poor deposit and laminated sediments were formed due to glacial scouring to induce slope failures and turbidity currents as well as transport of shelf sediments by meltwater pulses, depending on the partial or full glacial advance.

(2) Paleoproductivity change in terms of biogenic components in LC42

TOC, TN, and biogenic opal contents of glaciomarine sediments serve as an indicator of surface water productivity in the Ross Sea, although their preservation potentials are different, depending on diverse environmental factors (e.g., Langone et al. 1998). For example, Bahr et al. (2014) reported the XRD scanning geochemical data of contourites in the Gulf of Cadiz, and suggested that the bromine (Br) record represents TOC content in response to the climate signals. Their results indicate that the geochemical information was influenced by the bottom water activity rather than the surface water properties, despite the millennial time-scale. Downcore variation of TOC, TN, and biogenic opal contents of LC42 exhibits remarkable characteristics throughout the core (Fig. 3). All biogenic contents of laminated mud are consistently higher compared to other two sediment facies. Despite the low-resolution sampling interval (5 cm), variations of these components are more common within the laminated mud layer. In particular, variation of these three properties shows a clearly parallel pattern in laminated mud layer throughout the core (Fig. 3).

The linear relationship between TOC and TN contents provides evidence of their typical marine origin (Fig. 4a). The strong positive relationship between TOC and biogenic opal contents further supports the interdependence of these components. Their relationship in LC42 shows that the biogenic opal content during the interglacial period is similar to that of the Holocene surface sediments (Figs. 4b and 4c) and that the variation range of TOC and biogenic opal contents in LC42 is not much different between the interglacial and glacial periods (Fig. 4b). High TOC and biogenic opal contents of laminated mud layers are characteristic, because they were formed during the glacial periods. On the other hand, high C/N ratios of laminated mud layers result from the different degradation between TOC and TN, which reflects that the organic matters of laminated mud layers experienced the differential degradation before the deposition. Such high C/N ratios of laminated mud layers are different from those of diamicton and calving ice that contain the terrestrial organic matters in the Ross Sea (Smith et al. 2019). Based on the climate-productivity model, high productivity occurred during the interglacial periods, which was verified by the higher deposition of TOC and biogenic opal content during the warm conditions in the Ross Sea as shown in cores ANTA91-8 (Ceccaroni et al. 1998) and RS15-GC41 (Kim et al. 2020) (Fig. 4c). In LC42, thus, it can be simply interpreted that the deposition of the laminated mud reflects a higher productivity condition, representing the warm interglacial periods. However, it contradicts the interpretation by the glaciomarine depositional processes as described in the previous section.

In general, the paleoproductivity increased from the glacial periods to the deglacial-to-interglacial periods in the Antarctic continental margin including the Ross Sea (Frank et al. 1995; Ceccaroniet al. 1998; Frignani et al. 1998; Cunninghamet al. 1999; McKay et al. 2008; Tolottiet al. 2013; Wu et al. 2017; Kim et al. 2020; Hartman et al. 2021; Li et al. 2022; Lu et al. 2022). Such increase can be attributed to the reduction of sea ice coverage, which promoted the light availability for photosynthesis, and to more nutrient supply by the current system such as the Antarctic Slope Current. In the Ross Sea continental margin, similar to other Antarctic continental margins, interglacial sediments are characterized by high biogenic components, compared to glacial sediments (Cunninghamet al. 1999; Tolottiet al. 2013; Kim et al. 2020; Hartman et al. 2021; Li et al. 2022). Hence, considering the depositional evolution by the temporal succession of sediment lithology in LC42, the high content of biogenic components in the laminated mud layers is unusual.

(3) False paleoproductivity signal by recycled biogenic components in LC42

The laminated terrigenous muds, which are lack of biogenic components, have been reported in the continental slope and rise of the Antarctic continental margins and are thought to be the products of contour currents during the glacial periods (e.g., Venuti et al. 2011). On the other hand, the laminated biosiliceous muds show circum-Antarctic distribution in the inner shelf basins and troughs of the Antarctic continental shelves (e.g., Leventer et al. 2006; Tesi et al., 2020). In particular, varved couplets, representing seasonality, of diatomaceous lamina reflect extremely high primary productivity in the calving bays of the Antarctic ice sheet during the deglaciation (Stickley et al. 2005). However, the laminated mud layers in LC42 are not typical of both types of laminated muds in the Antarctic continental margin.

BSEI verifies that the light and dark laminae are millimeter- to submillimeter-thick and composed mainly of silty and clayey particles, respectively (Fig. 5a, 5e, and 5i). In this laminated mud layer, due to the low resolution sampling interval, the fluctuation of biogenic components (TOC and biogenic opal) depends on the sampling horizons of light or dark laminae (Fig. 3

and 5). The coarse-grained light lamina consists of very fine sand- to silt-sized angular to subangular quartz and feldspar grains, and contains considerable amounts of sand- to silt-sized biogenic fragments and sand-sized lumps of coagulated very small diatom fragments and clay particles (Fig. 5b, 5f, 5j, and 5k). In contrast, the fine-grained dark lamina consists of sparsely scattered silt-sized particles of terrigenous or biogenic origin in a diatomaceous clayey matrix (Fig. 5a and 5l). Nonetheless, high biogenic components of these laminae in the laminated mud are attributed to the tiny fragments of diatom and clay-sized powder with eroded diatom-rich lumps or chips (Fig. 5b, 5c, 5f, 5g, and 5j). Although some diatom archives are preserved (Fig. 5h), it is clearly discernible that most diatoms are tiny fragments, clay-sized powders, and semi-consolidated pieces, which were principally recycled (Fig. 5c, 5f, 5g, and 5j). In addition, Bollen et al. (2022) reported that diatom species in the laminated mud layers are mostly old (Pliocene to Miocene) and reworked. Thus, high TOC, TN, and biogenic opal contents of the laminated mud layers in LC42 were not related to the enhanced biological productivityin the surface water of the Central Basin at the time of mud deposition.

During the Last Glacial Maximum, the ice sheet did not advance to the shelf edge in the central and western Ross Sea (e.g., Lee et al. 2017). The glacial activity near the grounding line of ice sheet have influenced the depositional condition in the Central Basin of the northwestern Ross Sea. The gravity flow or mass flow including slope failure and turbidity currents occurred frequently at the front of grounding line (e.g., Anderson et al. 1984; Domack and Powell 2018). The preservation of laminated mud layers in the Central Basin seem spatially limited, because the same kind of sediment facies has not been reported yet. The laminated muds were deposited due to the continuous supply of a milky plume generated by meltwater underneath the advancing glacier. This milky plume contained the eroded lumps of semi-consolidated diatom-rich fossiliferous sediments. Following the glacial pumping, the lamination may have been formed by the density-based segregation of grain size and selective settling during the continuous flow. Khim et al. (2024) observed pinch-and-swelling and low-angle inclined lamination from the light laminae with possible internal truncation surfaces and particle imbrication, which suggests that the mud deposition might have occurred by dilute density currents (Mulder et al. 2003; Tripsanas and Piper 2008). These density currents could have been fed by subglacial meltwater discharges or buoyant suspensions associated with mass wasting processes, such as slide/slump or slope failure and debris flows including turbidity currents, near the grounding lines (Bollen et al. 2022). In addition, framboidal pyrites observed in the laminated muds evidenced that the dissolved oxygen concentration was low during the deposition or postdeposition (Fig 5d). In the similar way, the deglacial and glacial sediments in the continental slope and rise of the Ross Sea are characterized by higher levels of biogenic components than the Holocene sediments (Khim et al. 2021; Ha et al. 2022), which were interpreted to be due to the glacial supply of reworked diatom-rich shelf sediments (Fig. 4d). Our finding thus confirms that the degree of paleoproductivity should be judged cautiously by considering the recycling of biogenic particles to avoid a wrong or overly simplistic interpretation based on the current climate-productivity model in the Antarctic continental margin.

4. Conclusions

Glaciomarine sediments around the Antarctic continental margin provided important paleoceanographic and paleoclimatic information in association of ice sheet dynamics. The climate-productivity model in the Antarctic continental margin defines the coupling of climate change and biological productivity, i.e., high productivity during the warm interglacial and *vice versa*. In the Ross Sea continental margin, the glacial productivity was reduced due to thewider expansion of seasonal or permanent sea ice coverageand limited nutrient availability. Core LC42 from the Central Basin contains a series of laminated mud layer that were characterized by high biogenic components, compared to the IRD-poor bioturbated sandy mud and IRD-rich massive mud layers, although the laminated mud deposition might have occurred during the glacial periods. Such unexpected contrast was solved by BSEI observation that mostbiogenic components of the laminated muds were recycled from older deposits, containing old and reworked diatom fragments, eroded sand-sized lumps of fossil-bearing mud, and diatomaceousclayey particles. *In situ* paleoproductivity information seems difficult to obtain in terms of conventional biogenic proxies in the case of the laminated mud deposition in the Central Basin. Finally, reworking of older biogenic components in the Antarctic depositional system should have been considered, avoiding the misinterpretation of the paleoclimate and paleoenvironment.

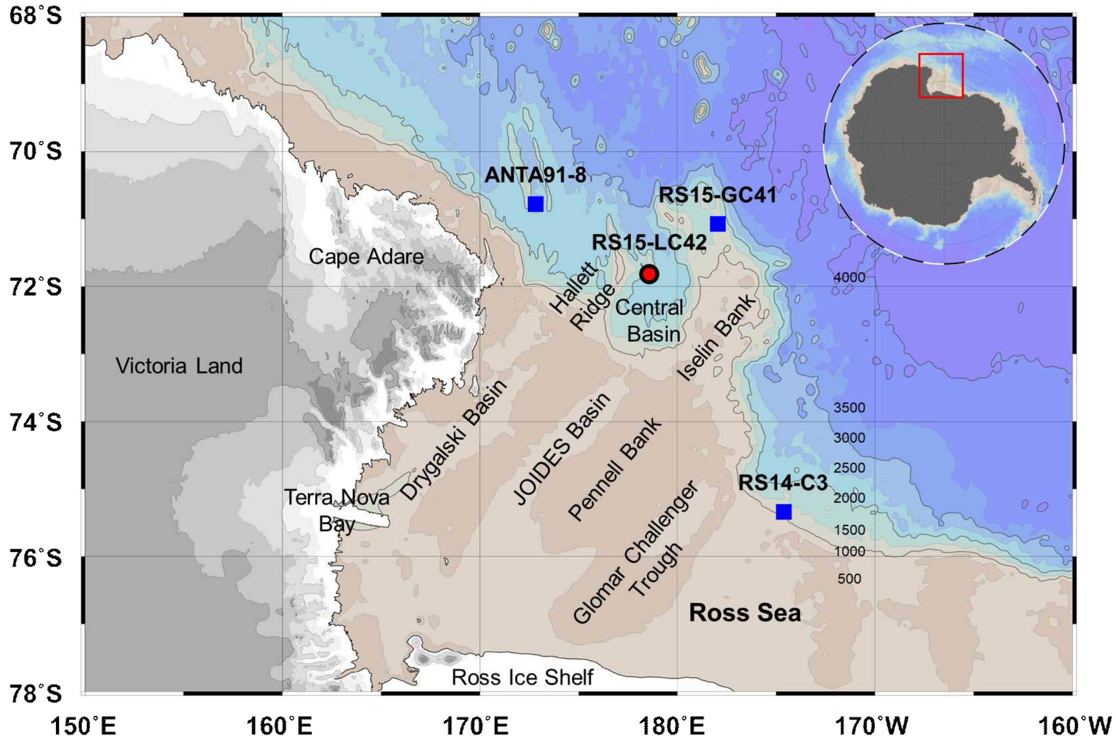

Fig. 1. Bathymetric map showing the geomorphologies in the Ross Seawith the location of core RS15-LC42 (this study) and other studied cores ANTA91-8 (Ceccaroni et al. 1998), RS15-GC41 (Kim et al. 2020), and RS14-C3 (Ha et al. 2022).

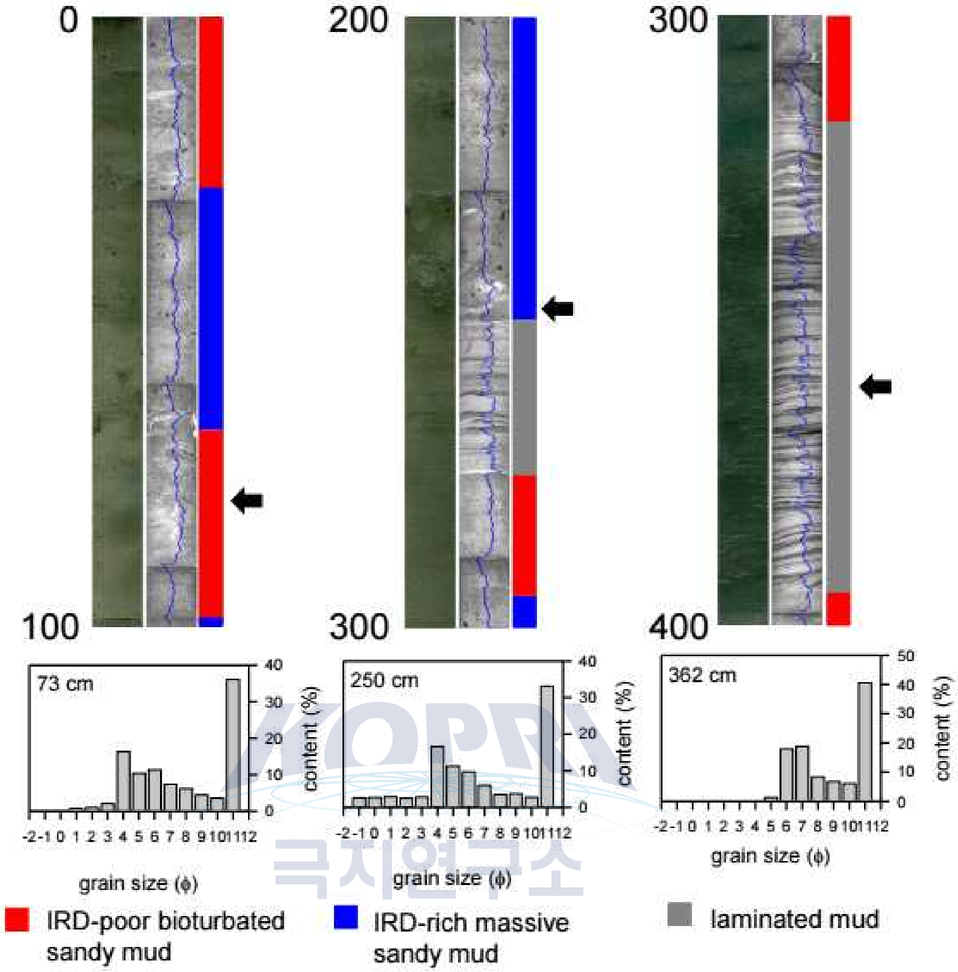

Fig. 2. Selected core photos and X-ray photographs of core LC42, consisting of three major lithologic facies (IRD-poor bioturbated sandy mud, IRD-rich massive mud, laminated mud). Three sediment facies were distinguished by the grain size distribution of horizon marked by the black arrow. Blue line on the X-ray photograph shows the gray scale to delineate the laminations.

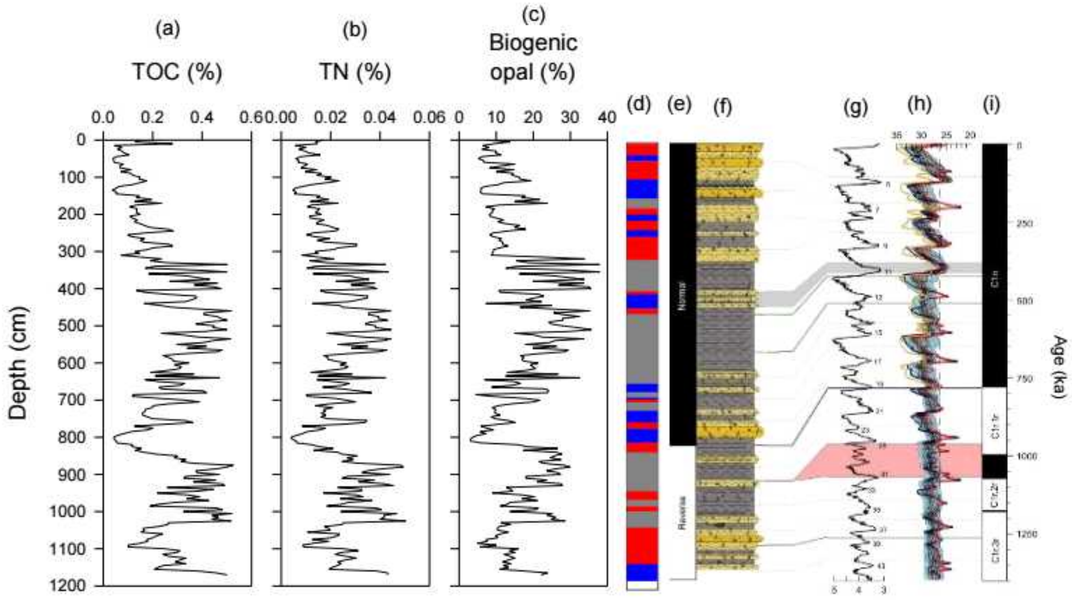

Fig. 3. (a)-(c) downcore variation of TOC, TN, and biogenic opal content, (d) schematic summary of sediment facies, (e) geomagnetic polarity (after Bollen et al. 2022), (f) sediment lithology (after Ohneiser et al. 2019), (g) the global benthic foraminifera $\delta^{18}O$ stack (Lisiecki and Raymo 2005), (h) modelled Antarcticice volume (Sutteretal. 2019), and (i) the global polarity time scale (Ogg 2020). The grey shaded area aligns the gravel peak from 4.0 to 4.5 mbsf to MIS 11 for reference and the red shaded area shows the missing time period over the interpreted hiatus at ~9.34 mbsf (Bollen et al. 2022).

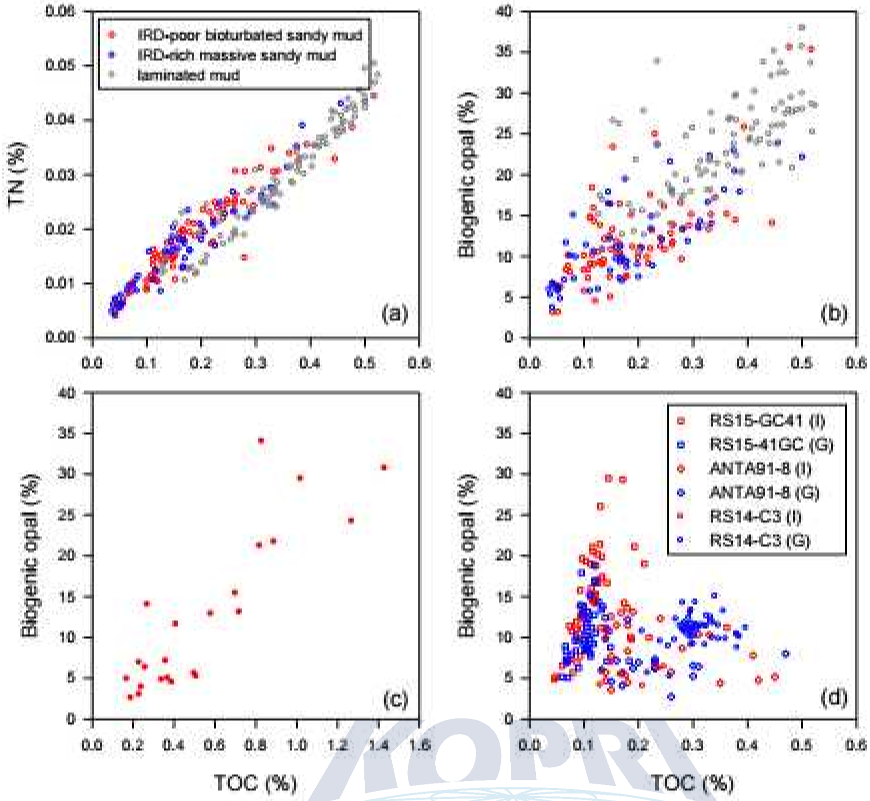

Fig. 4. (a) correlation between TOC and TN contents of each lithology in LC42. (b) correlation between TOC and biogenic opal contents of each lithology in LC42. (c) correlation between TOC and biogenic opal contents of surface sediments (Langone et al. 1998). (d) correlation between TOC and biogenic opal contents of cores RS15-GC41 (Kim et al. 2020), ANTA91-8 (Ceccaroniet al. 1998), and RS14-C3 (Ha et al. 2022) between the interglacial and glacial periods.

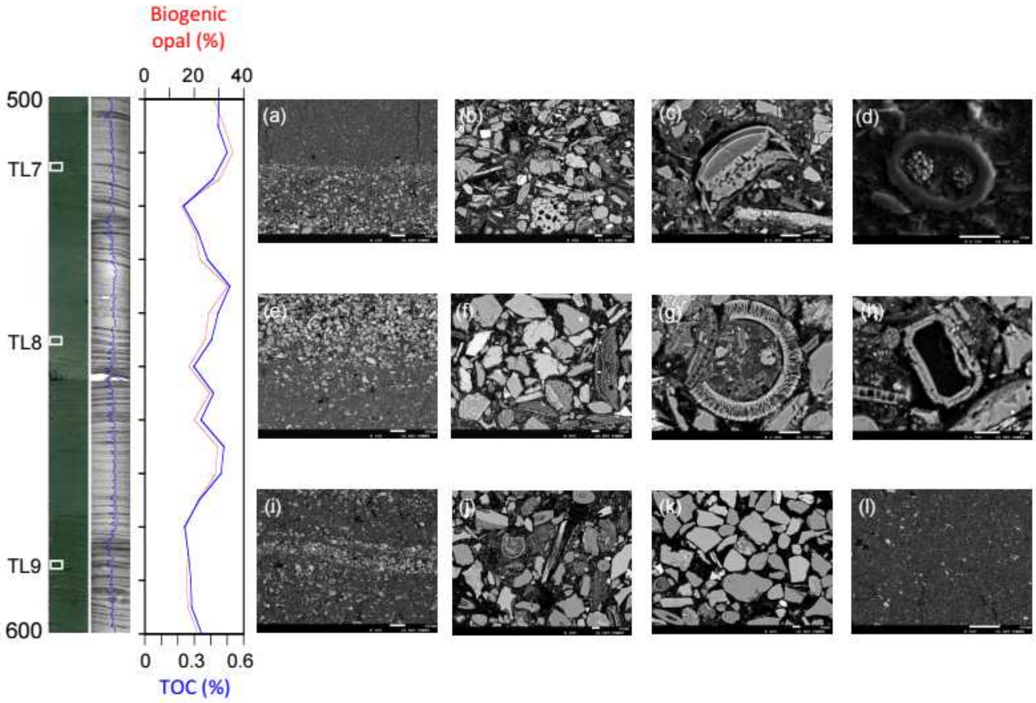

Fig. 5. Core photo, X-ray photograph, and downcore variation of biogenic opal and TOC contents between 500 and 600 cm of LC42, representing the laminated mud layer, with three positions of polished sections (TL7, TL8, and TL9). Blue line on the X-ray photograph shows the gray scale to delineate the laminations. BSEI of polished sections (a to d from TL7, e to h from TL8, and i to l from TL9): (a) alternations of light and dark laminae with sharp boundary, scale bar: 100 μm (×100), (b) coarse-grained componentry of fragmented diatoms, scale bar: 10 μm (×500), (c) fragmented diatom, scale bar: 10 μm (×1300), (d) framboidal pyrite, scale bar: 100 μm (×2700), (e) alternations of light and dark laminae with gradual boundary,scale bar: 100 μm (×100), (f) coarse-grained componentry of semi-consolidated eroded lump contained diatom fragments, scale bar: 10 μm (×500), (g) semi-consolidated diatom fragments infilled in the biogenic fossil, scale bar: 10 μm (×1400), (h) archive diatom, scale bar: 10 μm (×1700), (i) alternations of submillimeter-thick, light and dark laminae,scale bar: 100 μm (×100), (j) coarse-grained componentry of semi-consolidated eroded lump contained diatom fragments, scale bar: 10 μm (×500), (k) angular to subangular silt-sized grains, scale bar: 10 μm (×500), (l) diatomaceous clayey matrix with very fine silt particles, scale bar: 100 μm (×200). More BSEI of polished sections of LC42refers to Khim et al. (2024).

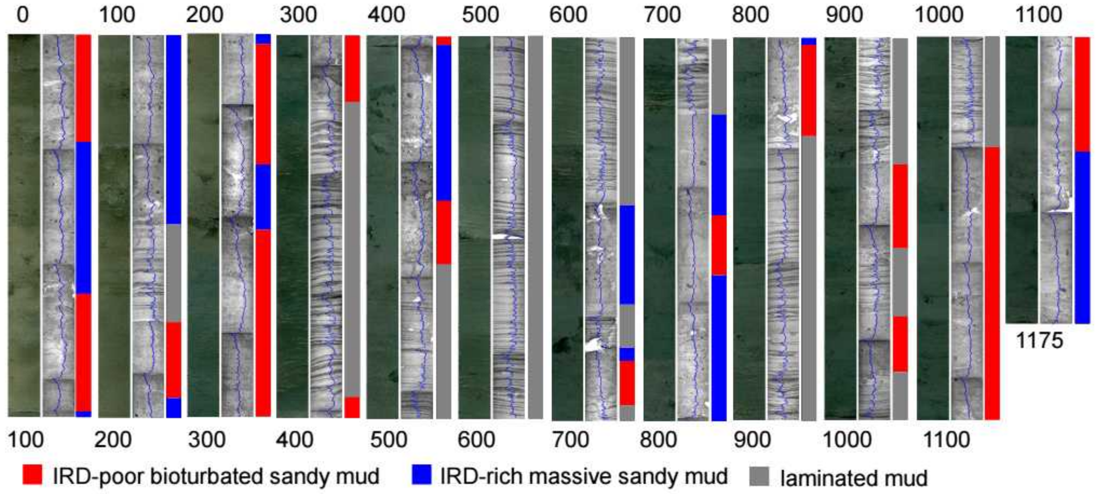

Supplementary figure S1. Core photos and X-ray photographs of core LC42, consisting of three major lithologic facies (IRD-poor bioturbated sandy mud, IRD-rich massive mud, laminated mud). Blue line on the X-ray photograph shows the gray scale to delineate the laminations. (modified from Khim et al., 2023)

2 절. Paleoenvironmental reconstruction of glaciomarine sediments in the Drygalski Basin of the western Ross Sea since the Last Glacial Maximum

1. Introduction

In the Ross Sea, the bathymetry and topography such as the north-northwest oriented deep and narrow basins (e.g., Glomar-Challenger Basin, Joides Basin, and Drygalski Basin) and shallow banks (e.g., Ross Bank, Pennell Bank, and Crary Bank) have been generated by the advanced ice sheet during the glacial periods (Fig. 1). The Drygalski Basin is located in the western Ross Sea and includes the deepest area on the Ross Sea continental shelf.Numerous outlet glaciers along the coastline of the western Ross Sea originated from the ice domes (Dome C (Charlie), Taylor dome, and Talos dome) on the Victoria Land (Giovinetto and Bentley, 1985; Frezzotti et al., 2000). After the LGM, the outlet glaciers on Northern Victoria Land retreated as the global sea level rose, whereas those on Southern Victoria Land retreated after Meltwater Pulse 1A (~14 ka) (Goehring et al., 2019; Christ and Bierman, 2020). The David Glacier, which is largest, forms the Drygalski Ice Tongue (DIT) that protrudes into Terra Nova Bay (Fig. 1). The deposition of biogenic particles in the Drygalski Basin is locally high, because Terra Nova Bay is the major polynya formed by the persistent katabatic wind from the Nansen Ice Shelf and characterized by the high spring diatom blooms leading to the increased primary productivity in the surface water (Arrigo et al., 2000, 2003). The study on the paleoenvironmental reconstruction of the Drygalski Basin could provide the retreating history of ice sheet and ice shelf related to the global sea level change and climate warming since the Last Glacial Maximum (LGM).

During the LGM, the ice sheet advanced to reach the continental shelf edge at the eastern side of the Ross Sea, but did not reach the shelf edge at the western side (Anderson et al., 2014; Halberstadt et al., 2016; Bart et al., 2018; Prothro et al., 2020). The retreat history of the grounded ice sheet after the LGM was reported by several studies using the sediment cores and seismic surveys in many areas of the Ross Sea (e.g. Conway et al., 1999; Domack et al., 1999; McKay et al., 2008; Prothro et al., 2020). Although the precise timing of the ice sheet retreat could not be determined due to the uncertainty of age dating, the ice sheet retreated from ~16 ka to ~8 ka in the northern Drygalski Basin (McKay et al., 2008; Prothro et al., 2020), and continued retreating toward the present-day position after ~8 ka (Conway et al., 1999; McKay et al., 2008; Lowry et al., 2019). The ice shelf in the Ross Sea also moved to the outer continental shelf and shelf edge with the ice sheet expansion during the LGM. Previous studies summarized glaciomarine sedimentation related to the retreating ice shelf during the deglacial period (e.g. McGlannan et al., 2017; Prothro et al., 2018; Smith et al., 2019). Although the retreat timing of the ice shelf in the northern Drygalski Basin is still unclear, the retreat of the ice shelf was later than that of the ice sheet (Prothro et al., 2020).

The types of sediment facies in the Antarctic continental shelf depend mainly on the distance from the grounding line, the position of the calving line, and the open marine condition. These are closely related to the variation of the ice sheet and ice shelf between the glacial and interglacial periods (Domack et al., 1999; McKay et al., 2008; Tolotti et al., 2013; Prothro et al., 2018; Smith et al., 2019). In addition, the hydrographic conditions such as sea ice, meltwater, water masses, and currents affect sediment deposition on the Antarctic continental shelf (Grobe and Mackensen, 1992; Gilbert et al., 1998; Anderson, 1999; Ehrmann et al., 2011). Smith et al. (2019) differentiated the depositional sequences in relation to changes in the ice sheet in the Antarctic continental shelf; the stiff diamicton beneath the ice sheet and the diatom-bearing mud or diatomaceous mud under the seasonal open marine conditions. In particular, under ice shelf conditions, the sediment grain size decreased as an increased distance from the grounding line. Far from the grounding line and near the calving line of the ice shelf, the coarse-grained particles as ice-rafted debris (IRD) and the biogenic particles increase to deposit under the seasonal open marine conditions. In the Drygalski Basin, change in the sediment facies from diamicton during the glacial period to open marine sediment deposit during the interglacial period was also reported (Brambati et al., 1997; Frignani et al., 1998; Domack et al., 1999; Licht et al., 1999; Prothro et al., 2018).

Hillenbrand et al. (2009) reported that the source of sediments changed by the shift of the ice flow direction in the Bellingshausen Sea. In the Bellingshausen Sea, the main provenance of the sediments supplied by the advanced ice sheet was the English Coast located at the southeastern side of the continental shelf during the LGM. On the other hand, the main provenance was shifted to the Beethoven Peninsula, located at the eastern side of the continental shelf, with the ice sheet retreat during the Holocene. Later, McGlannan et al. (2017) established the glaciomarine sedimentation variation related to the retreating ice sheet and ice shelf based on the sediment properties and geochemical proxies on the Wales Deep Basin located at the eastern continental shelf of the Ross Sea since the LGM. In this basin, the transported sediments by the ice sheet and meltwater decreased and biogenic materials from the open mains increased, following the retreating ice sheet.

In the Drygalski Basin, based on the grounding zone wedge and moraines on the seafloor, the ice flow directions were southward and westward during the deglacial period (Greenwood et al., 2018; Prothro et al., 2020; Rhee et al., 2020). These previous studies suggest glaciomarine sedimentation in the Drygalski Basin could be affected by the sediment transport of the ice flow since the LGM. For example, based on the ^{10}Be contents of sediments, Yokoyama et al. (2016) reported that the local ice shelf was pinned on the shallow bank or inner shelf in the western Ross Sea, which affected the glaciomarine sedimentation after the retreat of the grounded ice sheet. Nevertheless, the study on the ice flow using gravity cores has not been conducted at the northern part of the DIT in the Drygalski Basin.

This study aims at reconstructing the paleoenvironments of glaciomarine sediment deposition since the LGM and determining the effect of the ice flow direction from the local glacier at the north of the DIT using sediment properties, geochemical proxies, clay mineral compositions of fine-grained sediments, and diatom assemblage along with the accelerator mass spectrometry (AMS) ^{14}C age dating of the gravity (and box) cores.

2. Regional setting

Many paleoenvironmental and sedimentological studies on the advance and retreat of the ice sheet have been conducted in the continental shelves of the Ross Sea (Anderson et al., 1984; Domack et al., 1999; Salvi et al., 2006; Mosola and Anderson, 2006; McKay et al., 2008; McGlannan et al., 2017; Majewski et al., 2020). The advanced ice sheet during the glacial periods formed mega-scale glacial lineationsand large-scale erosion on the seafloor of the continental shelf (e.g., Shipp et al., 1999). Above mega-scale glacial lineations, the remolding and deformation of the redeposited sediments formed subglacial diamictons during the last glacial period from 26.5 to 19.5 ka (Anderson et al., 1992; Domack et al., 1999; Bart et al., 2000). The retreat of the grounding line and calving line since ~11 ka formed diverse sediment facies such as stratified diamicton by debris flow or turbidity currents at the front of the grounding line, laminated or massive mud by the meltwater plume from the grounding line, and massive mud with abundant IRDs under the calving line (Domack et al., 1999; McKay et al., 2008; Smith et al., 2019; Prothro et al, 2020). Following the retreat of the calving line, the seasonal open marine condition began to control the diatom bloom, resulting in the deposition of mainly diatom-bearing or diatomaceous mud on the continental shelf in the Ross Sea (Melis and Salvi, 2009; Smith et al., 2012; McGlannan et al., 2017).

Diamicton deposition during the LGM indicated that the Drygalcki Basin was covered with an advanced ice sheet (Brambati et al., 1997; Domack et al., 1999; Melis and Salvi, 2009; Prothro et al., 2020). After the LGM, the advanced ice sheet retreated rapidly along with the ice shelf (McKay et al., 2008; Prothro et al., 2020). In general, a complete sequence of sediment deposits indicating ice sheet or ice shelf retreat is rarely observed due to the relatively short duration of the sediment deposition (Smith et al., 2019). In the northern Drygalski Basin, Domack et al. (1999) reported the complete sequence of the sediment facies since the LGM from even only one sediment core that differentiates diamicton, fining-upward sediments related to the retreat of the grounding line, null zone, calving line deposit, and siliceous sediments under the seasonal open marine condition. In contrast, other core sediments from the central part of the Drygalski Basin generally preserve the diamicton, short glaciomarine sediments, and Holocene biogenic sediments (e.g. Brambati et al., 1997; Frignani et al., 1998; Licht et al., 1999; McKay et al., 2008). Based on the depositional sediment sequence, Prothro et al. (2020) reported that a seasonal open marine environment began to develop at ~8 ka in the Drygalski Basin.

The geochemical properties (TOC, TN, biogenic opal, $CaCO_3$, and C/N ratio) and $\delta^{13}C_{SOM}$ values represent the degree of biological productivity in the surface water of the continental shelf in the Ross Sea (e.g. Dunbar et al., 1998; Frignani et al., 1998; Villinski et al., 2000; Salvi et al., 2004; Salvi et al., 2006; McGlannan et al., 2017).These geochemical properties exhibit distinct difference between the glacial condition due to the wide coverage of ice sheet on the continental shelf and the interglacial condition characterized by the retreat of the ice sheet and more influence of the seasonal open marine condition in the Ross Sea (Domack et al., 1999; Salvi et al., 2006; McKay et al., 2008; McGlannan et al., 2017). The $\delta^{13}C_{SOM}$ values are controlled by various factors such as primary production in surface water, temperature and CO_2 concentration of seawater, terrestrial organic carbon, and heterotrophy etc (Rau et al., 1982; Villinski et al., 2000; Crosta et al.,2005;Henleyetal.,2012;Bergetal.,2013;Tesietal.,2020),amongwhichδ $^{13}C_{SOM}$values of the Ross Sea continental sediments are mainly determined by the biogenic fractionation and productivity within the water column (Villinski et al., 2000; Tesi et al., 2020).

The provenance of clay minerals in the Ross Sea embayment has been still poorly investigated mainly owing to the thick ice sheet on the bedrock of the continent. Nevertheless, previous studies reported the possible provenance of clay minerals in the Ross Sea (e.g. Kyle, 1990; Ehrmann et al., 2005; Ehrmann, 1998; Smellie and Hole, 1998; Giorgetti et al., 2009; Frank and Ehrmann, 2010).Illite is thought to originate from the erosion of the Beacon Super Group or crystalline rock of the Transantarctic Mountains under the ice sheet, whereas smectite is supplied from the McMurdo Volcanic Group (Erebus, Melbourne, and Hallett volcanic province). The source of chlorite was estimated as the bedrock or sedimentary rock of the Transantarctic Mountains. Despite unidentified, the source of kaolinite was estimated as paleosoils or sedimentary rock containing kaolinite around the Ross Sea. For example, Salvi et al. (2006) reported that the clay mineral compositions changed as the ice sheet retreated or advanced since the LGM on the JOIDES Basin of the Ross Sea. During the deglaciation, the retreating ice sheet supplied a large amount of smectite that originated from the McMurdo Volcanic Group at the Victoria Land coast. Nevertheless, the sediments at the front of the grounding zone and the Holocene sediments contain high levels of illite and chlorite, which might have been transported from the rocks in the East Antarctic interior.

The diatom assemblage of the continental shelf sediments in the Ross Sea was used to interpret the environmental condition of the surface water, such as sea ice extent or open marine conditions, despite the caution on reworking species (Cunningham and Leventer, 1998; Crosta et al., 2004, 2005; Armand et al., 2005; Tolotti et al., 2013; Tesi et al., 2020). *Chaetoceros* resting spores are linked to the seasonal stratified meltwater from sea ice melting in spring. *Thalassiosira antarctica* (cold type), *E. antarctica*var. *recta*, *F. curta*, and *F. obliquecostata* indicate seasonal sea ice condition. In the Ross Sea continental shelf, Tolotti et al. (2013) reported that the diatom assemblage was changed by the depositional condition since the LGM. They emphasized that the diatom abundance increased with the formation of seasonal open marine condition. On the other hand, *P. sulcata* has been used as an indicator of the reworking deposition. For example, McGlannan et al. (2017) reported that the dominant diatom assemblage was shifted from the reworked species to the modern species at an increasing distance from the grounding line related to the retreating ice sheet.

3. Materials and Methods

Gravity cores (GC01, GC02, and GC04) were collected each at three sites (DG12-01, DG12-02, and DG12-04) along the central floor of the Drygalski Basin and another gravity core (GC05) was collected at site DG12-05 on the southwestern flank of the Crary Bank (Fig. 1). At each site, box cores (BC01, BC02, BC04, and BC05) were also collected (Table 1). These cores were split, visually described, and X-ray photographed at the Korea Polar Research Institute (KOPRI).

The magnetic susceptibility (MS), water content (WC), grain size, total carbon (TC), total nitrogen (TN), total organic carbon (TOC), and $CaCO_3$ were measured at KOPRI. The MS was measured at 1 cm interval using Bartington MS-2B susceptibilitymeter. The WC was also measured at 1 cm interval using 1 cm thick subsamples by calculating the following equation with an assumption of 35 psu for the salinity of seawater.

The grain size was measured at 4 cm intervals. After removing organic matter using 10% H_2O_2 and biogenic silica using 2N NaOH, the coarse fraction (>63μm) was analyzed using 1 phi interval sieves. In contrast, the fine fraction (<63 μm) was analyzed using Micrometrics Sedigraph III 5120. The grain size classification followed the scheme of Folk and Ward (1957). The TC and TN contents were analyzed using an elemental analyzer (FLASH 2000 NC Analyzer) with an analytical precision of less than 0.1%. Total Inorganic Carbon (TIC) was measured using UIC CO_2 coulometer (Model CM5240). $CaCO_3$ concentration was calculated by multiplying TIC content by 8.333 (i.e., the ratio of $CaCO_3$ and carbon). TOC content was calculated as the difference between TC and TIC contents.

Biogenic silica concentration was measured at 8 cm intervals (GC01, GC04, and GC05) and 4 cm intervals (GC02) using the wet alkaline sequential extraction method using 1N NaOH solution at 85°C modified from DeMaster (1981) at Pusan National University. Biogenic opal content was calculated by multiplying biogenic silica concentrations by 2.4 (i.e., the ratio of biogenic opal and Si) (Mortlock and Froelich, 1989). The analytical precision for the biogenic opal measurement was ±1%.

The carbon isotope composition ($\delta^{13}C_{SOM}$) of the sediment organic matter was measured for selected sediment samples at 10 cm intervals from GC01 and at 8 or 16 cm intervals from GC02, 04, and 05 using element alanalysis-isotope ratio mass spectrometry (EA-IRMS: EuropaScientific20-20 isotope ratio mass spectrometer) at Iso-Analytical Ltd. (UK). The $\delta^{13}C_{SOM}$ values were expressed in conventional delta notation, which is the permil deviation from the V-PDB standard. The analytical precision for $\delta^{13}C_{SOM}$ was approximately ±0.08‰.

The samples for clay mineral compositions were collected from GC01 and GC04 at 10 or 20 cm intervals. The organic matter was removed using 10% H_2O_2, and the fine fraction (<63μm) was separated using a sieve. The fraction under 2 μm was extracted using Stokes' law, smeared on the slide, and air-dried following Stokke and Carson (1973). An air-dried slide was treated with ethylene-glycol for 24 h. X-ray diffraction (XRD) was performed using a Siemens/Brucker D5005 at Gyeongsang National University with Cu-Kαradiation (40 kV, 35mA). The clay mineral composition was identified based on the basal reflections recorded in the XRD patterns, following the methods of Brown and Brindley (1980) and Moore and Reynolds (1989). The four major clay minerals (illite, smectite, chlorite, and kaolinite) were estimated by semi-quantitative calculation using the method of Biscaye (1965). The analytical precision for the clay mineral composition was approximately ±5%.

The samples for diatom assemblage were selected at nine horizons from GC01 and GC04, respectively. The sediment treatment, slide preparation, and diatom counting were carried out at Jeonbuk National University. The quantitative analysis of the diatom slides was performed according to the procedure described in Scherer (1994).

AMS ^{14}C dating was conducted at the core-top (0–1 cm) of BC01 and BC04, two horizons of GC01, and three horizons of GC04 (Table 2). The ^{14}C activity was measured using the acid-insoluble organic matter (AIOM) of the bulk sediments at Beta Analytic (USA) due to the scarcity of foraminifera in the core sediments. The AMS ^{14}C ages obtained by AIOM of bulk sediments are generally biased by old carbon in the Antarctic seawater, reworking of sediments, and glacial erosion of old sediments (e.g., Andrews et al., 1999; Pudsey et al., 2006; Mezgec et al., 2017; Tesi et al., 2020; Ha et al., 2022). As a result, these ages incorporate the regional marine reservoir effect (MRE) as well as the local contamination offset (LCO) by dead carbon. The LCO should be corrected before calibrating AMS ^{14}C ages, assuming that the MRE and LCO are not different between the glacial periods and the Holocene (Hall et al., 2010; Hillenbrand et al., 2010). The MRE near Terra Nova Bay was estimated to be about 1.2 ka by Hall et al. (2010). The AMS ^{14}C ages of AIOM were dated 3.7 ka and 4.1 ka at the core-top of BC01 and BC04, respectively (Table 2). Similar old ages of the surface sediments are normally found on the Antarctic continental shelf (e.g. Licht et al., 1996; Andrews et al., 1999; Hall et al., 2010; Anderson et al., 2014). Consequently, the LCO at BC01 (2510 years) and BC04 (2890 years) was judged by subtracting the MRE (1.2 ka) from the core-top AMS ^{14}C age. This LCO was then applied to GC01 and GC04 for the reliable age correction. The LCO-corrected ages were subsequently converted to the calibrated AMS ^{14}C age using Calib 8.2 with calibration curve MARINE 20 (Heaton et al., 2020; Stuiver et al., 2021).

4. Results

Based on the core description, X-ray photographs, and grain size results, seven sediment facies are defined (Fig. 2 and 3): (a) clast-rich muddy diamicton, (b) clast-rich sandy diamicton, (c) massive mud, (d) laminated mud, (e) bioturbated mud, (f) massive sandy mud, and (g) bioturbated sandy mud. The clast-rich sandy or muddy diamicton contained large amounts (average ~75% and ~35%, respectively) of coarse grains in a fine sand or mud matrix and the mean grain sizes are 5.3ø and 6.6ø, respectively. They were observed at the lower part of GC01, GC04, and GC05 (Fig. 3). The massive mud is structureless fine-grained sediment (>90% of silt and clay) with a mean grain size of 10.3ø, whereas the laminated mud shows thin laminations with a similar mean grain size of 10.4ø (Fig. 2). These two sediment facies are intercalated in the middle part (~2 m thick) of GC04 with a thin (~2 cm) sandy mud at 147 cm (Fig. 3). The bioturbated mud is the fine-grained sediment (>8.7ø of mean grain size) showing a mixture by biogenic activity and containing scattered ice-rafted debris (IRD) (Fig. 2). This material was observed mostly at the upper part of the core (GC01, GC02, and GC05) (Fig. 3). However, the bioturbated sandy mud (7.8ø of mean grain size) with IRD was observed at the upper part of GC04 (Fig. 3). The massive sandy mud (30–40% sand fraction) characterized by a mean grain size of ~7ø is lack of primary sedimentary structure (Fig. 2). The intercalation of massive sandy mud and bioturbated sandy mud was also observed at GC02 and GC04 (Fig. 3). Finally, based on the association of sediment facies, four lithologic units (Unit 1 to 4 from core-bottom to core-top) were determined (Fig. 3).

(1) Lithologic unit 1

Lithologic unit 1 consisted of clast-rich sandy diamicton (GC01 and GC04) or clast-rich muddy diamicton (GC05), characterized by generally high MS (up to 200 at GC01 and GC04, ~130 at GC05) and low WC (~25%) (Fig. 4). The geochemical and isotope properties of this unit are characterized by very low TN (mostly below detection limit), TOC (~0.25%), and biogenic opal (<7%), $CaCO_3$(<0.8%exceptforGC01),andhighC/Nratio(>15)(Fig.5).The $\delta^{13}C_{SOM}$ values of Unit 1 are mostly constant ranging between ~-24‰ and ~-26‰ (Fig. 5). The clay mineral compositions of Unit 1 are characterized by relatively high smectite (10-23%) and chlorite (14-22%) and low illite (48-67%) content (Fig. 6). The preservation of the diatom in this unit is very poor and only *Paralia sulcata* appeared at GC04 (Fig. 7). The calibrated AMS ^{14}C ages above the unit boundary date 13.3 ka at GC01 and 22.9 ka at GC04, respectively (Fig. 4).

Unit 1 was observed at the bottom part of GC01, GC04 and GC05. The sediments of Unit 1 were characterized by sorted or unsorted granulometry with a large amount of coarse sand or mud matrix (Fig. 2 and 3). The sediment properties of Unit 1 are characterized by relatively high and low WC (Fig. 4). The advanced ice sheet during the last glacial period eroded the underlying bedrock and sediments, forming massive unconsolidated diamictons on the continental shelf in the Ross Sea (Licht et al., 1999).The diamictons are characterized by commonly high shear strength and MS intensity, poorly sorted granulometry, large amount of coarse fraction, low WC, and absent or little biogenic materials (Domack et al., 1999; Licht et al., 1999; Smith et al., 2019). These geochemical properties are related to the transported old biogenic fragments and lithogenic materials by the advanced ice sheet (Sjunneskog and Scherer, 2005; McGlannan et al., 2017; Smith et al., 2017; Smith et al., 2019).The geochemical proxies of Unit 1 indicate very low biogenic productivity due to the wide coverage of the ice sheet and, particularly, high C/N ratios might be attributed to eroded terrestrial sediments (Anderson et al., 1984; Domack et al., 1999; Salvi et al., 2006; McGlannan et al., 2017; Prothro et al., 2018; Smith et al., 2019).

(2) Lithologic unit 2

Lithologic unit 2 consists of the thick massive mud intercalated with thin laminated mud occurring only at the middle part of GC04 (Fig. 3), which is characterized by low MS (~30) and high WC (~70%) (Fig. 4). The geochemical and isotope properties of Unit 2 are mostly consistent with tiny fluctuations, showing TN (~0.03%), TOC (~0.5%), C/N ratio (~18), $CaCO_3$ (~0.02%), biogenic opal (~2%), and $\delta^{13}C_{SOM}$ (–24.5‰) (Fig. 5). The clay mineral composition of this unit is similar to that of Unit 1 such as relatively high smectite (9–26%) and chlorite (13–18%) and low illite (53–67%) content (Fig. 6). The occurrence of diatom is barren similar to Unit 1, except for the appearance of *Fragilariopsis curta* and *F. kergulensis* at the middle of Unit 2 (Fig. 7).

Unit 2 was observed only at the middle part of GC04, consisting of massive mud intercalated with laminated mud, although a sand layer (2 cm thick) was intervened at 148 cm (Fig. 3). Based on X-ray photograph, the sand layer seems to be deposited accidentally by lateral transport from the topographic high of the inner bay at the western side of the basin rather than the deposition of IRDs. The sediment properties of Unit 2 are characterized by a thick massive mud layer with homogeneous MS and high WC and without pebbles (Fig. 4). Similar sediment properties were reported in the massive or faint laminated mud in the Ross Sea and Amundsen Sea (McGlannan et al., 2017; Simkins et al., 2017; Smith et al., 2019). The old AMS ^{14}C ages in Unit 2 are, without doubt, due to the incorporation of old organic matters. The geochemical proxies of Unit 2 are characterized by a slight increase in TOC, TN, and $\delta^{13}C_{SOM}$ values and a decrease in C/N ratios and biogenic opal and $CaCO_3$ contents (Fig. 5). Domack et al. (1999) reported that the fine-grained sediments deposited by meltwater plume from the grounding line contained more biogenic materials than the diamicton. The increasing biogenic materials are not generated in the surface water under the ice shelf condition, but transported to deposit farther by the currents from the calving line which is located under the seasonally open marine condition (Prothro et al., 2018; Smith et al., 2019). The geochemical proxies of Unit 2 indicate that the fine sediment was transported by the meltwater plume from the grounding line with little amount of biogenic material from the open marine area farther from the DIT.

(3) Lithologic unit 3

Lithologic unit 3 consists of alternating sandy mud and massive mud at the lower part of GC02 and at the upper part of GC04 (Fig. 3), showing the fluctuation of MS (50–200) and WC (20–74%) (Fig. 4). The geochemical and isotope properties (TN: ~0.02%, TOC: ~0.4%, C/N: ~16, $CaCO_3$: ~0.05%, biogenic opal: ~2%, and $\delta^{13}C_{SOM}$: ~–24.6‰) of Unit 3 are similar to those of Unit 2, despite the slight fluctuations (Fig. 5). The clay mineral composition of this unit falls between Units 2 and 4 (Fig. 6). The occurrence of diatom in Unit 3 is also similar to that of Unit 2, with only the appearance of *F. curta* and *F. kergulensis* and mostly absence (Fig. 7).

Unit 3, observed at cores GC02 and GC04, is characterized by the alternation of mud and sandy mud layer with rich pebbles, gravels, and sand fractions (Fig. 4). Despite the uncertainty of the precise timing, while the retreating position of the ice shelf edge is unclear, the grounding line located at the coast of the Victoria Land and DIT until about 4 ka (Prothro et al., 2020). When the ice shelf was broken up, many dropstones from the icebergs were deposited on the seafloor. However, it is difficult to find the sediment layer indicating the deposition at the calving line due to its unstable position and the random supply of dropstones (Smith et al., 2019; Prothro et al., 2020). Nonetheless, the sediment layer deposited at the calving line was reported by previous studies on the Ross Sea, Antarctic Peninsula and Prydz Bay (Domak and Harris, 1998; Domack et al., 1998; Kilfeathe et al., 2011; McGlannan et al., 2017). The geochemical proxies of Unit 3 are similar to those of Unit 2 as relatively low TN, TOC, and biogenic opal content with high C/N ratios and $\delta^{13}C_{SOM}$ values (Fig. 5). Previous studies reported the different geochemical characteristics at the calving line showing the increasing biogenic materials due to the seasonal open marine condition or similar properties to the diamicton proximal at the grounding line such as a large amount of sediments by the meltwater discharge (Domack et al., 1999; McGlannan et al., 2017). The geochemical proxies of Unit 3 indicate that the sediments contained the transported sediments from the inner shelf or Antarctic continent similar to Unit 2.

(4) Lithologic unit 4

Lithologic unit 4 occupies the upper part of all cores as the bioturbated mud (GC01, GC02, and GC05) and bioturbated sandy mud (GC04) containing scattered IRDs (Fig. 3). In general, the MS is low (20–60) and the WC is high (~60%) in this unit, but the MS depends on the IRDs and sand fraction (Fig. 4). The geochemical properties of Unit 4 are characterized by a gradual increasing trend (TN: from 0.02% to 0.15%, TOC: from 0.2% to 1.0%, and biogenic opal: from 2% to 35%) with constantly low C/N ratios (~8) (Fig. 5). $CaCO_3$ content is also mostly low (<0.02%) and all core-tops mark the minimum (Fig. 5). The $\delta^{13}C_{SOM}$ values range between −27.1 and −23.8‰, particularly showing the lowest value (~−27‰) at the middle part of Unit 4 (Fig. 5). The clay mineral composition of this unit is characterized by high illite (64–88%) and low smectite (0–14%) and chlorite (8–15%, except for 21% in GC04) (Fig. 6). Unit 4 preserves a high number (>7 ´10^{-1}/g) of diatom valves consisting of diverse species (Fig. 7). The calibrated AMS ^{14}C ages in Unit 4 are 4.6 ka at middle part of GC01 and 20.6 ka and 7.7 ka at the bottom and middle parts GC04 (Fig. 4).

Unit 4 is observed at the top of all gravity cores and consists of bioturbated mud or sandy mud with dispersed IRDs (Figs. 2 and 3). The AMS ^{14}C ages at the middle of Unit 4 in GC01 confirmed that the sediments were deposited during the Holocene, although the ages at the bottom were relatively old due to the inclusion of old carbon. While the sediments transported from the subglacial ice and Antarctic continent decreased dramatically, the biogenic materials originating from the surface water increased to depositon the continental shelf under the seasonal open marine conditions after the retreat of the ice sheet and ice shelf on the continental shelf (e.g. Smith et al., 2011; Hillenbrand et al., 2014; Larter et al., 2014; Ó Cofaigh et al., 2014; McGlannan et al., 2017). The geochemical proxies of Unit 4 are characterized by the gradual increase in TOC, TN, and biogenic opal contents and a decrease in C/N ratios (Fig. 5). The $CaCO_3$ contents of Unit 4 are mostly very low. Generally, these geochemical proxies indicate that the biogenic productivity in the surface water increased after the onset of the seasonal open marine system in the continental shelf of the Ross Sea (Domack et al., 1999; Mosola and Anderson et al., 2006; Salvi et al., 2006; McGlannan et al., 2017; Prothro et al., 2018). The geochemical proxies of Unit 4 indicate that the biogenic productivity in the surface water increase under the seasonal open marine condition after the retreat of the ice shelf on the northern Drygalski Basin.

5. Discussion

(1) Paleoenvironmental reconstruction of Unit 1 in the Drygalski Basin

Prothro et al. (2018) divided the types of the diamicton in the Ross Sea: subglacial diamicton as till on the topset of the grounding zone wedge, proglacial diamicton on the foreset of the grounding zone wedge, and proglacial diamicton near the grounding zone. The subglacial diamicton which is deposited under the advanced ice sheet is characterized by constantly high MS, low sand content, constant pebble abundance, and low WC (Anderson et al., 1980; Cunningham et al., 1999; Licht et al., 1999; Prothro et al., 2018; Smith et al., 2019). The proglacial diamicton deposited mostly by debris flow is characterized by a sandy silt matrix, constant pebble abundance, constantly high MS, and relatively low WC, whereas proglacial (or pelletized) diamicton near the grounding zone deposited by basal debris melt-out is characterized by the sandy silt matrix, variable MS and pebble abundance, and relatively high WC (Anderson et al., 1980; Cunningham et al., 1999; Licht et al., 1999; McKay et al., 2012; Prothro et al., 2018). The sediment properties (MS, granulometry, and WC) of Unit 1 in GC01 fluctuated, while those in GC04 and GC05 were mostly constant (Fig. 4). The sediment properties of Unit 1 in GC01 corresponds to the diamicton deposited by the basal debris melt-out under the glaciomarine environment at the front of the grounding line during the retreating of the ice sheet. On the other hands, Unit 1 in GC04 and GC05 is the diamicton deposited by the debris flow proximal to the grounding line.

The poor relationship among geochemical proxies in Unit 1 confirms that *in situ*surface water productivity was not their main source (Fig. 8). Almost barren diatoms in Unit 1, except for the upper boundary (Fig. 7), also confirms that the biogenic fragments were recycled. These results are supported by previous studies reporting the absence of diatoms or the presence of reworked species in the glaciomarine diamicton on the Ross Sea continental shelf (Licht et al., 1996; McKay et al., 2008; Tolotti et al., 2013; McKay et al., 2016). The appearance of the reworked and sea ice taxa at the top of Unit 1 may suggest the lift-off of the retreating ice sheet and the intrusion of seawater in the study area.

The $CaCO_3$ content of the diamicton is generally low, except for the supply of old reworked foraminifera fragments (Cunningham et al., 1999; Melis and Salvi, 2009; Kilfeather et al., 2011). Melis and Salvi (2006) found out the reworked foraminifera fragments from the diamicton on the JOIDES Basin, where the diamicton consisted of the old inner shelf sediments eroded by the WAIS. On the other hand, the foraminifera are completely barren in the diamicton formed by the directly in the Drygalski Basin. The slightly high $CaCO_3$ content (~2 %) of Unit 1 in GC05 is due to the reworked foraminifera from the inner shelf. The $\delta^{13}C_{SOM}$ values of Unit 1 are almost constant (about −25 to−26‰) (Fig. 5). Ohkouchi and Eglinton (2006) reported that the $\delta^{13}C_{SOM}$ values of the terrestrial sediments from the Antarctic continent are −24‰ to −32‰. Because of the diamicton components, the $\delta^{13}C_{SOM}$ values are mainly affected by the old organic matters transported by the ice sheet rather than the fresh organic matters generated in the surface water. In addition, the invariant δ

$^{13}C_{SOM}$ values of Unit 1 indicate that the sediment source of diamicton was not changed during deposition.

The smectite content of the shelf sediments in the Ross Sea is locally different up to 80% at the McMurdo Sound (Ehrmann, 1998; Salvi et al., 2006; Franke and Ehrmann, 2010; Jung et al., 2021). The supply of smectite from the McMurdo Volcanic Group changed, depending on the advanced ice sheet and surface currents in the continental shelf (Brambati et al., 1997; Salvi et al., 2006; Ha et al., 2022). On the Pennell Trough, more smectites were supplied from the McMurdo Sound during the LGM (Salvi et al., 2006). The smectite content of Unit 1 is high (10–24%) during the last glacial and deglacial period (Fig. 6). The smectite provenances are known as the Erebus volcanic province (>60%) near the McMurdo Sound and the Melbourne volcanic province (~12%) near Terra Nova Bay (Ehrmann et al., 2005; Jung et al., 2021). The advanced ice sheet from the Erebus volcanic province supplied smectite-rich sediments to the Drygalski Basin whereas the ice sheet from the Melbourne volcanic province transported smectite-poor and illite-rich sediments to the northern part of Drygalski Ice Tongue. Thus, the smectite-rich sediments of Unit 1 were deposited during the retreat of the grounding line of the advanced ice sheet.

(2) Paleoenvironmental reconstruction of Unit 2 in the Drygalski Basin

The grounded ice sheet retreated to the western and southern sides of the Drygalski Basin during the deglacial period (Greenwood et al., 2018; Rhee et al., 2020). Although the ice shelf and grounding line in the Drygalski Basin retreated continuously during about 11–8 ka to the Victoria Land coast, the retreat of the ice shelf is much slower than that of the grounding line (Halberstadt et al., 2016; Prothro et al., 2020; Rhee et al., 2020). The northern basin of the DIT could be located under the ice shelf environment. The fine-grained sediments can be transported by meltwater plume from the grounding line farther by 250 km along the continental shelf under the ice shelf (Domack et al., 1999; Simkins et al., 2017; Smith et al., 2019).In addition, the current from the open marine area transported the open marine diatom and fine sediment to the sub-ice shelf (Domack and Harris, 1998).Domack et al. (1999) already reported that, during the retreat of the ice shelf on the Ross Sea, the structureless silty clay interval was deposited at the northern part of the Drygalski Basin. Based on our results, the massive and laminated mud layer of Unit 2 could be deposited until 8 ka by continuous or temporal supply of the fine-grained particles by the meltwater from the grounding line during the ice sheet retreat (e.g. Simkins et al., 2017; Smith et al., 2019).

The poor relationship among the geochemical proxies also indicates that the biogenic materials are not produced by the surface water productivity, similar to Unit 1 (Fig. 8). The increasing TOC and TN contents were attributed to more transport of fine-grained sediments containing biogenic materials by the currents from the ice-uncovered areas. In contrast, the decreasing C/N ratios are due to the decreasing meltwater plume from the grounding line. Cunningham et al. (1999) reported that the biogenic silica in the massive mud facies of the Drygalski Basin was a mixture of the transport from the grounding line and supply by *in situ*diatom production. Although the diatom valves appeared nearly barren, the sea ice diatom taxa were observed at middle part of Unit 2 (Fig. 7). However, the biogenic opal content of Unit 2 is almost minimum (Fig. 5). It implies that the distance of GC04 from the grounding line and the seasonal open marine area might be too far to transport the reworked and *in situ*produced diatoms.

The $CaCO_3$ content of Unit 2 is lower than that of Unit 1. The $CaCO_3$ content consists mainly of the benthic or planktonic foraminifera in the continental shelf on the Ross Sea (Anderson et al., 1984; Capotondi et al., 2018). The intrusion of Circumpolar Deep Water (CDW) into the continental shelf could dissolve $CaCO_3$ on the surface sediments (Anderson, 1975; Kim et al., 2020). The very low $CaCO_3$ content of Unit 2 resulted from the limited carbonate production due to the subglacial ice shelf environment. Furthermore, $CaCO_3$ might be dissolved by the modified CDW from the outer continental shelf. The constant $\delta^{13}C_{SOM}$ values (about −25‰) of Unit 2 are higher than those of Unit 1 (Fig. 5). While the retreat of the grounding line ceased temporally in the Drygalski Basin, Unit 2 indicates that the sediment is delivered mainly by the meltwater plume under the ice shelf from the grounding line with the sediment transported by the currents from the seasonally open areas.

The clay mineral compositions of Unit 2 are similar to those of Unit 1, characterized by relatively high smectite and low illite (Fig. 6). The relatively high smectite content is interpreted as the transport of eroded sediment from the McMurdo volcanic province located at the south of Drygalski Basin. The clay mineral composition of Unit 2 indicates that the sediments were still supplied by the meltwater plume from the grounding line at the southern side of the Drygalski Basin to the northern side under the subglacial ice shelf system.

(3) Paleoenvironmental reconstruction of Unit 3 in the Drygalski Basin

Following the retreat of the ice shelf, the calving line retreated landward. The MS and WC of Unit 3 fluctuated with the coarse fraction (Fig. 4). McGlannan et al. (2017) reported the ice shelf breakup facies in the outer continental shelf of the Whales Deep Basin in the eastern Ross Sea. This sediment facies is characterized by the massive sandy silt to mud matrix with large IRDs and variable MS and WC. The sediment properties of Unit 3 are similar to those of sediments deposited under the calving line. In addition, the alternation of the sandy mud and mud layer in Unit 3 might form by the temporal meltwater plume under the remaining local ice shelf near Terra Nova Bay. The sorting of transported sediments is controlled by the amount of meltwater discharge and the current velocity under the ice shelf (Kirshner et al., 2012; Simkins et al., 2017). Yokoyama et al. (2016) suggested the possibility of the remaining local ice shelf at the western coast of the Ross Sea, although the ice shelf had already retreated to the southern side of the Drygalski Basin. Hence, the sediments of Unit 3 were deposited by the meltwater plume beneath the local ice shelf from the grounding line with many IRDs at the calving line.

The geochemical proxies characterized by the low biogenic productivity and high C/N ratio might reflect little increase of the biogenic production in the surface water. However, the correlation among the geochemical proxies is relatively stronger than Unit 2 (Fig. 8). The better relationship reflects that more biogenic materials of *in situ* production in the surface water were deposited under the calving line.

Despite a slight increase in $CaCO_3$ content of Unit 3, carbonate productivity by the planktonic or benthic foraminifera did not increase at the calving line due to the very low values (<0.1%) (Fig. 5). The foraminifera community observed at the inner and outer sides of the calving line in the Ross Sea was controlled by the position of the calving line, multi-year sea ice, water mass, or katabatic wind (Pawlowski et al., 2005; Majewski et al., 2018). However, the skeleton of the dead foraminifera on the surface water could be easily dissolved by the corrosive water mass (Majewski and Anderson, 2009; Melis and Salvi. 2009; Majewski et al., 2016). The very low $CaCO_3$ values of Unit 3 seem to be affected by the intrusion of the corrosive water mass, despite the presence of foraminifera community. The $\delta^{13}C_{SOM}$ values of Unit 3 were also similar to those of Unit 2 (Fig. 5). Based on the results of the geochemical proxies of Unit 3, the increased biogenic particles by *in situ* production could change the $\delta^{13}C_{SOM}$ values. However, the sediments of Unit 3 were still affected strongly by the meltwater plume from the grounding line based on the sediment properties. The constant $\delta^{13}C_{SOM}$ values of Unit 3 compared to Unit 2 were affected by the meltwater plume more than the biogenic productivity under the calving line.

The appearance of diatom is not abundant, but diatom assemblage (*Chaetoceros*resting spore, *F. kerguelensis,* and *F. curta*) indicate a seasonal sea ice environment and biogenic productivity in the surface water during the Holocene (Fig. 7). Sjunneskog and Scherer (2005) reported that the diatom assemblage was a mixture of reworked and modern taxa at the calving line sediments in the central Ross Sea. The low diatom abundance and low diatom assemblage are a result of winnowing and transport by the current (Cunningham et al., 1999; Taylor et al., 2001; Sjunneskog and Scherer, 2005). The presence of modern diatom taxa suggests *in situ* biogenic productivity in the surface water, but the low diatom abundance might indicate low productivity in the surface water or poor preservation of the diatom frustule under the calving line.

The clay mineral composition of Unit 3 is characterized by relatively high smectite and low illite contents with an upward decreasing smectite toward Unit 4. Furthermore, kaolinite and chlorite contents are relatively high at several intervals. As explained, the main source of the smectite is restricted in the Ross Sea. The transport by the current, iceberg, wind, and meltwater in the continental shelf controlled the clay mineral compositions (Hillenbrand et al., 2003; Ehrmann et al., 2011). The decreasing smectite content indicate that the supply from the source area is limited by the weakening of erosion and/or transport. Lee et al. (2017) suggested the eastern and east-western ice flow from the southern Victoria Land to the southern part of the DIT during the deglacial period. This ice flow could block sediment transportation from the southern to the northern Drygalski Basin. The source area of kaolinite and chlorite is not clear, but its basement rock was distributed at the Transantarctic Mountains on Victoria Land (Cooper and Davey, 1985). The decreasing smectite and increasing kaolinite and chlorite indicate that the sediment supply declined from the southern Drygalski Basin and increased from the bedrock in the local coastal area.

(4) Paleoenvironmental reconstruction of Unit 4 in the Drygalski Basin

The sediments of Unit 4 are characterized by the lower MS and higher WC due to the less coarse fractions, compared to Unit 1 diamicton (Fig. 4). The low MS intensity of the Holocene sediments is generally attributed to the lowernumber of IRDs transported by the icebergs or sea ice during the warm climate conditions (Hillenbrand et al., 2010; Weber et al., 2014; Shin et al., 2020; Ha et al., 2022). The coarse particles of the Holocene sediments on the continental shelf of the Ross Sea are generally transported by IRDs or gravity flow or otherwise they were the remanent sediments winnowed by the strong bottom current (Anderson et al., 1984; Langone et al., 1998; Salvi et al., 2006; McKay et al., 2008). The northern side of the DIT has experienced seasonal open marine conditions since 8 ka, resulting in increased biogenic productivity in the surface water (Hall et al., 2004; McKay et al., 2008; Yokoyama et al., 2016; Prothro et al., 2020). Based on the results, Unit 4 reflects the seasonal open marine condition after the complete retreat of the ice shelf during the Holocene.

The biogenic materials from the surface water increase during middle to late the Holocene on the Ross Sea (Prothreo et al., 2018; Tesi et al., 2020). The variation of the geochemical proxies of Unit 4 is similar to the result of previous studies reporting that biogenic materials by the surface productivity increased under the seasonal open marine condition and carbonate was dissolved by the corrosive water on the continental shelf. Additionally, the relationship among the geochemical proxies indicates that the biogenic materials in Unit 4 originated from *in situ*production in the surface water (Fig. 8).

The variation of $\delta^{13}C_{SOM}$ values, showing the upward decrease and increase with the lowest value at the middle part, is different from that of TOC and biogenic opal contents, showing continuous increase without a peak in GC01 (Fig. 5). The decrease in $\delta^{13}C_{SOM}$ values is generally affected by the terrestrial organic matter under the sub-ice sheet or ice shelf environment. However, more deposition of terrestrial organic matter is difficult after the complete retreat of the grounding line, and the $\delta^{13}C_{SOM}$ values are strongly influenced by the primary production under the seasonal open marine condition in the Ross Sea (Villinski et al., 2000; Tesi et al., 2020). The degree of the primary production is controlled by the duration of the open water, sea ice formation, diatom taxa and nutrient utilization, etc (Fischer, 1991; Leventer et al., 1993; Cunningham et al., 1999; Arrigo et al., 2000, 2003; Smith et al., 2014; Alderkamp et al., 2019). The diatom assemblage and sea ice formation at the western coast of the Ross Sea during the warmer middle Holocene were different from the modern condition (Mezgec et al., 2017; Jones et al., 2021; Hall et al., 2023). Tesi et al. (2020) reported that the relationship between the low $\delta^{13}C_{SOM}$ values and the long duration of the open marine environment was characterized by the dominant diatom species (*Corethron pennatum*) during the middle to late Holocene in the northwestern Ross Sea. The decrease in $\delta^{13}C_{SOM}$ values at the middle part of Unit 4 may be attributed to the different diatom species under the gradual increase of primary productivity during the warm Holocene, although other additional factors cannot be ruled out.

The diatom assemblage at the middle part of Unit 4 is also characteristic (Fig. 7). At the lower part of Unit 4, the reworking diatom (*P. sulcata*) is dominant, but *C. criophilum* accounts for up to 17% with the highest at 129 cm in GC01. This open marine species indicating the spring melting season in the continental shelf is distributed widely in the Antarctic Ocean (Gersonde and Wefer, 1987; Leventer et al., 1993; Crawford, 1995). The absence of *C. criophilum* in GC04 might be due to poor preservation. At the upper part, *F. curta*, *F. kereguelensis*, *T. antarctica*, and *E. antarctica* var. *recta*, indicating the seasonal sea ice formation, are dominant. The deposition of Unit 4 reflects the seasonal open marine environmental conditions after the complete retreat of the ice shelf during the Holocene. Mezgec et al. (2017) reported that the diatom species during the middle Holocene (5.8–3.6 ka) at the Victoria Land coast was different, characterizing the early sea ice retreat and a long ice-free season. During the middle Holocene, the warm climate leads to the bloom of *C. criophilum* and the appearance of open marine species *F. obliquecostata* (Fig. 7). During the late Holocene, the neoglacial climate cooling maintains the long duration of sea ice characterized by dominant sea ice species in the northern Drygalski Basin. Fischer (1991) reported the different relationship between the low $\delta^{13}C_{SOM}$ values and dominant *C. criophilum* and between high $\delta^{13}C_{SOM}$ values and dominant *Thalassiosira* spp. around the Antarctic continental margin. The diatom assemblage and $\delta^{13}C_{SOM}$ values in Unit 4 were related to the climate change during the middle to late Holocene.

The clay mineral composition of Unit 4 is characterized by relatively lower smectite and higher illite contents (Fig. 6). Under the seasonal open marine system, the clay mineral composition of the fine-grained sediments on the continental shelf is controlled by the current rather than ice flow (Hillenbrand et al., 2003, 2009). Salvi et al. (2006) reported the significant decrease of smectite content during the late Holocene which was caused by a decline in the glacial transport of sediment from the inner shelf. The decreasing smectite content in Unit 4 is caused by the reduction of the eroded and transported sediments from the McMurdo Sound by the glacial ice. The other clay minerals are still supplied from the basement rocks on Victoria Land underneath the glacier to the Drygalski Basin. Although the smectite could be supplied from the Melbourn Volcanic province near Terra Nova Bay, its content was not comparable to that from the McMurdo Sound province (Frank and Ehrmann, 2010; Jung et al., 2021). The clay mineral composition of Unit 4 indicates that the sediment supply from the southern side of the Drygalski Basin decreased while that from the local source area was continuous to the northern Dryaglaksi Basin.

(5) Paleoenvironmental evolution in the Drygalski Basin since the Last Glacial Maximum

Although AMS ^{14}C ages could not provide the exact timing on the retreat of the ice sheet and ice shelf presumably due to the incorporation of old carbons, the variation of sediment deposition suggests that a successive change of glaciomarine depositional environment in the northern Drygalski Basin of the Ross Sea.

The subglacial circumstance at the northern part of the DIT maintained until at least 11 ka and the grounding line retreated southward between 11-10 ka (Licht and Andrew, 2002; Halberstadt et al., 2016). Unit 1 is characterized by unsorted granulometry, high MS, low WC, high smectite content, low $\delta^{13}C_{SOM}$values,andlessbiogenicmaterialswithalmostbarrenofdiatomandreworkeddiatomtaxa.The depositional process of Unit 1 in the Drygalski Basin was strongly affected by the advanced ice sheet from the western and southern sides of the Drygalski Basin under the proximal to the grounding line condition (Fig. 9a).

The grounding line in the Drygalski Basin retreated to the present DIT position at about 8 ka and the ice shelf covering its northern part was pinned to stop retreating by the Crary Bank and the Terra Nova Bay (Halberstadt et al., 2016; Greenwood et al., 2018; Prothro et al., 2020; Rhee et al., 2020). Unit 2 consists exclusively of the massive mud characterized by relatively low MS, a slight increase of biogenic materials, slightly high $\delta^{13}C_{SOM}$ values, a decrease of C/N ratio, high smectite content, and a barren of diatom with the appearance of sea ice taxa.The sediments of Unit 2 were supplied continuously by the meltwater plume during the sub-ice shelf condition from the near local ice shelf to the northern part of the DIT (Fig. 9b). In addition, the sediments from the seasonally open marine areas were transported to deposit by the currents under the ice shelf. On the other hand, the debris flow proximal to the grounding line could not influence the study area.

After the retreat of the grounding line ceased at the DIT, the calving line retreated continuously toward the DIT and the small bay at the Victoria

Land coast. Unit 3 is characterized by the alternating sandy mud and mud with many coarse fractions and fluctuating MS and WC. The geochemical proxies and $\delta^{13}C_{SOM}$ values are similar to those of Unit 2. The breakup of the ice shelf supplies a large amount of IRDs and the meltwater plume from the grounding line transport the mud or sandy mud to the northern Drygalski Basin. In addition, the seasonal open marine condition developed by the breakup of the ice shelf and the biogenic materials were deposited at the north side of DIT (Fig. 9c). Although biogenic production in the surface water began around the calving line, the influence of the meltwater plume from the nearby grounding line was stronger at the northern part of the DIT.

The northern Drygalski Basin retained the seasonal open marine condition after the complete retreat of the ice shelf (Yokoyama et al., 2016; Prothro et al., 2020; Rhee et al., 2020). Unit 4 consists of the bioturbated sediment facies, which is characterized by relatively low MS, C/N ratio and smectite content, distinct increase of biogenic materials, and an upward decrease and increase of $\delta^{13}C_{SOM}$ values with abundant diatoms and diverse diatom taxa. The biogenic components of the Holocene sediments increased by the enhanced biogenic productivity in the surface water, while the sediments transported by the ice and meltwater decreased dramatically (Fig. 9d). The variation of sea ice duration by the climate change during the middle Holocene strongly affected the diatom assemblage and $\delta^{13}C_{SOM}$ values. In addition, the detrital fine-grained sediments were delivered mainly from near the Victoria Land coast.

5. Conclusions

Gravity and box core sediments were analyzed in terms of the sediment and geochemical properties, carbon isotopic values of sediment organic matter, clay mineral compositions of fine-grained sediments, and diatom assemblage along with AMS ^{14}C dating of bulk sediments. These results determine the paleoenvironmental change and depositional evolution in the glaciomarine sediments related to the retreat of the ice sheet and ice shelf in the northern Drygaski Basin since the LGM. The relatively old AMS ^{14}C ages of the bulk sediments are generally due to the incorporation of old and reworked carbons on the continental shelf, as dated by 3.7 and 4.1 ka at the core-top sediments. Nevertheless, AMS ^{14}C ages distinguished pre-Holocene, early to middle Holocene, and late Holocene sediments. Based on the analytical results, the sediments were classified into seven sediment facies (clast-rich muddy or sandy diamicton, massive or laminated or bioturbated mud, and massive or bioturbated sandy mud), which were used to delineate four lithologic unit on the basis of depositional evolution since the LGM.

The glaciomarine sediment deposition in the northern Drygalski Basin was strongly affected by the retreating ice sheet and ice shelf since the LGM and the climate change during the Holocene. The advanced ice sheet transported a large amount of sediment toward the basin floor proximal to the grounding line. The ice shelf on the Drygalski Basin restricted the biogenic productivity. It resulted in the deposition of sorted sediments by the meltwater plume from the nearby grounding line at the Victoria Land coast. During the retreating calving line, abundant coarse particles were supplied to the seafloor at the north side of the DIT. The climate change during the middle Holocene was also essential in controlling the seasonal open marine condition and the diatom assemblage in the northern Drygalski Basin.

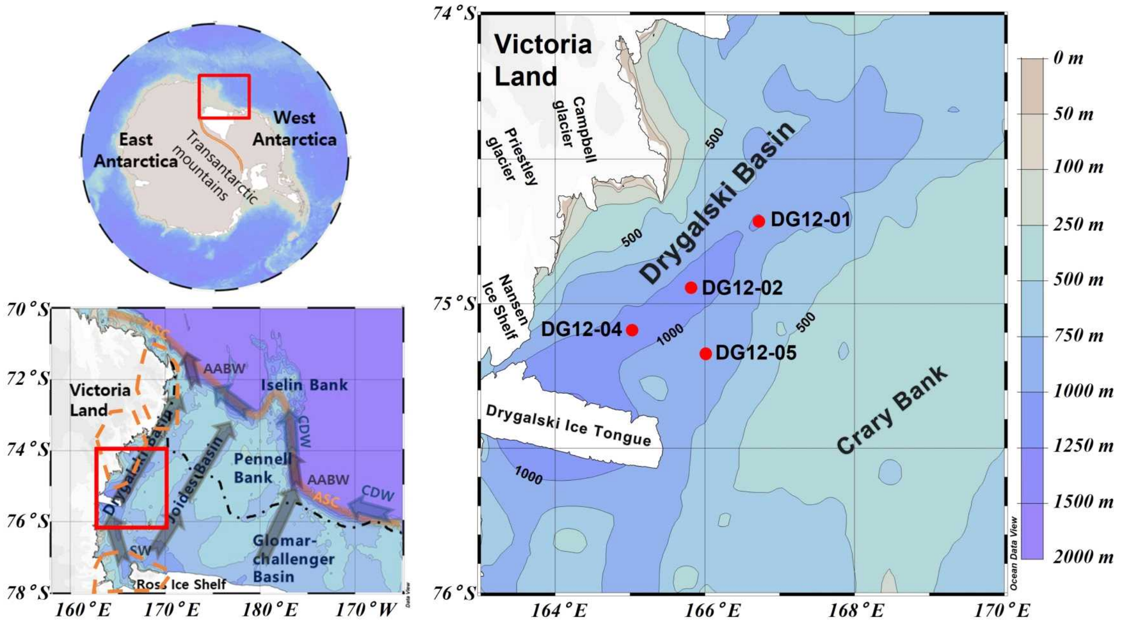

Figure 1. Study area (red rectangle in the Antarctic continent and the western Ross Sea) showing the Drygalski Basin. Coring sites (DG12-01, DG12-02, DG12-04, and DG12-05) were located in the northern Drygalski Basin. The orange dotted line marks the source area of smectite (the Hallett, Melbourne, and Erebus volcanic provinces from north to south). CDW: Circumpolar Deep Water, ASC: Antarctic Slope Current, AABW: Antarctic Bottom Water, SW: Shelf Water (Orsi and Wiederwohl, 2009).

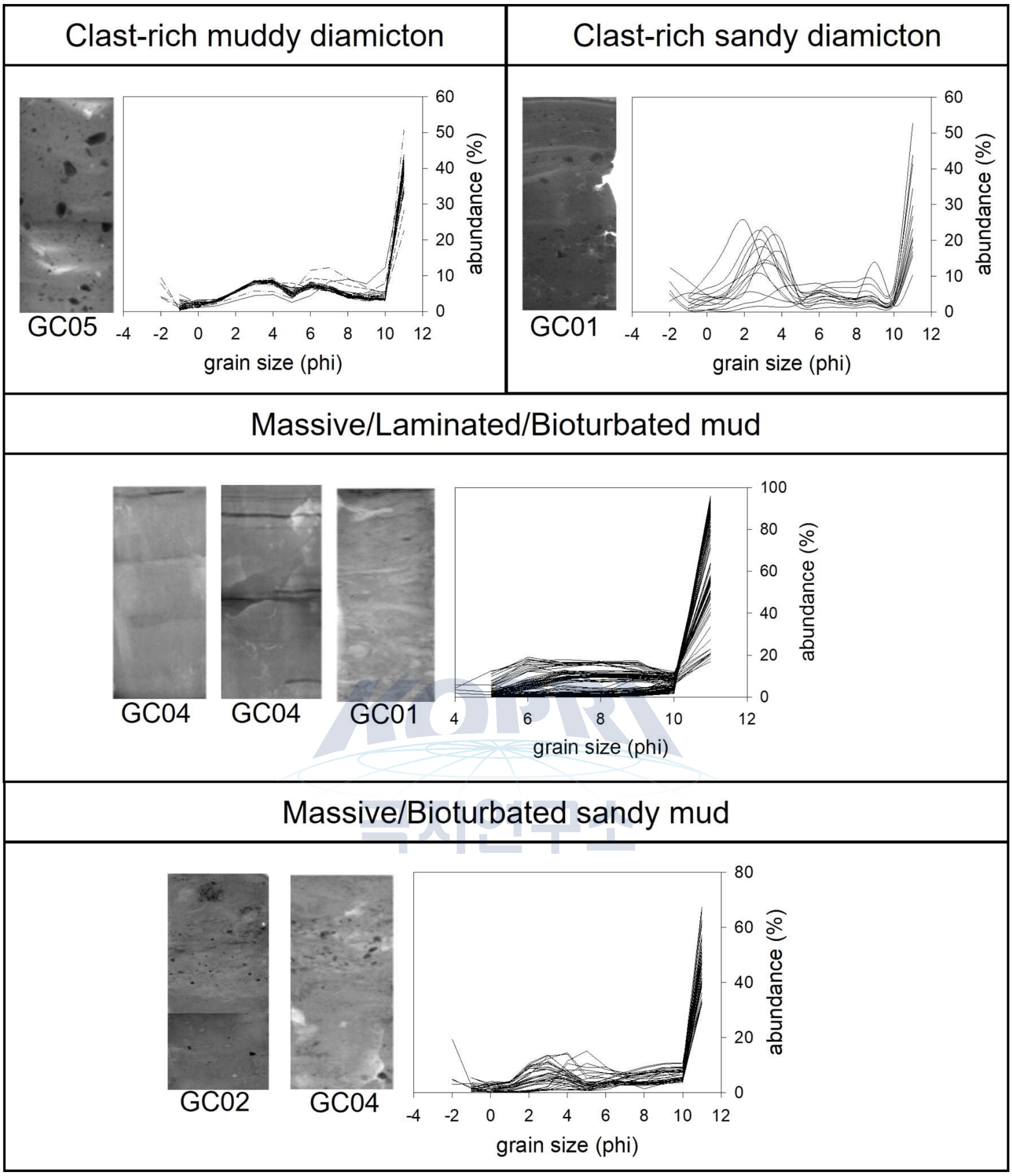

Figure 2. Classification of seven sediment facies based on the X-ray photographs and grain size distribution of four gravity cores (DG12-GC01, DG12-GC02, DG12-GC04, and DG12-GC05).

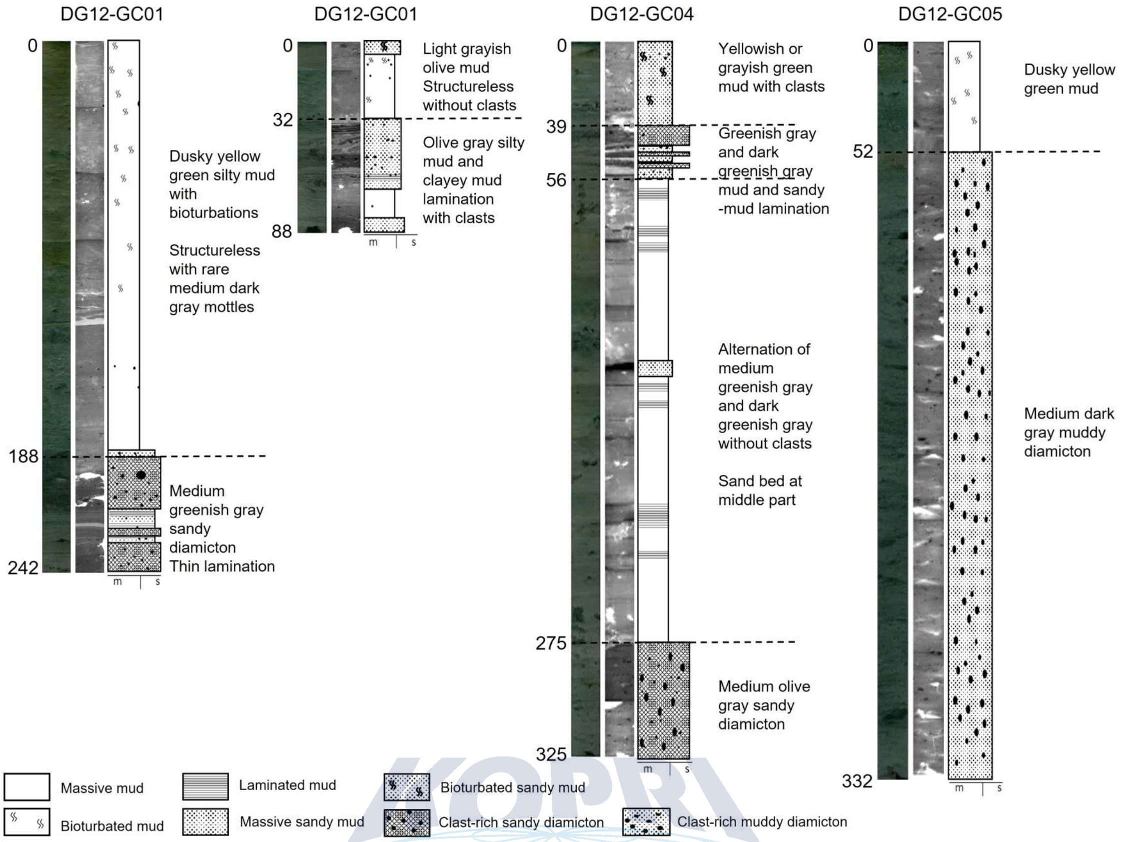

Figure 3. Core descriptions with photograph, X-ray radiograph, and sediment facies of four gravity cores (DG12-GC01, DG12-GC02, DG12-GC04, and DG12-GC05).

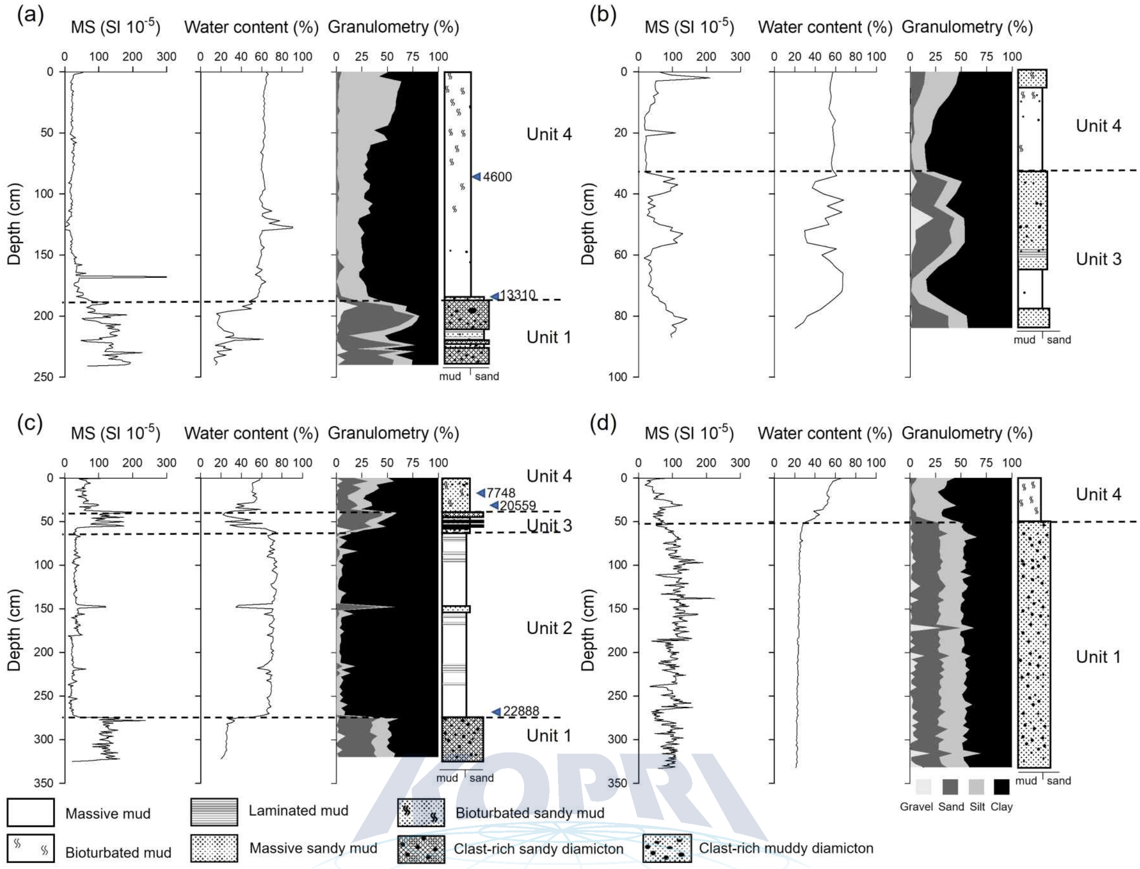

Figure 4. Downcore variation of sediment properties (magnetic susceptibility (MS), water content, and granulometry) with sediment facies. (a) GC01, (b) GC02, (c) GC04, and (d) GC05. Lithologic units (1, 2, 3, and 4) are divided by the dotted lines and calibrated ages are shown.

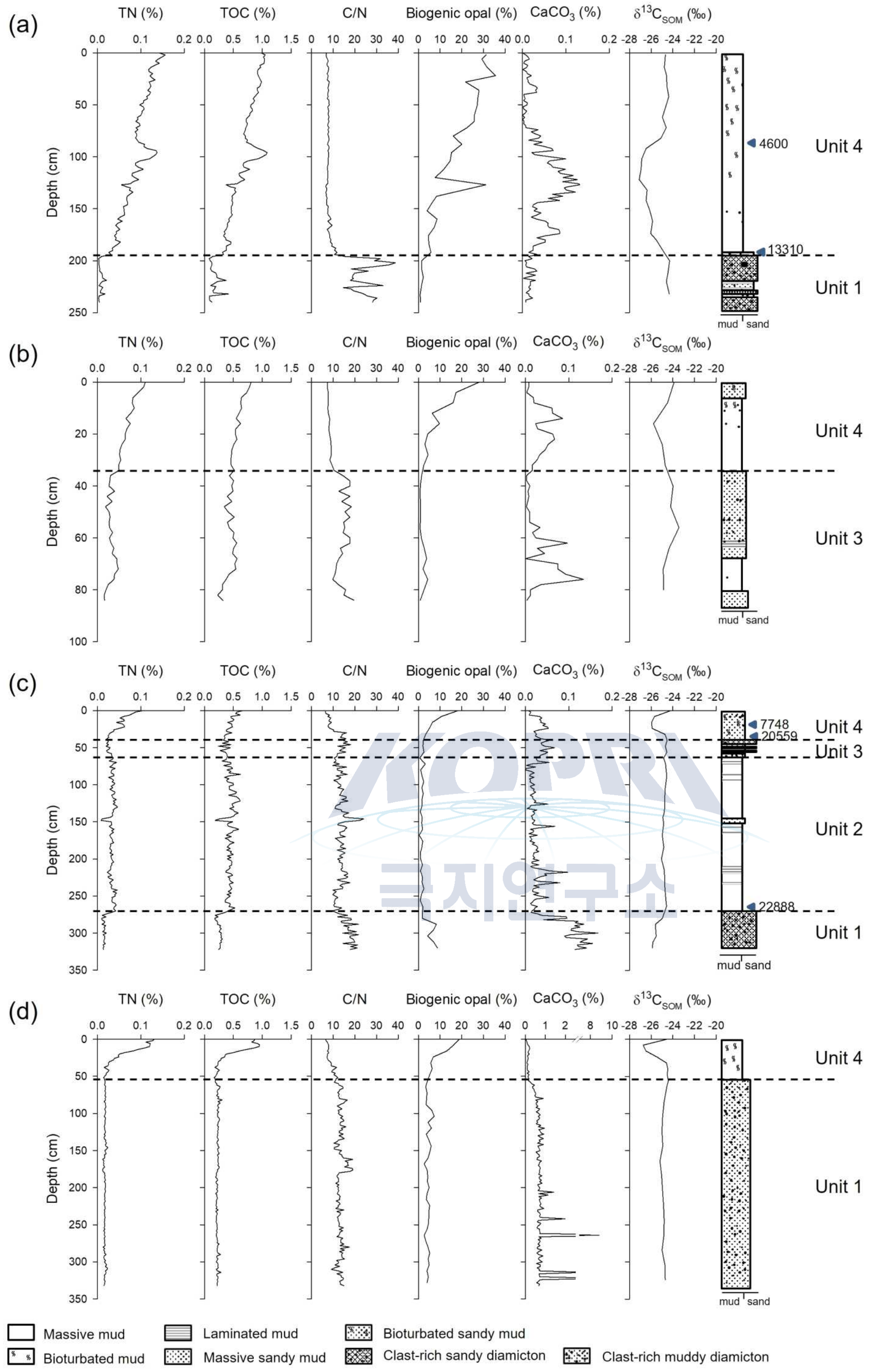

Figure 5. Downcore variation of geochemical proxies (total nitrogen (TN), total organic carbon (TOC), TOC/TN (C/N), biogenic opal, and $CaCO_3$)and$\delta^{13}C$ values of sediment organic matter with the columnar section of sediment facies. (a) GC01, (b) GC02, (c) GC04, and (d) GC05. Lithologic units (1, 2, 3, and 4) are divided by the dotted lines, and calibrated ages are shown.

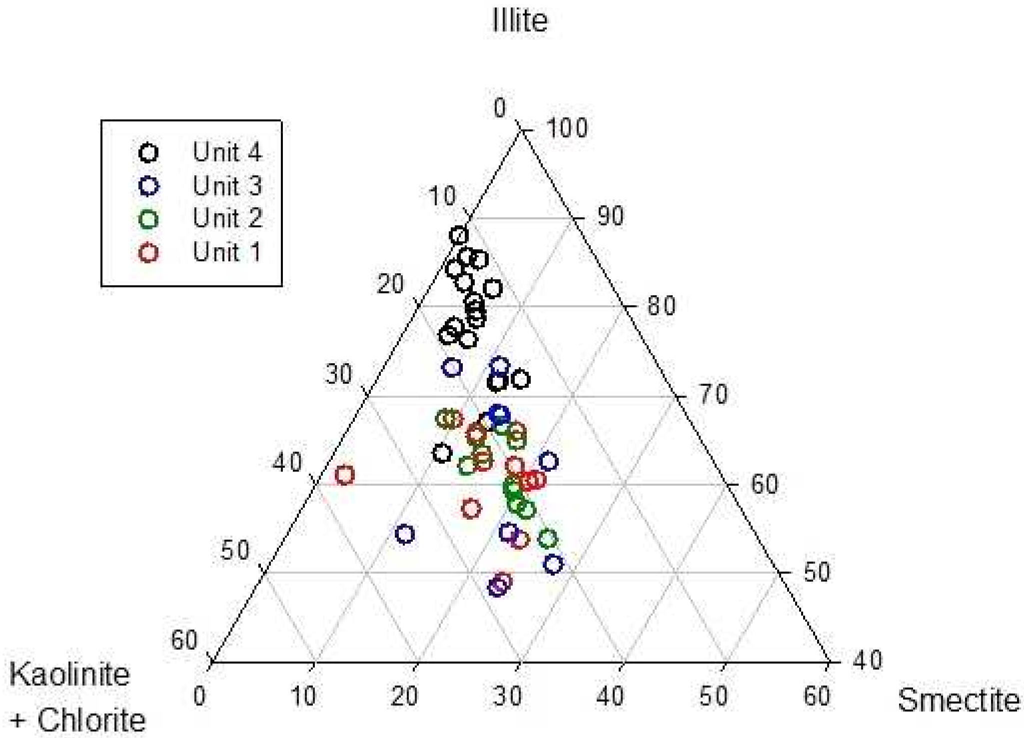

Figure 6. Ternary diagram of fine-grained clay mineral compositions of the lithologic unit at cores GC01 and GC04.

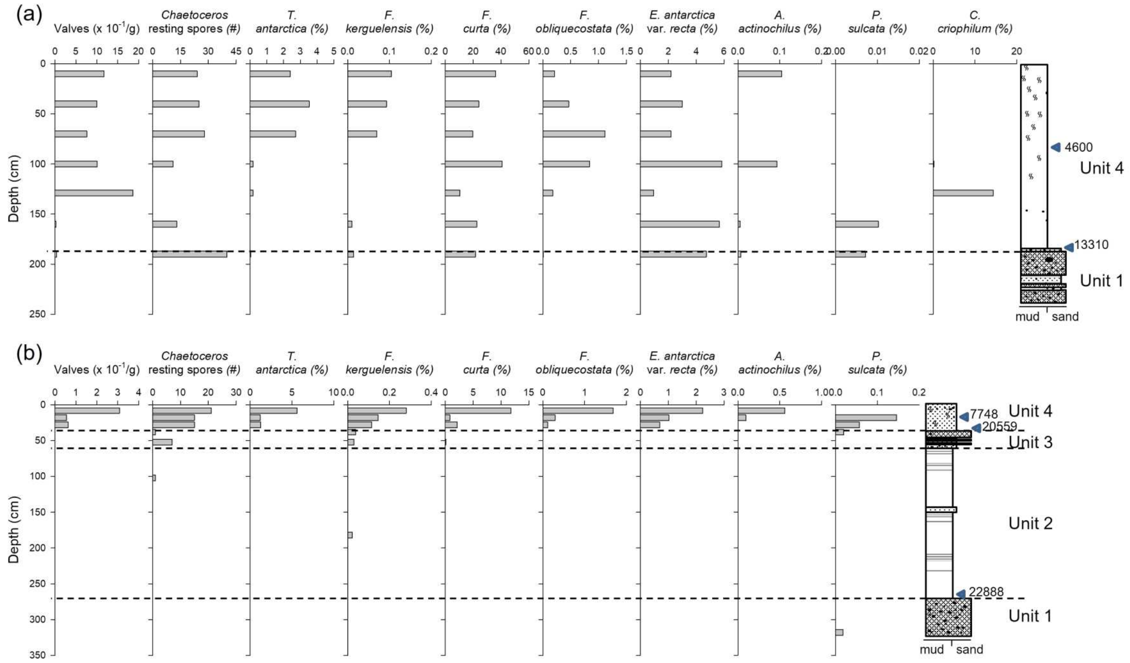

Figure 7. Downcore variation of diatom assemblage with the columnar section of sediment facies. (a) GC01, (b) GC04. Lithologic units (1, 2, 3, and 4) are divided by the dotted lines, and calibrated ages are shown.

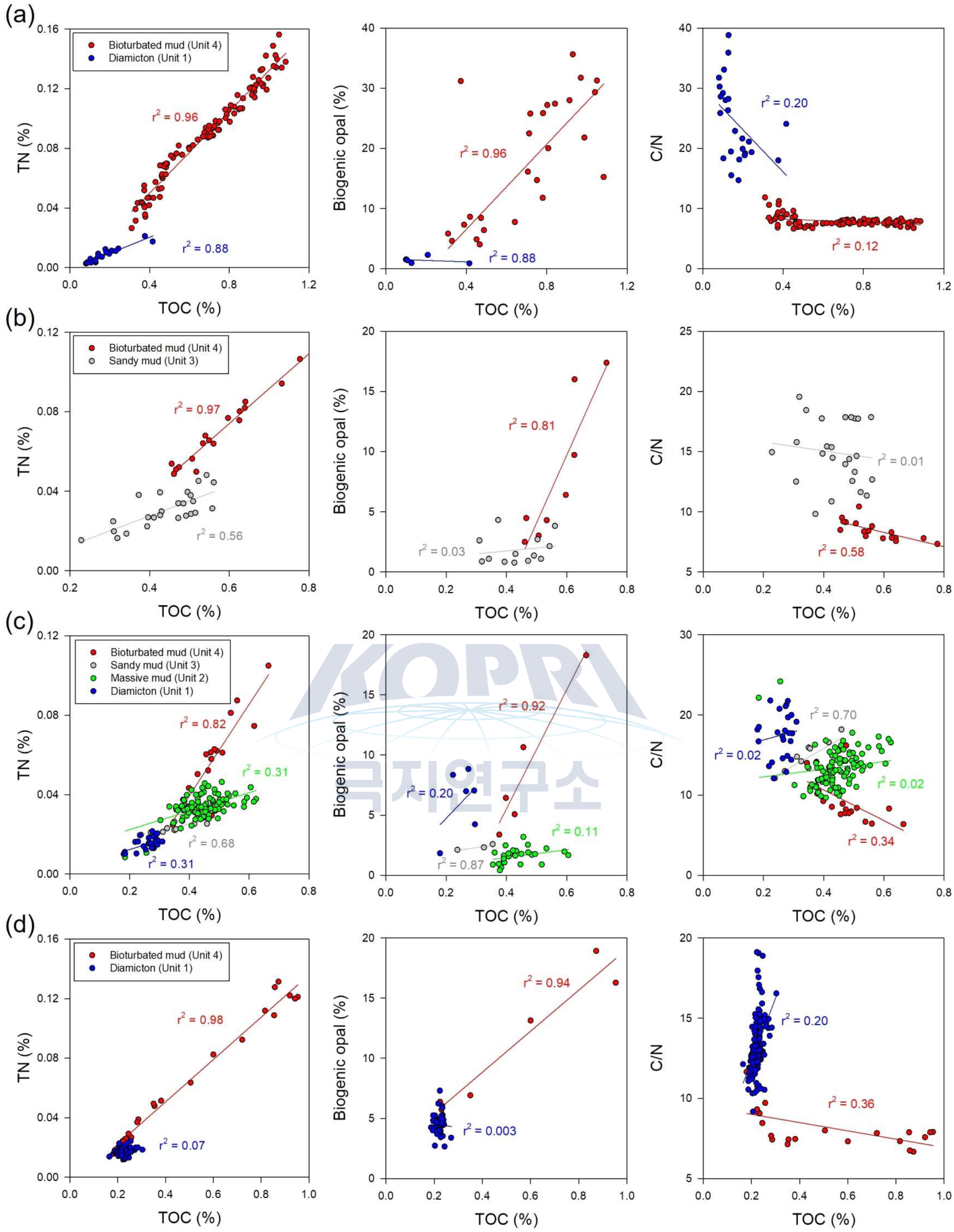

Figure 8. Correlation between TOC and TN, between TOC and biogenic opal, and between TOC and C/N ratio of the lithologic unit. (a) GC01, (b) GC02, (c) GC04, and (d) GC05.

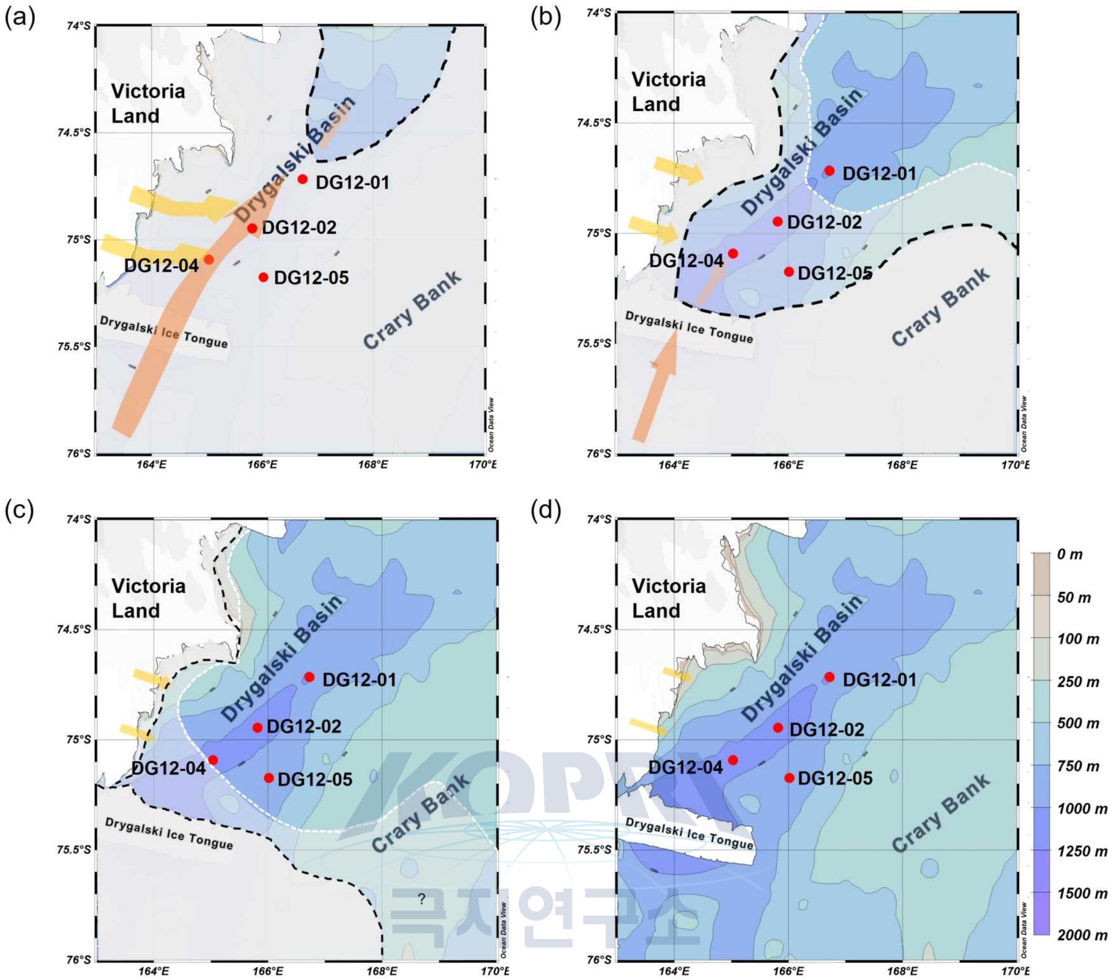

Figure 9. Schematic model showing the evolution of northern Drygalski Basin characterized by the sediment transport during the retreat of the ice sheet and ice shelf. The dotted black line and white line represent the grounding line and calving line, respectively. Orange and yellow arrows represent the sediment transport from the southern Drygalski Basin and the Victoria Land coast, respectively. The retreat of the grounding and calving lines was modified from Rhee et al. (2020) and Prothro et al. (2020).

제 4 장 연구개발목표 달성도 및 대외기여도

지난 6년 간의 과제 수행동안 아래와 같이 국제학술논문 8편을 게재하는 성공적인 성과를 내어 연구 목표의 달성도는 100%를 넘는 결과를 거두었다.

Khim, B.K.*, Kim, S., Lee, M.K.*, Sohn, Y.K., Lee, J.I, Yoo, K.C. (2024) Fallacy of paleoproductivity signals by the recycled biogenic components: case study in the Central Basin of the northwestern Ross Sea. *Geoscience Letters*, vol. 11, 50, DOI : 10.1186/s40562-024-00365-3 (*co-corresponding author)

Khim, B.K.*, Sohn, Y.K., Lee, M.K., Kim, S., Lee, J.I, Yoo, K.C. (2024) Pleistocene laminated muds in the Central Basin of the northwestern Ross Sea and their paleoceanographic records. *Terra Nova*, vol. 36, no. 1, p.37-44. (*corresponding author) (DOI:10.1111/ter.12688)

Ha, S., Lee, J.I., Bak, Y.S., Yoo, K.C., **Khim, B.K.*** (2023) Paleoenvironmental reconstruction of glaciomarine sediments in the Drygalski Basin of the western Ross Sea since the Last Glacial Maximum. *Sedimentary Geology*, vol. 456, Article 106495. (*corresponding author)

Ha, S., Colizza, E., Torricella, F., Langone, L., Giglio, F., Kuhn, G., Marci, P., **Khim, B.K.*** (2022) Glaciomarine sediment deposition on the continental slope and rise of the central Ross Sea since the Last Glacial Maximum. *Marine Geology*, vol. 445, Article 106752. (*corresponding author)

Khim, B.K.*, Kim, S., Park, Y.H., Lee, J., Ha, S., Yoo, K.C. (2021) Holocene sedimentation in the Hupo Trough of the southwestern East Sea (Japan Sea) and the development of the East Korea Warm Current. *The Holocene*, vol. 31, no. 7, p.1148-1157.

Khim, B.K.*, Colizza, E., Lee, J.I., Giglio, F., Ha, S., Bak, Y.S. (2021.06) Biological productivity and glaciomarine sedimentation in the Central Basin of the northwestern Ross Sea. *Polar Science*, vol. 28, Article 100682. (*corresponding author)

Torricella, F., Melis, R., Malinverno, E., fontolan, G., Capotondi, L., Del Carlo, P., Di Roberto, A., Geniram, A., Kuhn, G., **Khim, B.K.**, Morigi, C., Scateni, B., Colizza, E. (2021) Environmental and oceanographic conditions at the continental margin of the Central Basin, Northwestern Ross Sea (Antarctica) since Last Glacial Maximum. *Geosciences*, vol. 11, 155.

Melis, R., Capotondi, L., Torricella, F., Ferretti, P., Geniram, A., Hong, J.K.,

Kuhn, G., **Khim, B.K.**, Kim, S., Malinverno, E., Yoo, K.C., Colizza, E. (2021) Last Glacial Maximum to Holocene paleoceanography of the northwestern Ross Sea inferred from sediment core geochemistry and micropaleontology at Hallett Ridge. *Journal of Micropaleontology*, vol. 40, p.15-35.

본 연구 성과들은 남극 로스해(Ross Sea)를 중심으로 한 빙하–해양–퇴적 상호작용과 고해양·고생태 환경 변화를 고해상도로 규명함으로써, 남극 빙상 안정성 및 해수면 상승 예측의 핵심 과학적 근거를 국제사회에 제공하였다. 특히 마지막 빙기 이후부터 플라이스토세에 이르는 다양한 시간 규모에서의 퇴적·생산성·해빙 메커니즘을 종합적으로 해석함으로써, 기존의 단순화된 고생산성 및 빙하 후퇴 해석의 한계를 극복하는 데 기여하였다.

구체적으로, 재순환된 생물기원 성분에 의한 고생산성 신호 왜곡 가능성을 최초로 체계적으로 제시함으로써(Geoscience Letters, 2024), 고기후·고해양 프록시 해석의 신뢰도 향상과 국제 연구 방법론 개선에 기여하였다. 또한 로스해 중앙 분지 및 주변 대륙사면·라이즈 지역에서의 빙하성 퇴적과 생물 생산성 변화를 정밀 복원함으로써(Marine Geology, Sedimentary Geology, Polar Science 등), 서남극 빙상의 해빙 시기와 해양 환경 변화의 연계성을 규명하였다.

아울러 플라이스토세 라미네이티드 머드의 형성과 고해양 기록(Terra Nova, 2024)을 통해 빙상–해양 상호작용의 단주기 변동성에 대한 새로운 해석 틀을 제시하였으며, 이는 IODP 및 ICDP 등 국제 공동 시추 프로그램에서 확보되는 퇴적 기록 해석에 직접적으로 활용 가능한 지식 기반을 제공한다. 이러한 연구 결과들은 SCAR, IODP 등 국제 극지 연구 커뮤니티에서 요구하는 핵심 과제에 부합하며, 한국 연구진이 남극 고환경 및 빙상 연구 분야에서 주도적 학문적 기여를 수행하고 있음을 입증하였다.

종합적으로 본 논문들은 남극 빙상 변화와 미래 해수면 상승 예측의 불확실성을 저감하는 데 기여함과 동시에, 국제 공동연구에서의 한국의 학문적 위상과 발언권을 강화하는 중요한 성과로 평가된다.

Khim *et al. Geoscience Letters* (2024) 11:50
https://doi.org/10.1186/s40562-024-00365-3

Geoscience Letters

RESEARCH LETTER

Open Access

Fallacy of paleoproductivity signals by the recycled biogenic components: case study in the Central Basin of the northwestern Ross Sea

Boo-Keun Khim[1*], Sunghan Kim[2], Min Kyung Lee[2*], Young Kwan Sohn[3], Jae Il Lee[2] and Kyu-Cheul Yoo[2]

Abstract

Core LC42, retrieved from the Central Basin of the northwestern Ross Sea, contains three distinct sediment facies (IRD (ice-rafted debris)-poor bioturbated sandy mud, IRD-rich massive sandy mud, and laminated mud) that are interleaved with each other and deposited over the last 1 Ma. The biogenic components (biogenic opal, total organic carbon, and total nitrogen) of the laminated mud layers are consistently higher than the other two facies throughout the core. Based on the depositional succession of sediment facies and IRD-related depositional processes in the Antarctic continental margin, the laminated mud layers without IRD have been deposited during the glacial periods, but the enhanced paleoproductivity in terms of biogenic components during the mud deposition is unexpected. Backscattered electron imagery substantiates distinctly different componentry of the alternating light and dark laminae in the laminated mud. In particular, the light laminae contain scattered diatom fragments and eroded sand-sized lumps of fossil-bearing mud, whereas the dark laminae are clayey and diatomaceous. Both laminae thus are characterized by the high biogenic components, but they are interpreted to have been principally recycled from older deposits because diatom fragments are mostly reworked and old and their archives are poorly preserved. During the glacial periods, these laminated muds were deposited downward by milky plumes of meltwater discharged underneath the advancing glaciers that scoured the earlier-deposited and semi-consolidated diatom-rich sediments. Our study thus highlights that the recycling of biogenic particles should be precautious to avoid the fallacy of paleoclimatic interpretation in formulating climate-productivity models in the Antarctic continental margin.

Keywords Climate-productivity model, Antarctic continental margin, Biogenic components, Recycled diatoms, Ross Sea

*Correspondence:
Boo-Keun Khim
bkkhim@pusan.ac.kr
Min Kyung Lee
mklee@kopri.re.kr
Full list of author information is available at the end of the article

Received: 9 August 2022 | Revised: 14 August 2023 | Accepted: 21 September 2023
DOI: 10.1111/ter.12688

RESEARCH ARTICLE

Terra Nova WILEY

Pleistocene glaciomarine laminated muds in the Central Basin of the northwestern Ross Sea and their palaeoceanographic records

Boo-Keun Khim[1] | Young Kwan Sohn[2] | Min Kyung Lee[3] | Sunghan Kim[3] | Jae Il Lee[3] | Kyu Cheul Yoo[3]

[1]Department of Oceanography and Marine Research Institute, Pusan National University, Busan, Korea
[2]Department of Geology, Gyeongsang National University, Jinju, Korea
[3]Division of Glacial Environment Research, Korea Polar Research Institute, Incheon, Korea

Correspondence
Boo-Keun Khim, Department of Oceanography and Marine Research Institute, Pusan National University, Busan 46241, Korea.
Email: bkkhim@pusan.ac.kr

Funding information
Korea Polar Research Institute, Grant/Award Number: PE23090; the Ministry of Oceans and Fisheries; National Research Foundation of Korea, Grant/Award Number: 2022R1A2B5B01001811

Abstract
Glaciomarine laminated muds around the Antarctic continental margin are important in the marine geological record related to ice sheet dynamics. Microscopic observation and backscattered electron imagery of Pleistocene laminated muds in the Central Basin (Ross Sea) reveal that the light laminae comprise terrigenous angular to subangular silt-sized particles, scattered diatom fragments, and eroded sand-sized lumps of fossil-bearing mud. In contrast, the dark laminae are clayey and biogenic with very tiny pieces of fossils. These laminated muds are interpreted to have been deposited by subglacial meltwater plumes underneath the advancing glaciers that torn off the earlier-deposited and semi-consolidated diatom-rich sediments. Thus, most biogenic components of these laminated muds were recycled from older deposits, indicating that they are not related to enhanced biological production during the mud deposition. Our study suggests that the recycling of biogenic particles should be considered when interpreting the palaeoclimatic and palaeoceanographic implications of Antarctic environmental system.

KEYWORDS
antarctic continental margin, glaciomarine laminated muds, paleoceanography

1 | INTRODUCTION

The Antarctic Ice Sheet (AIS) has played a crucial role in affecting the environmental conditions related to the sediment depositional system in the Southern Ocean. Colleoni et al. (2018) reviewed the responses of the Antarctic environmental system to the changes in ice sheet basal hydrology, continental margin evolution, and ocean circulation through the complicated processes across the ice-bed-ocean interfaces of the AIS. In particular, the Antarctic ice shelves are the terminus of the AIS glaciers that responds sensitively to the ice-sheet dynamics around the Antarctic continental margin (Smith et al., 2019). In this context, the marine geological signatures of glacial–interglacial cycles have been well recognized from the studies of the Antarctic continental margin related to the presence, absence, and collapse of ice shelves (Domack & Powell, 2018).

Studies of the depositional processes of glaciomarine sediments in the Antarctic marine settings have offered important clues to understanding the diverse interplay among the ice sheet, ice shelf, and ocean within the Antarctic depositional systems. In the Antarctic continental margins, two general types of glaciomarine laminated sediments have been reported: laminated terrigenous muds and laminated biosiliceous muds. The former generally occurs in the continental slope and rise and is thought to be the product of contour currents (e.g., Anderson, 1999). The glacial sediments in the Pacific margin of the Antarctic Peninsula consist of this type of muds (Lucchi & Rebesco, 2007; Pudsey, 2000; Venuti et al., 2011). In addition, Domack (1990) reported a rhythmically laminated sequence

Sedimentary Geology 456 (2023) 106495

Contents lists available at ScienceDirect

Sedimentary Geology

journal homepage: www.elsevier.com/locate/sedgeo

Paleoenvironmental reconstruction of glaciomarine sediments in the Drygalski Basin of the western Ross Sea since the Last Glacial Maximum

Sangbeom Ha [a,b], Jae Il Lee [b], Young-Suk Bak [c], Kyu-Cheul Yoo [b], Boo-Keun Khim [a,d,*]

[a] Department of Oceanography, Pusan National University, Busan 46241, Republic of Korea
[b] Division of Glacial Environment Research, Korea Polar Research Institute, Incheon 21990, Republic of Korea
[c] Earth Environmental System Research Center, Jeonbuk National University, Jeonju 54896, Republic of Korea
[d] Marine Research Institute, Pusan National University, Busan 46241, Republic of Korea

ARTICLE INFO

Article history:
Received 26 May 2023
Received in revised form 17 August 2023
Accepted 18 August 2023
Available online 26 August 2023

Editor: Dr. Brian Jones

Keywords:
Continental shelf sediments
Ice sheet
Ice shelf
Grounding line
Calving line
Drygalski Basin
Ross Sea

ABSTRACT

The repeated growth and reduction of the ice sheet have controlled the striking variation of the continental shelf environment in the Ross Sea. Particularly, glaciomarine shelf sedimentation is closely related to the ice sheet dynamics and ice shelf development since the Last Glacial Maximum (LGM). Using the four gravity (and box) cores obtained from the northern Drygalski Basin in the western Ross Sea, multi-proxies including sediment properties, geochemical proxies, carbon isotopic values of organic matter, clay mineral compositions of fine-grained sediments, and diatom assemblage were analyzed with AMS ^{14}C dating from bulk organic matters. Based on the core description, X-radiograph observation, and results of grain size distribution, the core sediments were classified into the seven sediment facies: clast-rich muddy diamicton, clast-rich sandy diamicton, massive mud, laminated mud, bioturbated mud, massive sandy mud, and bioturbated sandy mud. The association of these sediment facies defines the four lithologic units in terms of the depositional evolution. Lithologic unit 1 represents diamicton deposited proximal to the grounding line. When the ice sheet and ice shelf retreated since the LGM, the unsorted sediment mass was deposited proximal to the grounding line. Lithologic unit 2 consists of the massive mud deposited under the sub-ice shelf condition. During the ice sheet retreat, the fine-grained particles were transported by the meltwater plume to the sub-ice shelf floor. The biogenic materials were also transported from the seasonal open marine area to the sub-ice shelf by the currents. Lithologic unit 3 was composed of sandy mud and mud with abundant dropstones that might have been deposited at the calving line. As the calving line passed the Drygalski Basin, a large amount of the coarse fractions was deposited due to ice shelf breakup. The terrestrial sediments from the Victoria Land coast were transported from the grounding line of the remained local ice sheet, when the calving line passed the north side of Drygalski Ice Tongue. Lithologic unit 4 comprises the bioturbated mud and sandy mud that were deposited under the seasonal open marine condition. The biological productivity increased significantly during the late Holocene, while the terrestrial sedimentation decreased under seasonal open marine conditions. The diatom assemblage and $\delta^{13}C$ values of sediment organic matter indicate the mid-Holocene warm climate with more sea ice melting. Since the LGM, the paleoenvironmental change and glaciomarine depositional evolution on the northern Drygalski Basin were closely linked with the ice sheet dynamics and ice shelf activity, in addition to the climate change during the Holocene.

1. Introduction

In the Ross Sea, the bathymetry and topography such as the north–northwest oriented deep and narrow basins (e.g., Glomar–Challenger Basin, Joides Basin, and Drygalski Basin) and shallow banks (e.g., Ross Bank, Pennell Bank, and Crary Bank) have been generated by the advanced ice sheet during the glacial periods (Fig. 1). The Drygalski Basin is located in the western Ross Sea and includes the deepest area on the Ross Sea continental shelf. Numerous outlet glaciers along the coastline of the western Ross Sea originated from the ice domes (Dome C (Charlie), Taylor dome, and Talos dome) on the Victoria Land (Giovinetto and Bentley, 1985; Frezzotti et al., 2000). After the LGM, the outlet glaciers on Northern Victoria Land retreated as the global sea level rose, whereas those on Southern Victoria Land retreated after Meltwater Pulse 1A (~14 ka) (Goehring et al., 2019; Christ and Bierman, 2020). The David Glacier, which is the largest, forms the

* Corresponding author at: Department of Oceanography, Pusan National University, Busan 46241, Republic of Korea.
E-mail addresses: sb_ha@pusan.ac.kr (S. Ha), leeji@kopri.re.kr (J.I. Lee), sydin@jbnu.ac.kr (Y.-S. Bak), kcyoo@kopri.re.kr (K.-C. Yoo), bkkhim@pusan.ac.kr (B.-K. Khim).

https://doi.org/10.1016/j.sedgeo.2023.106495

Marine Geology 445 (2022) 106752

Contents lists available at ScienceDirect

Marine Geology

journal homepage: www.elsevier.com/locate/margo

Research article

Glaciomarine sediment deposition on the continental slope and rise of the central Ross Sea since the Last Glacial Maximum

Sangbeom Ha[a], Ester Colizza[b], Fiorenza Torricella[c], Leonardo Langone[d], Federico Giglio[d], Gerhard Kuhn[e], Patrizia Macrì[f], Boo-Keun Khim[a,*]

[a] Department of Oceanography, Pusan National University, Busan, Republic of Korea
[b] Department of Mathematics and Geosciences, University of Trieste, Trieste, Italy
[c] Department of Earth Sciences, University of Pisa, Pisa, Italy
[d] National Research Council-Institute of Polar Sciences, Bologna, Italy
[e] Alfred-Wegener-Institute Helmholtz-Zentrum für Polar- und Meeresforschung (AWI), Bremerhaven, Germany
[f] Istituto Nazionale di Geofisica e Vulcanologia, Rome, Italy

A R T I C L E I N F O

Editor: Adina Paytan

Keywords:
Sediment core
Ice sheet
Sea ice
Paleoproductivity
Continental margin
Ross Sea

A B S T R A C T

The continental margin of the Ross Sea has been consistently sensitive to the advance and retreat of the Ross Ice Sheet (RIS) between the interglacial and glacial periods. This study examines changes of the glaciomarine sedimentation on the continental slope and rise to the eastern side of Hillary Canyon in the central Ross Sea, using three gravity cores collected at increasing water depths. Besides older AMS ^{14}C ages of bulk sediments, based on the analytical results, sediment lithology was divided into units A, B1, and B2, representing Holocene, deglacial, and glacial periods, respectively. The sedimentation rate decreased as the water depth increased, with a higher sedimentation rate in the deglacial period (unit B1) than the Holocene (unit A). Biological productivity proxies were significantly higher in glacial unit B2 than in interglacial unit A, with transitional values observed in deglacial unit B1. Biological productivity generally decreased in the Antarctic continental margin during the glacial period because of extensive sea ice coverage. The higher biogenic contents in unit B2 are primarily attributed to the increased transport of eroded and reworked shelf sediments that contained abundant biogenic components to the continental slope and rise beneath the advancing RIS. Thus, glacial sedimentation on the continental slope and rise of the central Ross Sea was generally governed by the activity of the RIS, which generated melt-water plumes and debris flows at the front of the grounding line, although the continental rise might have experienced seasonally open conditions and lateral effects due to the bottom current.

1. Introduction

Approximately 98% of Antarctica is covered with ice; thus, the continental ice plays an important role in the global water cycle and climate change (Pattyn et al., 2018). If the entire Antarctic Ice Sheet (AIS) were to melt, the global sea level would rise as high as −60 m above the present-day level, which is equivalent to almost half of the range that it fell during the last glacial period (Nakada et al., 2000; DeConto and Pollard, 2016). The AIS is geographically divided into the West Antarctic Ice Sheet (WAIS) and East Antarctic Ice Sheet (EAIS) by the Transantarctic Mountains. The marine-based WAIS is largely below sea level and flows rapidly, compared to the EAIS (Fretwell et al., 2013). Hence, the WAIS is more sensitive to changes in seawater temperature and sea level (DeConto and Pollard, 2016). The AIS plays an important role in controlling global climate change, with variations in the extent of the AIS affecting the surface albedo, global sea level, ocean circulation, and the production of bottom water (e.g., Ogura and Abe-Ouchi, 2001; Mackensen, 2004; Ritz et al., 2015).

The WAIS discharges ice into the central and eastern sectors of the Ross Sea, while the EAIS supplies ice to the western sector (Rignot et al., 2008). The extensive Ross Ice Sheet (RIS) primarily developed from portions of both with a comparatively higher contribution from the WAIS. The RIS advanced to the shelf edge in the eastern Ross Sea during the Last Glacial Maximum (LGM) (Fig. 1; Anderson et al., 2019, Lowry et al., 2020). Contrastingly, the RIS did not reach the shelf edge in the central and western Ross Sea, where it ceased its advance at Mawson

* Corresponding author.
E-mail address: bkkhim@pusan.ac.kr (B.-K. Khim).

https://doi.org/10.1016/j.margeo.2022.106752
Received 18 October 2021; Received in revised form 5 February 2022; Accepted 6 February 2022
Available online 9 February 2022
0025-3227/

Research Paper

The Holocene
2021, Vol. 31(7) 1148–1157

Article reuse guidelines:
sagepub.com/journals-permissions
DOI: 10.1177/09596836211003238
journals.sagepub.com/home/hol
SAGE

Holocene sedimentation in the Hupo Trough of the southwestern East Sea (Japan Sea) and development of the East Korea Warm Current

Boo-Keun Khim,[1] Sunghan Kim,[2] Yu-Hyeon Park,[3] Jongmin Lee,[1] Sangbeom Ha[1] and Kyu-Cheul Yoo[2]

Abstract

Various sediment properties, such as mean grain size, total organic carbon, total nitrogen, C/N ratio, $CaCO_3$, and biogenic opal content, were analyzed for a box core (BC02; 45 cm long) and a gravity core (GC02; 628 cm long), which were collected from the western margin of the Hupo Trough located off the eastern coast of Korea. The study area has been affected by the East Korea Warm Current (EKWC), a branch of the Tsushima Warm Current (TWC). The analytical results obtained for BC02 and the upper part of GC02 were in agreement, affirming the core-top preservation of GC02. Based on the corrected calibrated AMS ^{14}C dates, the sedimentation rate of GC02 changed abruptly at ~8.2 ka from ~4.0–10.2 cm/kyr in the lower part to ~56.6–91.0 cm/kyr in the middle to upper part. This corresponds to the lithologic change from sandy mud to mud sediments showing the mean grain size change from 6.9 to 46.0 μm. Diverse paleoceanographic proxies representing the surface water condition exhibited varying degree of change at ~8.2 ka, after which all the properties remain almost unchanged, implying stable and continuous depositional conditions following the complete development of the EKWC. Furthermore, it indicated that the sediment depositional conditions in the Hupo Trough in response to the EKWC might have stabilized at ~8.2 ka since the opening of the Korea Strait during the Holocene sea level rise. Moreover, microfossil data from previous studies on the establishment of the TWC in the East Sea (Japan Sea) support our interpretation that the sediment properties revealed the Holocene development of the EKWC in the Hupo Trough.

Keywords

geochemical properties, paleoceanography, sea level, sediment deposition, Tsushima Warm Current

Received 1 February 2021; revised manuscript accepted 15 February 2021

Introduction

The eustatic sea level fluctuations by tectonic or glacial forcing have influenced the terrestrial and oceanographic environment. The Bering Strait throughflow connects the Bering Sea of the North Pacific with the Chukchi Sea of the Arctic Ocean. During the last glacial period, a drop in the sea level caused the closure of the Bering Strait, leading to a halt of the Bering Strait throughflow, which controlled the climatic variability in the North Atlantic (e.g. Hu et al., 2012). At the same time, the connection of Asia with Alaska by sea level lowering formed the Bering land bridge (i.e. Beringia), which provided a postulated route of human migration from Asia to America (Goebel et al., 2008). Similar to the Bering Strait region, the East Sea, known as the Japan Sea (hereafter the East Sea), as a marginal sea almost enclosed by the East Asian continent and the Japanese islands, is an exceptionally sensitive to the sea level change (Figure 1(a)).

The East Sea consists of three basins namely the Ulleung Basin, the Yamato Basin, and the Japan Basin. The sea is deeper than 2000 m, and is connected to neighboring seas through shallow straits (Tatarskiy Strait: 12 m, Soya Strait: 55 m, Tsugaru Strait: 130 m, and Korea Strait: 140 m) (Figure 1(a)). The relatively broad (approximately 150 km wide) Korea Strait between the Korean Peninsula and the Japanese islands acts as the main entrance for the Tsushima Warm Current (TWC) which is a branch of the Kuroshio Current (Figure 1(b)) (Chang et al., 2004). The TWC splits into three branches after flowing through the Korea Strait (Figure 1(b)) (Katoh, 1994). The first branch (i.e Nearshore Branch: NB) through the eastern channel of the strait roughly follows the 200-m isobath of the continental shelf along the Japanese coast. The second branch (i.e. Offshore Branch: OB) through the western channel of the strait flows along the continental shelf break and slope of the Japanese margin. The third branch, known as the East Korea Warm Current (EKWC), flows along the eastern coast of Korea as a western boundary current.

Glacio-eustatic sea level fluctuations are critical key processes that bring about dramatic environmental shift between the glacial and interglacial periods of the East Sea, because all the straits connecting the East Sea with the neighboring seas are very

[1]Department of Oceanography, Pusan National University, Busan, Korea
[2]Division of Glacial Environment Research, Korea Polar Research Institute, Incheon, Korea
[3]Marine Research Institute, Pusan National University, Busan, Korea

Corresponding author:
Boo-Keun Khim, Department of Oceanography, Pusan National University, Jangjeon-dong, Geumjeong-gu, Busan 46241, Korea.
Email: bkkhim@pusan.ac.kr

Polar Science 28 (2021) 100682

Contents lists available at ScienceDirect

Polar Science

journal homepage: http://www.elsevier.com/locate/polar

Biological productivity and glaciomarine sedimentation in the Central Basin of the northwestern Ross Sea since the last glacial maximum

Boo-Keun Khim[a,*], Ester Colizza[b], Jae Il Lee[c], Federico Giglio[d], Sangbeom Ha[a], Young-Suk Bak[e]

[a] Department of Oceanography, Pusan National University, Busan, 46241, South Korea
[b] Department of Mathematics and Geosciences, University of Trieste, Trieste, Italy
[c] Division of Glacial Environment Research, Korea Polar Research Institute, Incheon, 21341, South Korea
[d] National Research Council-Institute of Polar Science, Bologna, Italy
[e] Earth Environmental System Research Center, Jeonbuk National University, Jeonju, 54896, South Korea

A R T I C L E I N F O

Keywords:
Glaciomarine
Geochemistry
Productivity
Ice sheet
Continental margin
Antarctica

A B S T R A C T

This study documents multi-proxy data representing surface water productivity and AMS ^{14}C dates of box (BC3) and gravity (GC2) cores in the Central Basin of the northwestern Ross Sea. Based on AMS ^{14}C dates, a comparison of sediment properties between BC3 and GC2 reveals that BC3 records the complete Holocene (i.e., interglacial) history, which is correlated to the uppermost part of GC2. The lithostratigraphic succession of GC2 consists of the repetition of contrasting layers distinguished by the productivity proxies. In contrast to the uppermost sediment layer (i.e., interglacial), the subsurface sediment layer (i.e., deglacial) is distinctly characterized by very high biogenic components. Such pronounced biogenic remnants in the deglacial sediments are not explained exclusively by in situ enhanced productivity in the surface water. Our results, thus, suggest that eroded and reworked shelf sediments from a previous interglacial period enriched in biogenic components by the advancing ice sheet might be transported through the melt-water plumes from the grounding line to the Central Basin, to provide high geochemical properties of deglacial sediments. Thus, growth and retreat of the grounded ice sheet played an important role in glaciomarine sedimentation change in the Central Basin of the northwestern Ross Sea.

1. Introduction

The Antarctic polar system is characterized by interaction and interplay of oceanic, glaciological, atmospheric, and continental processes operated at multiple spatio-temporal scales (Colleoni et al., 2018). Despite such complicated environmental factors, the depositional model of glaciomarine sedimentation on the Antarctic continental shelf supports the biological productivity model proposed for the Weddell Sea continental margin by Grobe and Mackensen (1992). Based on the biological productivity model, more biogenic components are deposited on the seafloor of the continental margin during interglacial periods because of enhanced productivity under reduced sea ice cover, whereas fewer biogenic components are detected during glacial periods because of reduced productivity under more sea ice cover. Such a binary concept of biogenic sedimentation has also been applied successfully to the continental shelf of the Ross Sea (e.g., Frignani et al., 1998; Nishimura et al., 1998; Salvi et al., 2006).

The complex continental shelf morphology of the Ross Sea, characterized by a rugged topography with deep troughs and banks, has been shaped by the advance and retreat of the Ross Ice Sheet, preserving the signature of grounded and floating ice activity during the last glacial–interglacial cycle. The sedimentary stratigraphic sequence of the continental shelf (including shelf basins such as Drygalski Basin, JOIDES Basin, and Pennell Trough) in the Ross Sea has thus provided an unequivocal depositional model (Anderson et al., 1984; Domack and Harris, 1998; Anderson 1999; Domack et al., 1999). The typical sedimentary succession in the continental shelf of the Ross Sea shows an upward transition from subglacial or glaciomarine diamicton toward proximal to distal deglacial glaciomarine sediments, and late Holocene marine biogenic mud, recording a progressive retreat of the grounding line and the final onset of seasonal open marine conditions.

Much of the eroded debris excavated from the continental shelf by

* Corresponding author.
E-mail addresses: bkkhim@pusan.ac.kr (B.-K. Khim), colizzae@units.it (E. Colizza), leeji@kopri.re.kr (J.I. Lee), federico.giglio@cnr.it (F. Giglio), sb_ha@pusan.ac.kr (S. Ha), sydin@jbnu.ac.kr (Y.-S. Bak).

https://doi.org/10.1016/j.polar.2021.100682
Received 12 November 2020; Received in revised form 22 March 2021; Accepted 30 March 2021
Available online 6 April 2021
1873-9652/

geosciences

MDPI

Article

Environmental and Oceanographic Conditions at the Continental Margin of the Central Basin, Northwestern Ross Sea (Antarctica) Since the Last Glacial Maximum

Fiorenza Torricella [1,*], Romana Melis [2], Elisa Malinverno [3], Giorgio Fontolan [2], Mauro Bussi [2], Lucilla Capotondi [4], Paola Del Carlo [5], Alessio Di Roberto [5], Andrea Geniram [2], Gerhard Kuhn [6], Boo-Keun Khim [7], Caterina Morigi [1], Bianca Scateni [1,5] and Ester Colizza [2,*]

1 Dipartimento di Scienze della Terra, Università di Pisa, Via Santa Maria 53, 56126 Pisa, Italy; caterina.morigi@unipi.it (C.M.); bianca.scateni@ingv.it (B.S.)
2 Dipartimento di Matematica e Geoscienze, Università di Trieste, Via E. Weiss 2, 34128 Trieste, Italy; melis@units.it (R.M.); fontolan@units.it (G.F.); bussi@units.it (M.B.); andrea.geniram@phd.units.it (A.G.)
3 Dipartimento di Scienze dell'Ambiente e della Terra, Università di Milano-Bicocca, Piazza della Scienza 4, 20126 Milano, Italy; elisa.maliverno@unimib.it
4 Istituto di Scienze Marine-Consiglio Nazionale delle Ricerche ISMAR-CNR, Via P. Gobetti 101, 40129 Bologna, Italy; lucilla.capotondi@bo.ismar.cnr.it
5 Istituto Nazionale di Geofisica e Vulcanologia, Sezione di Pisa, Via C. Battisti 53, 56125 Pisa, Italy; paola.delcarlo@ingv.it (P.D.C.); alessio.diroberto@ingv.it (A.D.R.)
6 Alfred Wegener Institute Helmholtz Centre for Polar and Marine Research, Am Alten Hafen 26, 27568 Bremerhaven, Germany; gerhard.kuhn@awi.de
7 Department of Oceanography, Pusan National University, Busan 46241, Korea; bkkhim@pusan.ac.kr
* Correspondence: fiorenza.torricella@phd.unipi.it (F.T.); colizzae@units.it (E.C.)

Citation: Torricella, F.; Melis, R.; Malinverno, E.; Fontolan, G.; Bussi, M.; Capotondi, L.; Del Carlo, P.; Di Roberto, A.; Geniram, A.; Kuhn, G.; et al. Environmental and Oceanographic Conditions at the Continental Margin of the Central Basin, Northwestern Ross Sea (Antarctica) Since the Last Glacial Maximum. *Geosciences* 2021, *11*, 155. https://doi.org/10.3390/geosciences11040155

Academic Editors: Jesus Martinez-Frias and Angelos G. Maravelis

Received: 26 February 2021
Accepted: 26 March 2021
Published: 31 March 2021

Abstract: The continental margin is a key area for studying the sedimentary processes related to the advance and retreat of the Ross Ice Shelf (Antarctica); nevertheless, much remains to be investigated. The aim of this study is to increase the knowledge of the last glacial/deglacial dynamics in the Central Basin slope–basin system using a multidisciplinary approach, including integrated sedimentological, micropaleontological and tephrochronological information. The analyses carried out on three box cores highlighted sedimentary sequences characterised by tree stratigraphic units. Collected sediments represent a time interval from 24 ka Before Present (BP) to the present time. Grain size clustering and data on the sortable silt component, together with diatom, silicoflagellate and foraminifera assemblages indicate the influence of the ice shelf calving zone (Unit 1, 24–17 ka BP), progressive receding due to Circumpolar Deep Water inflow (Unit 2, 17–10.2 ka BP) and (Unit 3, 10.2 ka BP–present) the establishment of seasonal sea ice with a strengthening of bottom currents. The dominant and persistent process is a sedimentation controlled by contour currents, which tend to modulate intensity in time and space. A primary volcanic ash layer dated back at around 22 ka BP is correlated with the explosive activity of Mount Rittmann.

Keywords: diatoms; micropaleontology; sedimentology; cryptotephra; LGM to Holocene; Central Basin; Western Ross Sea; Antarctica

1. Introduction

The high-latitude continental margins are key areas where the sedimentary processes are influenced by the advance and retreat of the ice shelf and by different bottom water current activity on the continental slope between the glacial and interglacial periods [1–3].

The Ross Sea continental margins record the variation of the Antarctic Ice Sheet (AIS) due to the presence of the largest ice shelf, the Ross Ice Shelf (RIS), which promotes the production of dense shelf water which is the precursor for Antarctic Bottom Waters (AABW) [4]. The RIS dynamics that occurred during the Pleistocene and Holocene have

J. Micropalaeontology, 40, 15–35, 2021
https://doi.org/10.5194/jm-40-15-2021

Last Glacial Maximum to Holocene paleoceanography of the northwestern Ross Sea inferred from sediment core geochemistry and micropaleontology at Hallett Ridge

Romana Melis[1], Lucilla Capotondi[2], Fiorenza Torricella[3], Patrizia Ferretti[4], Andrea Geniram[1], Jong Kuk Hong[5], Gerhard Kuhn[6], Boo-Keun Khim[7], Sookwan Kim[5], Elisa Malinverno[8], Kyu Cheul Yoo[5], and Ester Colizza[1]

[1]Dipartimento di Matematica e Geoscienze, Università di Trieste, Via E. Weiss 2, 34127 Trieste, Italy
[2]Consiglio Nazionale delle Ricerche–Istituto di Scienze Marine (CNR-ISMAR), Via Gobetti 101, 40129 Bologna, Italy
[3]Dipartimento di Scienze della Terra, Università di Pisa, Via Santa Maria 53, 56126 Pisa, Italy
[4]Dipartimento di Scienze Ambientali, Informatica e Statistica, Università Ca' Foscari, Via Torino 155, Mestre, 30172 Venice, Italy
[5]Korea Polar Research Institute, Incheon, 21990, South Korea
[6]Alfred-Wegener-Institut Helmholtz Zentrum für Polar- und Meeresforschung, Am Alten Hafen 26, 27568 Bremerhaven, Germany
[7]Department of Oceanography, Pusan National University, Busan, 46241, South Korea
[8]Dipartimento di Scienze dell'Ambiente e della Terra, Università di Milano-Bicocca, Piazza della Scienza 4, 20126 Milan, Italy

Correspondence: Lucilla Capotondi (lucilla.capotondi@bo.ismar.cnr.it)

Received: 15 September 2020 – Revised: 1 February 2021 – Accepted: 2 February 2021 – Published: 10 March 2021

Abstract. During the Late Pleistocene–Holocene, the Ross Sea Ice Shelf exhibited strong spatial variability in relation to the atmospheric and oceanographic climatic variations. Despite being thoroughly investigated, the timing of the ice sheet retreat from the outer continental shelf since the Last Glacial Maximum (LGM) still remains controversial, mainly due to a lack of sediment cores with a robust chronostratigraphy. For this reason, the recent recovery of sediments containing a continuous occurrence of calcareous foraminifera provides the important opportunity to create a reliable age model and document the early deglacial phase in particular. Here we present a multiproxy study from a sediment core collected at the Hallett Ridge (1800 m of depth), where significant occurrences of calcareous planktonic and benthic foraminifera allow us to document the first evidence of the deglaciation after the LGM at about 20.2 ka. Our results suggest that the co-occurrence of large *Neogloboquadrina pachyderma* tests and abundant juvenile forms reflects the beginning of open-water conditions and coverage of seasonal sea ice. Our multiproxy approach based on diatoms, silicoflagellates, carbon and oxygen stable isotopes on *N. pachyderma*, sediment texture, and geochemistry indicates that abrupt warming occurred at approximately 17.8 ka, followed by a period of increasing biological productivity. During the Holocene, the exclusive dominance of agglutinated benthic foraminifera suggests that dissolution was the main controlling factor on calcareous test accumulation and preservation. Diatoms and silicoflagellates show that ocean conditions were variable during the middle Holocene and the beginning of the Neoglacial period at around 4 ka. In the Neoglacial, an increase in sand content testifies to a strengthening of bottom-water currents, supported by an increase in the abundance of the tycopelagic fossil diatom *Paralia sulcata* transported from the coastal regions, while an increase in ice-rafted debris suggests more glacial transport by icebergs.

Published by Copernicus Publications on behalf of The Micropalaeontological Society.

제 5 장 연구개발결과의 활용계획

본 연구에서 산출된 일련의 학술 논문들은 남극해 로스해를 중심으로 한 고해양·빙하성 환경 변화 복원 성과를 국제적으로 확산시키는 데 활용되었을 뿐만 아니라, 향후 남극 빙상 안정성 평가와 해수면 상승 예측 연구의 핵심 기초 자료로 활용되고 있다. 특히 퇴적물 기록에 기반한 빙하-해양-생물 생산성 간 상호작용에 대한 정밀한 해석은 국제 공동연구와 대형 연구 인프라 사업에서 요구하는 과학적 근거 자료로 활용 가능성이 높다.

우선, 재순환된 생물기원 성분에 의해 고생산성 신호가 왜곡될 수 있음을 규명한 연구(Geoscience Letters, 2024)는 기존 고생산성 프록시 해석의 한계를 명확히 제시함으로써, 향후 IODP 및 ICDP 시추 퇴적물 자료 해석 시 분석 전략 및 프록시 선택 기준을 재정립하는 데 활용될 수 있다. 이는 국제 극지 연구 커뮤니티에서 널리 적용되는 생산성 지표의 신뢰도를 제고하고, 고기후 해석의 불확실성을 저감하는 데 기여한다.

플라이스토세 엽리층 머드의 형성과 고해양 기록을 규명한 연구(Terra Nova, 2024)는 단주기 환경 변동과 빙상-해양 상호작용을 해석하는 새로운 개념적 모델을 제시함으로써, 고해상도 퇴적 기록을 보유한 국제 공동 시추 코어의 정밀 해석에 직접적으로 활용될 수 있다. 해당 연구는 빙하 후퇴 국면에서 나타나는 계절성 해빙, 수괴 층화, 저산소 환경의 복합적 영향을 해석하는 기준 자료로 기능한다.

또한 마지막 최대빙기 이후 로스해 전역의 빙하성 퇴적과 해양 환경 변화를 복원한 연구들(Marine Geology, Sedimentary Geology, Polar Science, Geosciences 등)은 서남극 빙상의 후퇴 시기와 공간적 비동시성(asynchrony)을 규명하는 데 활용되고 있다. 이들 성과는 로스해 대륙붕, 대륙사면, 중앙 분지 등 서로 다른 지형 단위에서 확보된 자료를 통합적으로 해석함으로써, 향후 빙상-해양 결합 모델의 경계조건 및 검증 자료로 제공될 수 있다.

아울러 해당 연구 성과들은 국제 공동연구 네트워크 내에서 후속 연구 기획과 시추 후보지 선정 과정에도 활용되고 있다. 특히 로스해 중앙 분지 및 주변 해역에 대한 고해상도 퇴적 환경 복원 결과는 IODP 및 향후 ICDP 기반 빙하 하부 시추 사업에서 우선 연구 대상 지역 설정과 과학적 목표 구체화에 참고 자료로 활용될 수 있다. 이는 단순한 학술 성과를 넘어, 대형 국제 연구 사업의 기획 단계에

서 실질적인 의사결정 자료로 기능한다는 점에서 중요한 의미를 갖는다.

더 나아가 본 연구에서 축적된 자료와 해석 결과는 국내외 연구진의 교육·인력 양성 측면에서도 활용되고 있다. 대학원 과정 및 국제 공동 워크숍을 통해 고해양 프록시 분석, 연대측정, 빙하성 퇴적 해석 기법이 전수되고 있으며, 이는 차세대 극지 연구 인력의 전문성 강화로 이어지고 있다. 이러한 인적 자원 양성 효과는 장기적으로 국내 극지 과학의 지속 가능성을 높이는 데 기여한다.

종합적으로, 본 논문들의 연구실적은 국제 학술지 게재에 그치지 않고, 국제 공동 시추 자료 해석 고도화, 빙상-기후 모델 검증, 대형 극지 연구 기획, 인력 양성 및 학문적 표준 정립 등 다양한 분야에서 실질적으로 활용되고 있다. 이는 본 연구가 남극 빙상 변화와 미래 기후 대응이라는 국제적 과제 해결에 기여하는 핵심 연구 성과임을 보여준다.

제 6 장 연구개발과정에서 수집한 해외과학기술정보

남극해 로스해는 남극 빙상과 해양 순환, 생물 생산성이 복합적으로 상호작용하는 핵심 해역으로, 전 지구 기후 변화와 해수면 변동을 이해하기 위한 전략적 연구 대상 지역으로 인식되고 있다. 이에 따라 최근 해외 고해양학 연구는 로스해에서의 과거 해빙-빙하 변동, 해양 순환 구조 변화, 생물 생산성의 장·단주기 변동을 정량적으로 복원하는 데 집중되고 있다.

우선, 로스해 고해양 환경 복원 연구의 핵심 기술은 심해 및 대륙붕 퇴적물 시추와 고해상도 퇴적 기록 분석이다. 국제해양시추프로그램(IODP)을 비롯한 다수의 국제 공동 연구를 통해 로스해 대륙주변부와 중앙 분지에서 장주기 퇴적물 코어가 확보되었으며, 이를 기반으로 신제3기 이후 서남극 빙상의 전진과 후퇴 과정이 단계적으로 규명되고 있다. 특히 빙하 기원의 퇴적물 분포와 입도 변화, 빙산기원퇴적물(IRD) 분석을 통해 빙상 후퇴 시기와 해빙 강도의 공간적 차이가 정밀하게 복원되고 있다.

해외 연구에서는 해빙(sea ice) 변화와 해양 순환의 연계성이 주요 과학기술 이슈로 부각되고 있다. 로스해는 남극 저층수(AABW)의 주요 형성 지역 중 하나로, 과거 해빙 면적과 폴리냐(polynya) 발달 정도에 따라 저층수 형성과 심층 해양 순환이 크게 변동한 것으로 해석된다. 이를 규명하기 위해 규조류 군집, 바이오마커(IP25, HBI), 산소·탄소 동위원소, 미량원소 분석 등이 복합적으로 활용되고 있으며, 이러한 다중 프록시 접근법은 해빙-해양 순환-기후 간의 상호작용을 정량적으로 재구성하는 데 기여하고 있다.

또한 로스해 고해양학 연구에서 중요한 기술적 진전은 빙하-해양 상호작용(glacier-ocean interaction)에 대한 정량화이다. 최근 해외 연구들은 빙저 용융에 의해 유입되는 담수의 영향을 퇴적물 지구화학 신호와 미세화석 기록을 통해 추적하고 있으며, 이를 통해 빙하 후퇴 시 해양 층화 강화, 영양염 공급 변화, 생물 생산성의 비선형적 반응이 나타났음을 보고하고 있다. 이는 단순한 온도 상승만으로는 설명할 수 없는 남극 해양 시스템의 복잡성을 보여주는 중요한 과학기술적 성과이다.

플라이스토세 및 홀로세 고환경 복원 연구 역시 로스해 해외 연구의 중요한 축을 이루고 있다. 마지막 최대빙기 이후 로스해의 해빙 시기, 해양 전선 이동, 생산성 회복 과정이 고해상도로 복원되었으며, 일부 연구에서는 단주기(수십~수백 년

규모)의 환경 변동이 빙상 동역학과 밀접하게 연관되어 있음을 제시하고 있다. 특히 라미네이티드 머드(laminated muds)의 형성과 보존 메커니즘에 대한 연구는 저산소 환경, 계절적 생산성 변화, 빙저 용융수 유입을 통합적으로 이해하는 새로운 해석 틀을 제공하고 있다.

최근에는 고기후 자료와 수치 모델을 결합하는 융합 연구가 해외에서 활발히 진행되고 있다. 로스해에서 복원된 고해양 자료는 빙상-해양-기후 결합 모델의 검증 자료로 활용되며, 이를 통해 서남극 빙상의 임계 반응과 해수면 상승 기여도를 보다 현실적으로 재현하려는 시도가 이루어지고 있다. 특히 플라이오세와 같은 과거 온난기의 로스해 환경은 미래 지구 평균기온 2℃ 이상 상승 시 남극 해양 시스템이 어떻게 변화할지를 예측하는 데 중요한 비교 기준으로 활용되고 있다.

종합적으로, 해외 과학기술 동향에서 로스해 고해양학 연구는 단순한 과거 환경 복원을 넘어, 미래 기후 변화에 따른 남극 빙상 안정성 평가와 해수면 상승 예측의 핵심 과학적 기반으로 자리매김하고 있다. 이러한 연구는 대규모 국제 공동 시추, 다중 프록시 분석 기술, 고성능 수치 모델링을 결합한 종합적 접근을 특징으로 하며, 향후 남극해 연구의 방향성을 결정하는 데 핵심적인 역할을 수행할 것으로 전망된다.

제 7 장 참고문헌

1 절. Fallacy of paleoproductivity signals by the recycled biogenic components: case study in the Central Basin of the northwestern Ross Sea

Anderson JB (1999) Antarctic Marine Geology. Cambridge (UK), Cambridge University Press.

Anderson JB, Brake CF, Myers NC (1984) Sedimentation on the Ross Sea continental shelf, Antarctica. Mar Geol 57:295–333

Anderson JB, Kurtz DD, Weaver FM (1979) Sedimentation on the Antarctic continental slope. In: Doyle LJ, Pilkey O (ed) Geology of Continental Slopes. SEPM Spec Pub 27, pp. 265–283

Bahr A, Jimenez-Espejo FJ, Kolasinac N, Grunert P, Hernandez-Molina FJ, Röhl U, Voelker AHL, Escutia C, Stow DAV, Hodell D, Alvarez-Zarikian CA (2014) Deciphering bottom current velocity and paleoclimate signals from contourite deposits in the Gulf of Cadiz during the last 140 kyr: An inorganic geochemical approach. Geochem Geophys Geosyst 15:3145–3160

Bollen M, Riesselman CR, Ohneiser C, Albot O, McKay R, Lee MK, Yoo KC, Kim S, Lee JI, Levy R (2022) Pleistocene oceanographic variability in the Ross Sea: A multiproxy approach to age model development and paleoenvironmental analyses. Global Planet Ch 216, 103901, doi.org/10.1016/j.glopalcha.2022.103901

Ceccaroni L, Frank M, Frignani M, Langone L, Ravaioli M, Mangini A (1998) Late Quaternary fluctuations of biogenic component fluxes on the continental slope of the Ross Sea, Antarctica. J Mar Syst 17:515–525

Cunningham WL, Leventer A, Andrews JT, Jennings AE, Licht KJ (1999) Late Pleistocene-Holocene marine conditions in the Ross Sea, Antarctica: evidence from the diatom record. The Holocene 9:129–139

DeMaster DJ (1981) The supply and accumulation of silica in the marine environment. Geochim Cosmochim Acta 45:1715–1732

Domack EW, Powell R (2018) Chapter 7 – Modern glaciomarine environments and sediments: An Antarctic perspective. In: Menzies J, van der Meer J (ed) Past Glacial Environments. Elsevier, pp. 181–272

Domack EW, Jacobson E A, Shipp S, Anderson JB (1999) Late Pleistocene–Holocene retreat of the West Antarctic Ice-Sheet system in the Ross Sea: Part 2—sedimentologic and stratigraphic signature. Geol Soc Am Bull 111:1517–1536

Dunbar RB, Leventer A, Stockton WL (1989) Biogenic sedimentation in McMurdo Sound, Antarctica. Mar Geol 85:155–179

Frank M, Eisenhauer A, Bonn WJ, Walter P, Grobe H, Kubik PW, Dittrich-Hannen B, Mangini A (1995) Sediment redistribution versus paleoproductivity change: Weddell Sea margin sediment stratigraphy and biogenic particle flux of the last 250,000 years deduced from ^{230}Thex,^{10}Beandbiogenicbariumprofiles. Earth Planet Sci Lett 136:559–573

Frignani M, Giglio F, Langone L, Ravaioli M, Mangini A (1998) Late Pleistocene-Holocene sedimentary fluxes of organic carbon and biogenic silica in the northwestern Ross Sea, Antarctica. Annals Glaciol 27:697–703

Ha S, Colizza E, Torricella F, Langone L, Giglio F, Kuhn G, MacríP, Khim BK (2022) Glaciomarine sediment deposition on the continental slope and rise of the central Ross Sea since the Last Glacial Maximum. Mar Geol 445, 106752

Hartman JD, Sangiorgi F, Barcena MA, Tateo F, Giglio F, Albertazzi S, Jtrincardi F, Bijl PK, Langone L, Asioli A (2021) Sea-ice, primary productivity and ocean temperatures at the Antarctic marginal zone during late Pleistocene. Quat Sci Rev 266, 107069

Hillenbrand CD, Crowhurst SJ, Williams M, Hodell DA, McCave IN, Ehrmann W, Xuan C, Piotrowski AM, Hernández-Molina FJ, Graham AGC, Grobe H, Williams TJ, Horrocks JR, Allen CS, Larter RD (2021) New insights from multi-proxy data from the West Antarctic continental rise: Implications for dating and interpreting Late Quaternary palaeoenvironmental records. Quat Sci Rev 257, 106842

Khim BK, Colizza E, Lee JI, Giglio F, Ha S, Bak YS (2021) Biological productivity and glaciomarine sedimentation in the Central Basin of the northwestern Ross Sea. Polar Sci28, 100682

Khim BK, Sohn YK, Lee MK, Kim S, Lee JI, Yoo KC (2024) Pleistocene glaciomarine laminated muds in the Central Basin of the northwestern Ross Sea and their paleoceanographic records. Terra Nova 36: 37–44, DOI: 10.1111/ter.12688

Khim BK,Song B, Cho HG, William T, Escutia C (2017) Late Neogene sediment properties in the Wilkes Land continental rise (IODP Exp. 318 Hole U1359A), East Antarctica. Geosci J21:21–32

Kim S, Lee JI, McKay RM, Yoo KC, Bak YS, Lee MK, Roh YH, Yoon HI, Moon HS, Hyun CU (2020) Late Pleistocene paleoceanographic changes in the Ross Sea–Glacial-interglacial variations in paleoproductivity, nutrient utilization, and deep-water formation. Quat Sci Rev 239, 106356

Langone L, Frignani M, Labbrozzi L, Ravaioli M (1998) Present-day biosiliceous sedimentation in the northwestern Ross Sea, Antarctica. J Mar Syst 17:459–470

Ledford-Hoffman PA, DeMaster DJ, Nittrouer CA (1986) Biogenic-silica accumulation in the Ross Sea and the importance of Antarctic continental-shelf deposits in the marine silica budget. Geochim Cosmochim Acta 50:2099–2110

Lee JI, McKay RM, Golledge NR, Yoon HI, Yoo KC, Kim HJ, Hong JK (2017) Widespread persistence of expanded East Antarctic glaciers in the

southwest Ross Sea during the last deglaciation. Geology 45:403–406
Leventer A, Domack E, Dunbar R, Pike J, Stickley C, Maddison E, Brachfeld S, Manley P, McClennen C (2006) Marine sediment record from the East Antarctic margin reveals dynamics of ice sheet recession. Geol Soc Am Today 16:4–10
Li G, Bu R, Yi L, Hu B, Li Y, Ji Y, Li Y, Wang L (2022) Geochronology and paleoenvironmental changes of Late Pleistocene sediments in the Ross Sea, Antarctica. Front Earth Sci 10, 863336
Lisiecki LE, Raymo ME (2005) A Pliocene-Pleistocene stack of 57 globally distributed benthic $\delta^{18}O$ records. Paleoceanography, 20, PA1003
Lu L, Zheng X, Chen Z, Yan W, Wu S, Zheng L-W, Wang X, Chen Y, Kao S (2022) One-to-one coupling between Southern Ocean productivity and Antarctica climate. Geophys Res Lett49, e2022GL098761.
McKay RM, Dunbar GB, Naish TR, Barrett PJ, Carter L, Harper M (2008) Retreat history of the Ross Ice Sheet (Shelf) since the Last Glacial Maximum from deep-basin sediment cores around Ross Island. Palaeogeogr Palaeoclimatol Palaeoecol 260:245–261
Mortlock RA, Froelich PN (1989) A simple method for the rapid determination of opal in pelagic marine sediments. Deep-Sea Res 36:1415–1426
Mulder T, Syvitski JPM, Migeon S, Faugere JC, Savoye B (2003) Marine hyperpycnal flows: initiation, behavior and related deposits. A review. Mar Petrol Geol 20:861–882
Ogg JG (2020) Chapter 5 - Geomagnetic Polarity Time Scale. Geologic Time Scale 2020 1:159–192
Ohneiser C, Yoo KC, Albot OB, Cortese G, Riesselman C, Lee JI, McKay R, Bollen M, Lee MK, Moon HS, Kim S, Beltran C, Levy R, Wilson G (2019) Magneto-biostratigraphic age models for Pleistocene sedimentary records from the Ross Sea. Global Planet Ch 176:36–49
Pike J, Kemp AES (1996) Preparation and analysis techniques for studies of laminated sediments. In: Kemp ASE (ed) Palaeoclimatology and Palaeoceanography from Laminated Sediments. Geological Society of London, Spec Publ 116, pp. 37–48
Prothro LO, Majewski W, Yokoyama Y, Simkins LM, Anderson JB, Yamane M, Miyairi Y, Ohkouchi N (2020) Timing and pathways of east Antarctic ice sheet retreat. Quat Sci Rev 230, 106166
Smith, JA, Graham AGC, Post AL, Hillenbrand CD, Bart PJ, Powell RD (2019) The marine geological imprint of Antarctic ice shelves. Nat Comm 10, 5635
Stickley CE, Pike J, Leventer A, Dunbar R, Domack EW, Brachfeld S, Manley P, McClennan C (2005) Deglacial ocean and climate seasonality in laminated diatom sediments, Mac. Robertson Shelf, Antarctica.Palaeogeogr Palaeoclimatol Palaeoecol 227:290–310
Sutter J, Fischer H, Grosfeld K, Karlsson NB, Kleiner T, Van Liefferinge B, Eisen O (2019) Modelling the Antarctic Ice Sheet across the mid-Pleistocene transition – implications for Oldest Ice. Cryosphere 13:2023–2041

Tesi T, Belt ST, Gariboldi K, Muschitiello F, Smik L, Finocchiaro F, Giglio F, Colizza E, Gazzurra G, Giordano P, Morigi C, Capotondi L, Nogarotto A, Köseoğlu D, Di Roberto A, Gallerani A, Langone L (2020) Resolving sea ice dynamics in the north-western Ross Sea during the last 2.6 ka: From seasonal to millennial timescales. Quat Sci Rev 237, 106299
Tolotti R, Salvi C, Salvi G, Bonci MC (2013) Late Quaternary climate variability as recorded by micropalaeontological diatom data and geochemical data in the western Ross Sea, Antarctica. Ant Sci 25:804–820
Tripsanas EK, Piper DJW (2008) Late Quaternary stratigraphy and sedimentology of Orphan Basin: Implications for meltwater dispersal in the southern Labrador Sea. Palaeogeogr Palaeoclimatol Palaeoecol 260:521–539
Venuti A, Florindo F, Caburlotto A, Hounslow MW, Hillenbrand CD, Strada E, Talarico FM, Cavallo A (2011) Late Quaternary sediments from deep-sea sediment drifts on the Antarctic Peninsula Pacific margin: Climatic control on provenance of minerals. J Geophys Res (Solid Earth) 116, B06104, doi:10.1029/2010JB007952.
Wu L, Wang R, Xia W, Ge S, Chen Z, Krijgsman W (2017) Productivity-climate coupling recorded in Pleistocene sediments off Prydz Bay (East Antarctica). Palaeogeogr Palaeoclimatol Palaeoecol 485:260–270

2 절. Paleoenvironmental reconstruction of glaciomarine sediments in the Drygalski Basin of the western Ross Sea since the Last Glacial Maximum

Alderkamp, A. C., van Dijken, G. L., Lowry, K. E., Lewis, K. M., Joy-Warren, H. L., van de Poll, W., Laan, P., Gerringa, L., Delmont, T.O., Jenkins, B.D., Arrigo, K. R., 2019. Effects of iron and light availability on phytoplankton photosynthetic properties in the Ross Sea. Marine Ecology Progress Series, 621, 33-50.
Anderson, J.B., 1975. Factors controlling $CaCO_3$ dissolution in the Weddell Sea from foraminiferal distribution patterns. Marine Geology, 19, 315-332.
Anderson, J.B., Kurtz, D.D., Domack, E.W., Balshaw, K.M., 1980. Glacial and glacial marine sediments of the Antarctic continental shelf. The Journal of Geology, 88, 399-414.
Anderson, J.B., Brake, C.F., Myers, N.C., 1984. Sedimentation on the Ross Sea continental shelf, Antarctica. Marine Geology, 57, 295-333.
Anderson, J.B., Shipp, S.S., Bartek, L.R., Reid, D.E., 1992. Evidence for a grounded ice sheet on the Ross Sea continental shelf during the late Pleistocene and preliminary paleodrainage reconstruction. In: Elliot, D.H. (Ed.), Contributions to Antarctic Research III, vol. 57, American Geophysical Union, pp. 39-62.

Anderson, J. B., 1999. Antarctic marine geology. Cambridge University Press, 289
Anderson, J.B., Conway, H., Bart, P.J., Witus, A.E., Greenwood, S.L., McKay, R.M., Hall. B.L., Ackert, R.B., Licht, K., Jakobsson, M., Stone, J.O., 2014. Ross Sea paleo-ice sheet drainage and deglacial history during and since the LGM. Quaternary Science Reviews, 100, 31-54.
Andrews, J.T., Domack, E.W., Cunningham, W.L., Leventer, A., Licht, K.J., Jull, A.T., DeMaster, D.J., Jennings, A.E., 1999. Problems and possible solutions concerning radiocarbon dating of surface marine sediments, Ross Sea, Antarctica. Quaternary Research, 52, 206-216.
Armand, L.K., Crosta, X., Romero, O., Pichon, J.J., 2005. The biogeography of major diatom taxa in Southern Ocean sediments: 1. Sea ice related species. Palaeogeography, Palaeoclimatology, Palaeoecology, 223, 93-126.
Arrigo, K.R., DiTullio, G.R., Dunbar, R.B., Robinson, D.H., VanWoert, M., Worthen, D.L., Lizotte, M.P., 2000. Phytoplankton taxonomic variability in nutrient utilization and primary production in the Ross Sea. Journal of Geophysical Research (Oceans), 105, 8827-8846.
Arrigo, K.R., Robinson, D.H., Dunbar, R.B., Leventer, A.R., Lizotte, M. P., 2003. Physical control of chlorophyll a, POC, and TPN distributions in the pack ice of the Ross Sea, Antarctica. Journal of Geophysical Research (Oceans), 108, 3316.
Bart, P.J., Anderson, J.B., Trincardi, F., Shipp, S.S., 2000. Seismic data from the Northern basin, Ross Sea, record extreme expansions of the East Antarctic Ice Sheet during the late Neogene. Marine Geology, 166, 31-50.
Bart, P.J., DeCesare, M., Rosenheim, B.E., Majewski, W., McGlannan, A., 2018. A centuries-long delay between a paleo-ice-shelf collapse and grounding-line retreat in the Whales Deep Basin, eastern Ross Sea, Antarctica. Scientific Reports, 8, 12392.
Berg, S., Leng, M.J., Kendrick, C.P., Cremer, H., Wagner, B., 2013. Bulk sediment and diatom silica carbon isotope composition from coastal marine sediments off East Antarctica. Silicon, 5, 19-34.
Biscaye, P.E., 1965. Mineralogy and sedimentation of recent deep-sea clay in the Atlantic Ocean and adjacent seas and oceans. Geological Society of America Bulletin, 76, 803-832.
Brambati, A., Fanzutti, G.P., Finocchiaro, F., Melis, R., Frignani, M., Ravaioli, M., Setti, M. 1997. Paleoenvironmental Record in Core Anta91-30 (Drygalski Basin, Ross Sea, Antarctica). Geology and Seismic Stratigraphy of the Antarctic Margin, 2, 71, 137-151.
Brown, G.T., Brindley, G.W., 1980. X-ray diffraction procedures for clay mineral identification. In: Brindley, G.W., Brown, G. (Eds.), Crystal structure of clay minerals and their X-ray identification, Mineralogical Society of London, pp. 305-359.
Capotondi, L., Bergami, C., Giglio, F., Langone, L., Ravaioli, M., 2018. Benthic foraminifera distribution in the Ross Sea (Antarctica) and its relationship to oceanography. Bollettino della Società Paleontologica Italiana, 57,

187-202.
Christ, A.J., Bierman, P.R., 2020. The local last glacial maximum in McMurdo Sound, Antarctica: Implications for ice-sheet behavior in the ross sea embayment. Geological Society of America Bulletin, 132, 31-47.
Conway, H., Hall, B.L., Denton, G.H., Gades, A.M., Waddington, E.D., 1999. Past and future grounding-line retreat of the West Antarctic Ice Sheet. Science, 286, 280-283.
Cooper, A.K., Davey, F.J., 1985. Marine geological and geophysical investigations in the Ross Sea, Antarctica. Antarctic Journal of the United States, 19, 80-82.
Crawford, R.M., 1995. The role of sex in the sedimentation of a marine diatom bloom. Limnology and Oceanography, 40, 200-204.
Crosta, X., Sturm, A., Armand, L., Pichon, J.J., 2004. Late Quaternary sea ice history in the Indian sector of the Southern Ocean as recorded by diatom assemblages. Marine Micropaleontology, 50, 209-223.
Crosta, X., Crespin, J., Billy, I., Ther, O., 2005. Major factors controlling Holocene δ13Corg changes in a seasonal sea-ice environment, Adélie Land, East Antarctica. Global Biogeochemical Cycles, 19, GB4029.
Cunningham, W.L., Leventer, A., 1998. Diatom assemblages in surface sediments of the Ross Sea: relationship to present oceanographic conditions. Antarctic Science, 10, 134-146.
Cunningham, W.L., Leventer, A., Andrews, J.T., Jennings, A.E., Licht, K.J., 1999. Late Pleistocene-Holocene marine conditions in the Ross Sea, Antarctica: evidence from the diatom record. The Holocene, 9, 129-139.
DeMaster, D.J., 1981. The supply and accumulation of silica in the marine environment. Geochimica et Cosmochimica Acta, 45, 1715-1732.
Domack, E.W., Harris, P.T., 1998. A new depositional model for ice shelves, based upon sediment cores from the Ross Sea and the Mac. Robertson shelf, Antarctica. Annals of Glaciology, 27, 281-284.
Domack, E.W., O'Brien, P., Harris, P., Taylor, F., Quilty, P.G., De Santis, L., Raker, B., 1998. Late Quaternary sediment facies in Prydz Bay, East Antarctica and their relationship to glacial advance onto the continental shelf. Antarctic Science, 10, 236-246.
Domack, E.W., Jacobson, E.A., Shipp, S., Anderson, J.B., 1999. Late Pleistocene–Holocene retreat of the West Antarctic Ice-Sheet system in the Ross Sea: Part 2—sedimentologic and stratigraphic signature. Geological Society of America Bulletin, 111, 1517-1536.
Dunbar, R.B., Leventer, A.R., Mucciarone, D.A., 1998. Water column sediment fluxes in the Ross Sea, Antarctica: atmospheric and sea ice forcing. Journal of Geophysical Research (Oceans), 103, 30741-30759.
Ehrmann, W., 1998. Implications of late Eocene to early Miocene clay mineral assemblages in McMurdo Sound (Ross Sea, Antarctica) on paleoclimate and ice dynamics. Palaeogeography, Palaeoclimatology, Palaeoecology, 139, 213-231.
Ehrmann, W., Setti, M., Marinoni, L., 2005. Clay minerals in Cenozoic sediments off Cape Roberts (McMurdo Sound, Antarctica) reveal palaeoclimatic

history. Palaeogeography, Palaeoclimatology, Palaeoecology, 229, 187-211.
Ehrmann, W., Hillenbrand, C.D., Smith, J.A., Graham, A.G., Kuhn, G., Larter, R.D. 2011. Provenance changes between recent and glacial-time sediments in the Amundsen Sea embayment, West Antarctica: clay mineral assemblage evidence. Antarctic Science, 23, 471-486.
Fischer, G., 1991. Stable carbon isotope ratios of plankton carbon and sinking organic matter from the Atlantic sector of the Southern Ocean. Marine Chemistry, 35, 581-596.
Folk, R.L., Ward, W.C., 1957. Brazos River bar [Texas]; a study in the significance of grain size parameters. Journal of Sedimentary Research, 27, 3-26.
Franke, D., Ehrmann, W., 2010. Neogene clay mineral assemblages in the AND-2A drill core (McMurdo Sound, Antarctica) and their implications for environmental change. Palaeogeography, Palaeoclimatology, Palaeoecology, 286, 55-65.
Frezzotti, M., Tabacco, I.E., Zirizzotti, A., 2000. Ice discharge of eastern Dome C drainage area, Antarctica, determined from airborne radar survey and satellite image analysis. Journal of Glaciology, 46, 253-264.
Frignani, M., Giglio, F., Langone, L., Ravaioli, M., Mangini, A., 1998. Late Pleistocene-Holocene sedimentary fluxes of organic carbon and biogenic silica in the northwestern Ross Sea, Antarctica. Annals of Glaciology, 27, 697-703.
Gersonde, R., Wefer, G., 1987. Sedimentation of biogenic siliceous particles in Antarctic waters from the Atlantic sector. Marine Micropaleontology, 11, 311-332.
Gilbert, I.M., Pudsey, C.J., Murray, J.W., 1998. A sediment record of cyclic bottom-current variability from the northwest Weddell Sea. Sedimentary Geology, 115, 185-214.
Giorgetti, G., Talarico, F., Sandroni, S., Zeoli, A., 2009. Provenance of Pleistocene sediments in the ANDRILL AND-1B drillcore: Clay and heavy mineral data. Global and Planetary Change, 69, 94-102.
Giovinetto, M. B., Bentley, C.R., 1985. Surface balance in ice drainage of Antarctica, Antarct. JUS, 20, 6-13.
Goehring, B.M., Balco, G., Todd, C., Moening-Swanson, I., Nichols, K. 2019. Late-glacial grounding line retreat in the northern Ross Sea, Antarctica. Geology, 47, 291-294.
Greenwood, S.L., Simkins, L.M., Halberstadt, A.R.W., Prothro, L.O., Anderson, J.B., 2018. Holocene reconfiguration and readvance of the East Antarctic Ice Sheet. Nature Communications, 9, 3176.
Grobe, H., Mackensen, A., 1992. Late Quaternary climatic cycles as recorded in sediments from the Antarctic continental margin. In: Kennett, J.P., Warnke, D.A. (Eds.), The Antarctic Paleoenvironment: A Perspective on Global Change, American Geophysical Union, pp. 349-376.
Ha, S., Colizza, E., Torricella, F., Langone, L., Giglio, F., Kuhn, G., Macri, P., Khim, B.K., 2022. Glaciomarine sediment deposition on the continental slope and rise of the central Ross Sea since the Last Glacial Maximum.

Marine Geology, 445, 106752.
Halberstadt, A.R.W., Simkins, L.M., Greenwood, S.L., Anderson, J.B., 2016. Past ice-sheet behaviour: retreat scenarios and changing controls in the Ross Sea, Antarctica. The Cryosphere, 103, 1003-1020.
Hall, B.L., Baroni, C., Denton, G.H., 2004. Holocene relative sea-level history of the Southern Victoria Land Coast, Antarctica. Global and Planetary Change, 42, 241-263.
Hall, B.L., Henderson, G.M., Baroni, C., Kellogg, T.B., 2010. Constant Holocene Southern-Ocean 14C reservoir ages and ice-shelf flow rates. Earth and Planetary Science Letters, 296, 115-123.
Hall, B.L., Koch, P.L., Baroni, C., Salvatore, M.C., Hoelzel, A.R., de Bruyn, M., Welch, A.J., 2023. Widespread southern elephant seal occupation of the Victoria land coast implies a warmer-than-present Ross Sea in the mid-to-late Holocene. Quaternary Science Reviews, 303, 107991.
Heaton, T.J., Köhler, P., Butzin, M., Bard, E., Reimer, R.W., Austin, W.E., Ramsey, C.B., Grootes, P.M., Hughen, K.A., Kromer, B., Reimer, P.J., Adkins, J., Burke, A., Cook, M.S., Olsen, J., Skinner, L.C., 2020. Marine20—the marine radiocarbon age calibration curve (0–55,000 cal BP). Radiocarbon, 62, 779-820.
Henley, S.F., Annett, A.L., Ganeshram, R.S., Carson, D.S., Weston, K., Crosta, X., Tait, A., Dougans, J., Fallick, A.E., Clarke, A., 2012. Factors influencing the stable carbon isotopic composition of suspended and sinking organic matter in the coastal Antarctic sea ice environment. Biogeosciences, 9, 1137-1157.
Hillenbrand, C.D., Grobe, H., Diekmann, B., Kuhn, G., Fütterer, D.K., 2003. Distribution of clay minerals and proxies for productivity in surface sediments of the Bellingshausen and Amundsen seas (West Antarctica)–Relation to modern environmental conditions. Marine Geology, 193, 253-271.
Hillenbrand, C.D., Kuhn, G., Frederichs, T., 2009. Record of a Mid-Pleistocene depositional anomaly in West Antarctic continental margin sediments: an indicator for ice-sheet collapse? Quaternary Science Reviews, 28, 1147-1159.
Hillenbrand, C.D., Smith, J.A., Kuhn, G., Esper, O., Gersonde, R., Larter, R.D., Maher, B., Moreton, S.G., Shimmield, T.M., Korte, M., 2010. Age assignment of a diatomaceous ooze deposited in the western Amundsen Sea Embayment after the Last Glacial Maximum. Journal of Quaternary Science, 25, 280-295.
Hillenbrand, C.D., Bentley, M.J., Stolldorf, T.D., Hein, A.S., Kuhn, G., Graham, A.G., Fogwill, C.J., Kristofferson, Y., Smith J.A., Anderson, J.B., Larter, R.D., Melles, M., Hodgson, D.A., Mulvanet, R., Sugden, D.E., 2014. Reconstruction of changes in the Weddell Sea sector of the Antarctic Ice Sheet since the Last Glacial Maximum. Quaternary Science Reviews, 100, 111-136.
Jones, R.S., Whitmore, R.J., Mackintosh, A.N., Norton, K.P., Eaves, S.R., Stutz, J., Christl, M., 2021. Regional-scale abrupt Mid-Holocene ice sheet

thinning in the western Ross Sea, Antarctica. Geology, 49, 278-282.
Jung, J., Ko, Y., Lee, J., Yang, K., Park, Y.K., Kim, S., Moon, H., Kim, H.J., Yoo, K.C., 2021. Multibeam bathymetry and distribution of clay minerals on surface sediments of a small bay in Terra Nova Bay, Antarctica. Minerals, 11, 72.
Kilfeather, A.A., Ó Cofaigh, C., Lloyd, J.M., Dowdeswell, J.A., Xu, S., Moreton, S. G., 2011. Ice-stream retreat and ice-shelf history in Marguerite Trough, Antarctic Peninsula: Sedimentological and foraminiferal signatures. Geological Society of America Bulletin, 123, 997-1015.
Kirshner, A.E., Anderson, J.B., Jakobsson, M., O'Regan, M., Majewski, W., Nitsche, F.O., 2012. Post-LGM deglaciation in Pine island Bay, west Antarctica. Quaternary Science Reviews, 38, 11-26.
Kim, S., Lee, J.I., McKay, R.M., Yoo, K.C., Bak, Y.S., Lee, M.K., Roh, Y.H., Yoon, H.I., Moon, H., Hyun, C.U., 2020. Late pleistocene paleoceanographic changes in the Ross Sea–Glacial-interglacial variations in paleoproductivity, nutrient utilization, and deep-water formation. Quaternary Science Reviews, 239, 106356.
Kyle, P.R., 1990. A. McMurdo volcanic group western Ross embayment. Volcanoes of the Antarctic Plate and Southern Oceans, 48, 18-145.
Langone, L., Frignani, M., Labbrozzi, L., Ravaioli, M., 1998. Present-day biosiliceous sedimentation in the northwestern Ross Sea, Antarctica. Journal of Marine Systems, 17, 459-470.
Larter, R.D., Anderson, J.B., Graham, A.G., Gohl, K., Hillenbrand, C.D., Jakobsson, M., Johnson, J.S., Kuhn, G., Nitsche, F.O., Smith, J.A., Witus, A.E., Bentley, M.J., Dowdeswell, J.A., Ehrmann, W., Klages, J.P., Lindow, J., Ó Cofaigh, C., Spiegel, C., 2014. Reconstruction of changes in the Amundsen Sea and Bellingshausen sea sector of the West Antarctic ice sheet since the last glacial maximum. Quaternary Science Reviews, 100, 55-86.
Lee, J.I., McKay, R.M., Golledge, N.R., Yoon, H.I., Yoo, K.C., Kim, H.J., Hong, J. K., 2017. Widespread persistence of expanded East Antarctic glaciers in the southwest Ross Sea during the last deglaciation. Geology, 45, 403-406.
Leventer, A., Dunbar, R.B., DeMaster, D.J., 1993. Diatom evidence for late Holocene climatic events in Granite Harbor, Antarctica. Paleoceanography, 8, 373-386.
Licht, K.J., Jennings, A.E., Andrews, J.T., Williams, K.M., 1996. Chronology of late Wisconsin ice retreat from the western Ross Sea, Antarctica. Geology, 24, 223-226.
Licht, K.J., Dunbar, N.W., Andrews, J.T., Jennings, A.E. 1999. Distinguishing subglacial till and glacial marine diamictons in the western Ross Sea, Antarctica: implications for a last glacial maximum grounding line. Geological Society of America Bulletin, 111, 91-103.
Licht, K.J., Andrews, J.T., 2002. The 14C record of Late Pleistocene ice advance and retreat in the central Ross Sea, Antarctica. Arctic, Antarctic, and Alpine Research, 34, 324-333.

Lowry, D.P., Golledge, N.R., Bertler, N.A., Jones, R.S., McKay, R., 2019. Deglacial grounding-line retreat in the Ross Embayment, Antarctica, controlled by ocean and atmosphere forcing. Science Advances, 58, eaav8754.
Majewski, W., Anderson, J.B., 2009. Holocene foraminiferal assemblages from Firth of Tay, Antarctic Peninsula: paleoclimate implications. Marine Micropaleontology, 73, 135-147.
Majewski, W., Wellner, J.S., Anderson, J.B., 2016. Environmental connotations of benthic foraminiferal assemblages from coastal West Antarctica. Marine Micropaleontology, 124, 1-15.
Majewski, W., Bart, P.J., McGlannan, A.J., 2018. Foraminiferal assemblages from ice-proximal paleo-settings in the Whales Deep Basin, eastern Ross Sea, Antarctica. Palaeogeography, Palaeoclimatology, Palaeoecology, 493, 64-81.
Majewski, W., Prothro, L.O., Simkins, L.M., Demianiuk, E.J., Anderson, J.B., 2020. Foraminiferal patterns in deglacial sediment in the western Ross Sea, Antarctica: Life near grounding lines. Paleoceanography and Paleoclimatology, 35, e2019PA003716.
McGlannan, A.J., Bart, P.J., Chow, J.M., DeCesare, M. 2017. On the influence of post-LGM ice shelf loss and grounding zone sedimentation on West Antarctic ice sheet stability. Marine Geology, 392, 151-169.
McKay, R.M., Dunbar, G.B., Naish, T.R., Barrett, P.J., Carter, L., Harper, M., 2008. Retreat history of the Ross Ice Sheet (Shelf) since the Last Glacial Maximum from deep-basin sediment cores around Ross Island. Palaeogeography, Palaeoclimatology, Palaeoecology, 260, 245-261.
McKay, R., Naish, T., Powell, R., Barrett, P., Scherer, R., Talarico, F., Kyle, P., Monien, D., Kuhn, G., Jackolski, C., Williams, T., 2012. Pleistocene variability of Antarctic ice sheet extent in the Ross embayment. Quaternary Science Reviews, 34, 93-112.
McKay, R., Golledge, N.R., Maas, S., Naish, T., Levy, R., Dunbar, G., Kuhn, G., 2016. Antarctic marine ice-sheet retreat in the Ross Sea during the early Holocene. Geology, 44, 7-10.
Melis, R., Salvi, G., 2009. Late Quaternary foraminiferal assemblages from western Ross Sea (Antarctica) in relation to the main glacial and marine lithofacies. Marine Micropaleontology, 70, 39-53.
Mezgec, K., Stenni, B., Crosta, X., Masson-Delmotte, V., Baroni, C., Braida, M., Ciardini, V., Colizza, E., Melis, R., Salvatore, M.C., Severi, M., Scarchilli, C., Traversi, R., Udisti, R., Frezzotti, M., 2017. Holocene sea ice variability driven by wind and polynya efficiency in the Ross Sea. Nature Communications, 8, 1334.
Moore, D.M., Reynolds Jr, R.C., 1989. X-ray Diffraction and the Identification and Analysis of Clay Minerals. Oxford University Press.
Mortlock, R.A., Froelich, P.N., 1989. A simple method for the rapid determination of biogenic opal in pelagic marine sediments. Deep Sea Research Part A, 36, 1415-1426.
Mosola, A.B., Anderson, J.B., 2006. Expansion and rapid retreat of the West

Antarctic Ice Sheet in eastern Ross Sea: possible consequence of over-extended ice streams? Quaternary Science Reviews, 25, 2177-2196.
Ó Cofaigh, C., Davies, B.J., Livingstone, S.J., Smith, J.A., Johnson, J.S., Hocking, E.P., Hodgson, D.A., Anderson J.B., Bentley, M.J., Canals, M., Comack, E., Dowdeswell. J.A., Evnas, J., Glasse, N.F., Hillenbrand, C.D., Larter, R.D., Roberts, S.J., Simms, A.R., 2014. Reconstruction of ice-sheet changes in the Antarctic Peninsula since the Last Glacial Maximum. Quaternary Science Reviews, 100, 87-110.
Ohkouchi, N., Eglinton, T.I., 2006. Radiocarbon constraint on relict organic carbon contributions to Ross Sea sediments. Geochemistry, Geophysics, Geosystems, 7, Q04012.
Orsi, A.H., Wiederwohl, C.L. 2009. A recount of Ross Sea waters. Deep Sea Research II, 56, 778-795.
Pawlowski, J., Fahrni, J.F., Guiard, J., Conlan, K., Hardecker, J., Habura, A., Bowser, S.S., 2005. Allogromiid foraminifera and gromiids from under the Ross Ice Shelf: morphological and molecular diversity. Polar Biology, 28, 514-522.
Prothro, L.O., Simkins, L.M., Majewski, W., Anderson, J.B., 2018. Glacial retreat patterns and processes determined from integrated sedimentology and geomorphology records. Marine Geology, 395, 104-119.
Prothro, L.O., Majewski, W., Yokoyama, Y., Simkins, L.M., Anderson, J.B., Yamane, M., Miyairi, Y., Ohkouchi, N., 2020. Timing and pathways of east Antarctic ice sheet retreat. Quaternary Science Reviews, 230, 106166.
Pudsey, C.J., Murray, J.W., Appleby, P., Evans, J., 2006. Ice shelf history from petrographic and foraminiferal evidence, Northeast Antarctic Peninsula. Quaternary Science Reviews, 25, 2357-2379.
Rau, G.H., Sweeney, R.E., Kaplan, I.R., 1982. Plankton 13C: 12C ratio changes with latitude: differences between northern and southern oceans. Deep Sea Research Part A, 29, 1035-1039.
Rhee, H.H., Lee, M.K., Seong, Y.B., Lee, J.I., Yoo, K.C., Yu, B.Y., 2020. Post-LGM dynamic deglaciation along the Victoria Land coast, Antarctica. Quaternary Science Reviews, 247, 106595.
Salvi, C., Salvi, G., Stenni, B., Brambati, A., 2004. Palaeoproductivity in the Ross Sea, Antarctica, during the last 15 kyr BP and its link with ice-core temperature proxies. Annals of Glaciology, 39, 445-451.
Salvi, C., Busetti, M., Marinoni, L., Brambati, A., 2006. Late Quaternary glacial marine to marine sedimentation in the Pennell Trough (Ross Sea, Antarctica). Palaeogeography, Palaeoclimatology, Palaeoecology, 231, 199-214.
Scherer, R.P., 1994. other silt-sized sedimentary particles. Journal of Paleolimnology, 12, 171-179.
Shin, J.Y., Kim, S., Zhao, X., Yoo, K.C., Yu, Y., Lee, J.I., Lee, M.K., Yoon, H.I., 2020. Particle-size dependent magnetic properties of Scotia Sea sediments since the Last Glacial Maximum: Glacial ice-sheet discharge controlling magnetic proxies. Palaeogeography, Palaeoclimatology,

Palaeoecology, 557, 109906.
Shipp, S., Anderson, J.B, Domack, E.W, 1999. Late Pleistocene–Holocene retreat of the West Antarctic Ice-Sheet system in the Ross Sea: part 1—geophysical results. Geological Society of America Bulletin, 111, 1486-1516.
Simkins, L.M., Anderson, J.B., Greenwood, S.L., Gonnermann, H.M., Prothro, L.O., Halberstadt, A.R.W., Strarns, L.A., Pollard, D., DeConto, R.M., 2017. Anatomy of a meltwater drainage system beneath the ancestral East Antarctic ice sheet. Nature Geoscience, 10, 691-697.
Sjunneskog, C., Scherer, R.P., 2005. Mixed diatom assemblages in glacigenic sediment from the central Ross Sea, Antarctica. Palaeogeography, Palaeoclimatology, Palaeoecology, 218, 287-300.
Smellie, J.L., Hole, M.J., 1998. Products and processes in Pliocene-Recent, sub-aqueous to emergent volcanism in the Antarctic Peninsula: examples of englacial Surtseyan volcano construction. Bulletin of Volcanology, 58, 628-646.
Smith Jr, W.O., Ainley, D.G., Arrigo, K.R., Dinniman, M.S., 2014. The oceanography and ecology of the Ross Sea. Annual Review of Marine Science, 6, 469-487.
Smith, J.A., Hillenbrand, C.D., Kuhn, G., Larter, R.D., Graham, A.G., Ehrmann, W., Moreton, S.G., Forwick, M., 2011. Deglacial history of the West Antarctic Ice Sheet in the western Amundsen Sea embayment. Quaternary Science Reviews, 30, 488-505.
Smith, J.A., Andersen, T.J., Shortt, M., Gaffney, A.M., Truffer, M., Stanton, T.P., Binschadler, R., Dutrieux, P., Jenkins, A., Hillenbrand, C.D., Ehrmann, W., Corr, H.F.J., Farley, N., Crowhurst, S., Vaughan, D.G., 2017. Sub-ice-shelf sediments record history of twentieth-century retreat of Pine Island Glacier. Nature, 541, 77-80.
Smith, J.A., Graham, A.G., Post, A.L., Hillenbrand, C.D., Bart, P.J., Powell, R.D., 2019. The marine geological imprint of Antarctic ice shelves. Nature Communications, 101, 5635.
Stokke, P.R., Carson, B., 1973. Variation in clay mineral X-ray diffraction results with the quantity of sample mounted. Journal of Sedimentary Research, 43, 957-964.
Stuiver, M., Reimer, P.J., Reimer, R.W., 2021. CALIB 8.2. CALIB Radiocarbon Calibration, URL: http://calib.org/calib/calib.html
Taylor, F., Whitehead, J., Domack, E., 2001. Holocene paleoclimate change in the Antarctic Peninsula: evidence from the diatom, sedimentary and geochemical record. Marine Micropaleontology, 41, 25-43.
Tesi, T., Belt, S.T., Gariboldi, K., Muschitiello, F., Smik, L., Finocchiaro, F., Giglio, F., Colizza, E., Gazzurra, G., Giordano, P., Morigi, C., Capotondi, L., Nogarotto, A., Koseoglu, D., Di Roberto, A., Gallerani, A., Langone, L., 2020. Resolving sea ice dynamics in the north-western Ross Sea during the last 2.6 ka: From seasonal to millennial timescales. Quaternary Science Reviews, 237, 106299.
Tolotti, R., Salvi, C., Salvi, G., Bonci, M.C., 2013. Late Quaternary climate

variability as recorded by micropalaeontological diatom data and geochemical data in the western Ross Sea, Antarctica. Antarctic Science, 25, 804-820.
Villinski, J.C., Dunbar, R.B., Mucciarone, D.A., 2000. Carbon 13/Carbon 12 ratios of sedimentary organic matter from the Ross Sea, Antarctica: A record of phytoplankton bloom dynamics. Journal of Geophysical Research (Oceans), 105, 14163-14172.
Weber, M.E., Clark, P.U., Kuhn, G., Timmermann, A., Sprenk, D., Gladstone, R., Zhang, X., Lohmann, G., Menviel, L., Chikamoto, M.O., Friedrich, T., Ohlwein, C., 2014. Millennial-scale variability in Antarctic ice-sheet discharge during the last deglaciation. Nature, 510, 134-138.
Yokoyama, Y., Anderson, J.B., Yamane, M., Simkins, L.M., Miyairi, Y., Yamazaki, T., Koizumi, M., Suga, H., Kusahara, K., Prothro, L.O., Hasumi, H., Southon, J.R., Ohkouchi, N., 2016. Widespread collapse of the Ross Ice Shelf during the late Holocene. Proceedings of the National Academy of Sciences, 1139, 2354-2359.

주 의

1. 이 보고서는 극지연구소 위탁과제 연구결과보고서 입니다.

2. 이 보고서 내용을 발표할 때에는 반드시 극지연구소에서 위탁연구과제로 수행한 연구결과임을 밝혀야 합니다.

3. 국가과학기술 기밀유지에 필요한 내용은 대외적으로 발표 또는 공개하여서는 안됩니다.